TRACE CHEMICAL EVALUATION OF CLOUD SEEDING IN THE PAYETTE BASIN

by

James Mitchell Fisher

A thesis

submitted in partial fulfillment

of the requirements for the degree of

Master of Science in Hydrologic Sciences

Boise State University

August 2017

BOISE STATE UNIVERSITY GRADUATE COLLEGE

DEFENSE COMMITTEE AND FINAL READING APPROVALS

of the thesis submitted by

James Mitchell Fisher

Thesis Title: Trace Chemical Evaluation of Cloud Seeding in the Payette Basin

Date of Final Oral Examination: 28 April 2017

The following individuals read and discussed the thesis submitted by student James Mitchell Fisher, and they evaluated his presentation and response to questions during the final oral examination. They found that the student passed the final oral examination.

Shawn Benner, Ph.D.	Chair, Supervisory Committee
Matthew J. Kohn, Ph.D.	Member, Supervisory Committee
Hans P. Marshall, Ph.D.	Member, Supervisory Committee
James P. McNamara, Ph.D.	Member, Supervisory Committee

The final reading approval of the thesis was granted by Shawn Benner, Ph.D., Chair of the Supervisory Committee. The thesis was approved by the Graduate College.

ACKNOWLEDGEMENTS

I wish to acknowledge the generous support and guidance of the meteorologists at Idaho Power Company, particularly Mel Kunkel, Derek Blestrud, and Vincent P. Holbrook. Their extremely detailed (and accurate) forecasts ensured that we collected relevant data every time we headed out in the field.

I also wish to thank all the individuals contributing to the sampling effort: Robert Florence, Andy Karlson, Kerrie Weppner, Clay Roehner, and the Idaho Power River Engineering team. A very special thanks to Larry Thomas Oltheim (aka "TomO") for sampling conducting real-time snow at abnormal times of the day (midnight).

I also wish to thank Reggie Walters, Katelyn Watson, and Miguel Aguayo for providing useful Python scripts to analyze large SNOTEL and/or WRF data efficiently.

Marion Lytle was essential to the success of this project – her expertise in finding optimal mass spectrometer settings, her assistance analyzing every sample (and, at times, analyzing samples by herself), and her ability to swiftly make adjustments in the laboratory necessary to lower the contamination potential at the part per trillion level.

I would like to give a big thanks to my primary advisor, Shawn Benner, for guiding this project and for teaching me how to make this project successful and learning the "soft skills" needed in the workforce. Shawn permitted me the flexibility to study whatever aspect I saw fit but frequently checked in to make sure I was on track.

Lastly, but most importantly, I thank my friends and family for the constant encouragement and support. They made my graduate experience a joyful one.

ABSTRACT

Glaciogenic cloud seeding increases the fraction of super cooled liquid water precipitating from a given storm. Orographic clouds tend to be inefficient at higher cloud temperatures due to the lack of active natural ice nuclei. Adding artificial ice nuclei active at temperatures greater than -12^{o}C (where most natural ice nuclei are inactive) may result in an increase in snow precipitation, especially in orographic clouds. Silver iodide (AgI) is typically the artificial nucleating agent for winter orographic cloud seeding. Recent estimates suggest the addition of AgI to orographic storm clouds enhance precipitation by 3 - 15%. However, the National Research Council stated "*the areas affected by AgI remains an open question*".

In this study, we seek to understand how well AgI is delivered to regions intended for cloud seeding in the central mountains of Idaho. To accomplish this, we develop and validate methods to detect sub-part-per-trillion silver concentrations in snow. These methods were specific to an ICP-MS laboratory not housed in a Class 100 Clean room. Unique laboratory layout and protocols are employed to reduce laboratory contamination potential. Using clean field methods, we sample a series of snow profiles within the target area of active cloud seeding. The results demonstrate the ability of these new methods to reproduce distinct elevated Ag concentrations over a small scale (0.25 km^2) and at the basin scale (2,400 km^2). A localized enrichment factor highlighted silver enrichments likely from AgI rather than from other local sources. This enrichment factor can delineate a seeding signature at sites far downwind from AgI sources, where Ag concentrations are

only 2 parts per trillion above background levels. The localized enrichment factors consistently correspond to known cloud seeding events.

After developing reliable trace chemical snow methods in the 2015 water year, the 2016 water year applied these methods to assess Idaho Power's overall AgI targeting in the Payette Basin. Improper targeting is regarded by some as the biggest obstacle to achieving statistically significant estimates of silver iodide (AgI) impacts on precipitation. To better understand AgI targeting, we (1) assessed AgI targeting effectiveness spatially for aerial and ground-based seeding, (2) quantified temporal variability of AgI targeting using real-time snow collection methods, and (3) determined the maximum distance from AgI sources at which seeding signatures in snow exist. We addressed these issues by analyzing more than 4,000 snow samples. Sample collection took place in the target zone and up to 180 km downwind of AgI sources using both real-time and traditional snow pit methods. We found silver enrichments in 90% of cases involving ground generators seeding, but in only 11% aircraft-only seeding events. We also assessed, for the first time, the maximum spatial extent of AgI enrichments (AgI > 3 ppt and an Enrichment Factor > 1) in snow using ultra-clean methods. All sites sampled beyond 80 km (n = 13) of the seeding source lacked detectable AgI signatures in snow.

We developed methods during the 2015 and 2016 water years to detect sub-ppt silver concentrations and validation of areas impacted by AgI. Next, we wanted to understand whether the AgI in snowpack would cause adverse environmental impacts. Based on the 2.8 ppb silver concentrations within measured within 5 m of ground generators, we concluded AgI is unlikely to harm known fauna. The toxicity of silver depends primarily on concentration, speciation, and bioavailability. The silver ion (Ag^+)

is a bioavailable and the most toxic form of silver known. Silver iodide is not soluble nor bioavailable, and secondary EPA standards are four orders of magnitude higher than concentrations found in all seeded snow samples. The silver ion is typically the dominant species in laboratory toxicity studies quantifying the toxicity of silver (where silver nitrate is used, a solution not found in natural environments). Modern cloud seeding programs disperse extremely small amounts of AgI annually (< 25 kg) over large areas (> 2,000 km^2). Environmental sampling indicated no adverse effects on wildlife, nor silver accumulating at detectable levels above background in soils, streams, or aquatic species in seeded areas.

INTRODUCTION

Glaciogenic cloud seeding is an important scientific technology for enhancing water resources across in the Western United States. Cloud seeding enriches orographic super cooled liquid water layers with plumes of ice nuclei, increasing water yield from a given storm. Weather model assessments of cloud seeding estimate controlled releases of the ice nucleating agent, silver iodide (AgI), increases snow precipitation between 5-15% annually. However, efficacy of cloud seeding programs are difficult to assess using statistical or modeling approaches alone. This study will develop a new field method evaluating the spatial and temporal abundance of AgI in snow using ultra-trace snow chemistry. Regions void of an AgI signature is evidence that snowflakes were not nucleated via AgI.

The field laboratory is Idaho Power Company (IPC). IPC has been cloud seeding since 2003 to provide additional aquifer to the Snake River Basin. Water in this basin feeds into the Snake River, and ultimately into the Hells Canyon Hydroelectric Dam Complex. This, in turn, produces additional clean energy for Southern Idaho, permits more water usage for irrigation, and benefits local fauna.

This thesis has three main objectives, each separated into a chapter. Chapter one asks ‘what are the methods necessary to detect AgI in snow?’ This chapter describes the field and laboratory methods necessary to detect enrichments of silver from AgI seeded snow. The second chapter asks ‘how well is AgI targeted in time and space, and is this program effectively increasing precipitation?’ This chapter highlights the methods to

collect and analyze snow in real-time, shows five basin-wide sampling campaigns to find AgI in space, and compares SNOTEL sites to Weather Research and Forecasting model outputs – to compute the percent increase in precipitation due to cloud seeding. In essence, this chapter is an application of chapter 1 methods. Finally, the third chapter asks ‘since we know the concentrations and locations of AgI, is it toxic?’. I perform a literature review on silver toxicity in the environment. I assess the environmental risks associated with cloud seeding based on this literature review and snow sampling effort.

TABLE OF CONTENTS

LIST OF TABLES

LIST OF FIGURES

LIST OF PICTURES

LIST OF ABBREVIATIONS

CHAPTER 1

BSU	Boise State University
IPC	Idaho Power Company
CEF	Crustal enrichment factor
ICP-MS	Inductively coupled plasma mass spectrometer
HR-ICPMS	High resolution inductively coupled plasma mass spectrometer
HDPE	High density polyethylene
LDPE	Low density polyethylene
PFA	Polyfluoroalkoxy
MQ	Milli-Q 18.2 mΩ water
ppt	Parts per trillion (10^{-12})
ppb	Parts per billion (10^{-9})
ppm	Parts per million (10^{-6})
mb	millibars
WRF	Weather Research and Forecasting
EPA	Environmental Protection Agency
WWMPP	Wyoming Weather Modification Pilot Project
SNOTEL	SNOw TELemetry
HNO_3	Nitric acid
AgI	Silver iodide

Ag	Silver
In_2O_3	Indium sesquioxide

CHAPTER 2

EC_{xx}	Effect concentration (xx% population experience adverse effects)
LC_{xx}	Lethal concentration (xx% mortality within a population)
NOEC	No observed effect concentration
NOAEL	No observed adverse effect concentration
LOEC	Lowest observed effect concentration

CHAPTER 3

SLW	Super cooled liquid water
SPERP	Snowy Precipitation Enhancement Research Project
ICP-MS	Inductively Coupled Plasma Mass-Spectrometer
HNO_3	Nitric acid
EPA	Environmental Protection Agency
CEF	Crustal Enrichment Factor
SNOTEL	SNOw TELemetry – network of meteorlogical gauges
LRR	Lost River Range, Idaho.
A	Aircraft seeding events
G	Ground generator seeding events
A + G	Mixed seeding events

DEFINITIONS FOR CHAPTER 2

Absorption – Process in which a substance is some entity (in this case, silver) that assumes the bulk phase of the adsorbing material. This entity is taken up by the *volume.*

Adsorption – Similar to absorption. This involves the adhesion of an entity (in this case, silver) to the surface of a bulk phase. This entity is taken up by the *surface*.

Acute Toxicity – Produces a significant effect within a short period of time, usually 96 hours or less. Acute toxicity may be a function of EC_{50}or LC_{50} (EPA Water Quality Handbook: Glossary, 2012). Typically, the concentration of a contaminant required to produce an acute response is much higher than that required to produce a chronic response (see chronic toxicity below).

Bioavailability – Bioavailability is the contaminant fraction available to cross an organism's cellular membrane. In other words, the fraction actively interacting with organisms are bioavailable (whether positive or negative). Fractions of the contaminant in the form of other chemical species inert to the organism of interest are not bioavailable.

Bioconcentration Factor (BCF) – Ratio of the contaminant concentration in an organism to the contaminant concentration in a medium of interest. Mediums used for this ratio are commonly water or air in the surrounding environment, or food commonly consumed. This is a measure of how much the contaminant accumulates within the organism.

Chronic Toxicity – This produces an effect that lingers for long periods of time after exposure, typically defined as 10% or more of the organism's lifespan. A few examples of chronic effects include reduced growth rates, mortality rates, or death (EPA

Water Quality Handbook: Glossary, 2012). Typically, the concentration of a contaminant required to produce a chronic response is much lower than that required to produce an acute response (see acute toxicity above).

Total Recoverable Silver – Total amount of silver that can be solubilized by strong acid digestion. EPA standards of silver concentrations utilize this metric. The EPA also states the term "total [silver]" and "total recoverable [silver]" are synonymous and can be used interchangeably as was listed on the EPA memorandum titled "Total vs. Total Recoverable Metals" on August 19, 1998.

parts per million (ppm) = mg/kg = 10^{-6} g g^{-1} = mg/L[1]

parts per billion (ppb) = µg/kg = 10^{-9} g g^{-1} = µg/L

parts per trillion (ppt) = ng/kg = 10^{-12} g g^{-1} = ng/L

DEFINITIONS FOR CHAPTER 3

Target zone – For this paper, the target zone is defined as areas less than 80 km downwind an AgI source. We defined 'downwind' as anything following the wind stream lines of the WRF-GFS model (1.8 km resolution). We assume dispersion between the outer-most generators is 100%. In other words, we assume the target zone is a continuous 2D area between the two outer-most generators.

Seeding signal – Samples with silver concentrations at least two standard deviations above background (μ = 1 ppt, σ = 1 ppt) and a crustal enrichment factor (CEF) greater than one.

---

[1] The units listed above are equivalent to the units in parenthesis assuming the density of water equals 1000 kg/m^3. This is approximately true (within 3%) amid temperatures and salinities of most natural waters.

Source-receptor approach – The source-receptor method correlates AgI timing releases to silver concentrations in snow.

Downwind effects – Effects of AgI beyond the target zone (> 80 km downwind).

CHAPTER ONE: TRACE CHEMICAL METHOD DEVELOPMENT

Glaciogenic cloud seeding with silver iodide (AgI) has been used to enhance precipitation for over 60 years. Assessments of AgI impact and dispersion are often quantified using atmospheric processes models with impact assessed by comparing models with and without the inclusion of cloud seeding modules. However, there is inherent uncertainty in these models. Quantifying AgI distribution in the snowpack following cloud seeding can both validate and improve model performance. The purpose of this study is to demonstrate the capacity to document the dispersion of AgI by measuring silver (Ag) enrichments in snow.

This study develops clean field and laboratory procedures to detect trace seeding signatures in alpine snowpack. Unique laboratory layout and protocols are employed to reduce contamination potential within a traditional ICP-MS laboratory setting (not housed in a Class 100 Clean Room). Using these methods, we sample a series of snow profiles within the target area of active cloud seeding in the central mountains of Idaho. The results demonstrate the ability of the new methods to reproduce distinct elevated Ag concentrations over a small scale (0.25 km^2) and at the basin (2,400 km^2) scale. The trace chemical analysis of snow samples from eight snow pits over an area of 0.25 km^2 and six sites separated up to 65 km (basin scale) identify potential seeding signatures from two seeded storms. A localized enrichment factor was used to identify and replicate this seeding signature at all six sites within the basin. This enrichment factor can delineate a seeding signature at sites far downwind from AgI sources, where Ag concentrations are

only 1-3 parts per trillion above background levels. The localized enrichment factors at all six sites contain chemical snow profiles generally corresponding to peak Ag concentrations and known cloud seeding events.

1. Introduction

1.1 Brief Description of Cloud Seeding

Glaciogenic cloud seeding is a method of enhancing the fraction of super cooled liquid water precipitating from a given storm. Precipitation tends to be inefficient at higher cloud temperatures due to the lack of active natural ice nuclei [1]. The addition of artificial ice nuclei active at temperatures, greater than -12^{o}C, may result in an increase in snow precipitation, especially in orographic clouds [2]. Silver iodide (AgI) is the artificial nucleating agent most often used in winter orographic cloud seeding. Recent estimates suggest the addition of artificial ice nuclei from AgI enhances precipitation by 3 - 15% [3, 4].

1.2 Current validation techniques

The impact of cloud seeding is often quantified using physical, statistical and modeling techniques. Models, such as the Weather Research and Forecasting (WRF) model, can be used to predict the spatial and temporal presence of AgI in the atmosphere and its associated impact on precipitation. However, AgI plumes can be difficult to model amid complex terrain. Some physical studies found AgI plumes can be trapped in valleys, lacking the uplift to effectively nucleate orographic clouds [5, 6]. A model may incorrectly identify enhancements downwind of a valley-trapped AgI plume. Therefore, there is a need for physical validation of these techniques [2, 7]. One such validation tool is trace chemical analysis, validating the success in AgI targeting only. Assessing the

magnitude of precipitation enhancement (using modeling and statistical techniques) with targeting effectiveness (trace chemical analysis) allows for a more comprehensive evaluation of cloud seeding effectiveness.

1.3 Prior efforts to quantify Ag seeding signals in snow

Trace chemical methods have been utilized to evaluate cloud seeding for years. This method was first used in 1968 using a neutron activation technique [7]. However, the importance of clean techniques was not universally understood until the early 1990's [8] and results prior to this period should be evaluated accordingly [9]. There have been several recent studies utilizing clean techniques that have provided reliable results. For instance, new approaches were developed to evaluate cloud seeding in a project at Lake Almanor, in California, including a source-receptor method and a dual-tracer method. The source-receptor method sought to correlate the timing of AgI releases to Ag concentrations in snow [10, 11]. Ag enrichments above typical background concentrations did not necessarily imply successful cloud seeding because anthropogenic contamination or dry deposits from dust could have elevated concentrations. Background Ag concentrations, on the other hand, imply poor targeting. The dual-tracer method provided better physical understanding of high Ag concentrations in target zones due to AgI seeding [12-14]. This method released AgI in conjunction with In_2O_3, a non-active nuclei of similar size as AgI. Because In_2O_3 does not participate in nucleation processes, the enhancement of indium concentrations in snow is likely due to scavenging processes only. Therefore, snow samples with Ag to In ratios greater than expected from scavenging (approximately one) implied that enhanced Ag concentrations were primarily due to nucleation. These dual-tracer techniques were replicated in the Payette Basin,

Idaho [15] and in the Snowy Mountains, Australia [16]. These dual-tracer studies showed that Ag concentrations above background (1 ppt and 3 ppt in the Payette Basin and Snowy Mountains, respectively) were almost always correlated to high Ag to In ratios, demonstrating the differential nucleating capacity of AgI. The most recent trace chemical analysis, Wyoming Weather Modification Pilot Project (WWMPP), found the source-receptor method useful in identifying seeded snow layers [4]. In the study presented here, like the WWMPP, the source-receptor method was used to identify seeded snow layers.

1.4 What is the gap in knowledge?

Although measuring Ag enrichments in snow has been done for years, there are limited field-based studies regarding the spatial distribution of AgI at various scales [16]. Understanding spatial variability is critical to both establishing the appropriate amount of samples to collect in the field, as well as the reliability of trace chemical methods in defining a seeded layer. Additionally, several recent studies utilized a Thermo-Scientific XR high resolution inductively coupled plasma mass spectrometer (HR-ICPMS) housed in a Class 100 Clean Room. The present study utilized a quadrupole ICP-MS with higher limits of detection and was not housed in a clean room. Because high resolution ICP-MS instruments housed in clean laboratories can be cost prohibitive as a validation tool, the feasibility of using a traditional laboratory for analyzing trace Ag and other trace metal concentrations was evaluated in this study.

1.5 Purpose and objectives of the research

The purpose of this study was to quantify trace Ag enhancements in snow from AgI cloud seeding using the source-receptor approach. This was accomplished by developing appropriate field and laboratory techniques to produce limits of detection for

Ag that were below one part per trillion (ppt). The analysis techniques were tested to determine if seeding signatures could be detected over a small scale (0.25 km^2) and also over a basin scale (2,400 km^2). The approach described in this paper can be used to assess the cloud seeding module in the WRF model and accuracy and cloud seeding impacts.

Specifically, the four questions posed by this study are:

1. Is a traditional quadrupole ICP-MS laboratory suitable for trace chemical analysis of snow samples?
2. Are low signal to noise Ag enhancements in field samples replicable and reliable?
3. Are the identification of Ag cloud seeding signals replicable over a small scale?
4. Can the distribution of seeding signals be reliably determined over a basin scale?

2. Methodology

2.1 Field Methods

The target area for the cloud seeding activities in this study is the Payette Basin, located in southwestern Idaho, USA (*Figure 1*). The Payette Basin is approximately 2,400 km^2 and is bounded by latitudes 43° 57'N to 44° 33'N and longitudes 115° 57'W to 116° 04'W. Elevations range between 970 and 2,830 m. A centrally located weather station near the median elevation reveals an average annual temperature and precipitation of 3.8^oC and 81.9 cm respectively (Deadwood Dam Meteorological Station, 1,640 m elevation). The sites sampled in this study primarily resided in the southern Payette Basin (*Table 1*).

The field and lab methods necessary to quantify trace amounts of Ag in snow have been outlined in several studies, primarily in Arctic regions [17-21]. Slight modifications of these methods were applied for this study. Note that all acids described in this paper were quartz double distilled in a Class 100 Clean Room. All acid percent concentrations were computed on a volume per volume basis.

Field equipment was cleaned and packaged to minimize the potential for contamination. Field equipment in direct contact with snow underwent three nitric acid baths while subsidiary equipment soaked in a 2% nitric acid bath until use (see *Laboratory Methods*). All field equipment used for sampling, including attire, was packed in a Class 100 Clean Room. Equipment was sealed within two polyethylene bags. Only the inner bags were acid washed [9]. Inner polyethylene bags were leached in 4% nitric acid (HNO_3) for 48 hours [22]. Bags were rinsed in ultra-pure water, and then dried in a vertical laminar flow station (AirClean PCR Workstation AC600) for 12 hours. Clean field equipment was packed and sealed under these workstations as well.

To prevent contamination, technicians wore clean room attire and constructed snow pits far from potential contamination sources. Clean gear attire consisted of a High-Density Polyethylene (HDPE) Tyvek suit, 2 pairs of nitrile gloves, face masks, and Low-Density Polyethylene (LDPE) bags tied around the technician's feet. Technicians approached the sampling location from downwind to prevent particulates migrating from the technician to the snow about to be sampled. Sampling locations were always in remote areas and at least 400 m from potential contamination sources, such as snow mobile tracks or roads.

Snow samples were collected from the wall of an excavated snow pit. The snow pit was first excavated using an aluminum shovel. Snow pit faces were then decontaminated prior to sampling by removing 2 cm of snow perpendicular to the pit face using a clean polypropylene scraper. The pit face was decontaminated again with a triple cleaned LDPE scraper, removing an additional 2 cm [23] of snow. Snow was then sampled using 50 mL, 3 cm diameter polypropylene centrifuge vials (FisherBrand, Pittsburg, PA, USA). Columns of vials were staggered 1.5 cm (*Figure 2*) to obtain a higher depth resolution [24].

A "clean hands/dirty hands" technique was employed while sampling in which one member of the team was designated as "clean hands", this person collected samples while a second member of the team was designated as "dirty hands" and conducted activities other than snow collection [22]. "Clean hands" would handle only the LDPE scraper for decontamination and areas of sample vials untouched by "dirty hands". "Dirty hands" would attend to tasks more susceptible to contamination, such as labeling vials with permanent markers and opening acid cleaned bags of vials.

After sample collection, vials were immediately double bagged (clean inner bag), shipped back to Boise State University in a dry ice cooler and then stored at -20^{o} C until analysis. Samples were kept frozen to mitigate trace element adsorption in the sampling vials.

2.2 Laboratory Methods

Our laboratory Milli-Q 18.2 mΩ (MQ) water and HNO_3 prepared in the laboratory were compared to known pure standards. Blanks were validated using SeaStar Chemicals (Sidney, BC, Canada) BASELINE® HNO_3 (Lot No. 1214070) and

BASELINE® water (Lot No. 9214020). SeaStar HNO_3 and water were both certified to less than 0.05 ppt Ag. Differences between our lab MQ water and SeaStar Chemicals were always less than 0.4 ppt for Ag, within our method detection limit. Upon dilution to 2% HNO_3, negligible differences resulted from SeaStar Chemicals HNO_3 and the reagent-grade HNO_3 double distilled in our Class 100 Clean Room. The importance of blanks cannot be understated. The quality of blanks, not the sensitivity of modern ICP-MS instruments, are often the most impactful factor in lowering an instrument-limit of detection [24].

Equipment in direct contact with samples or acid underwent a triple acid bath with increasing purity [9, 25, 26] and decreasing concentrations of HNO_3 (10%, 5%, and 0.1% respectively). MQ water rinses followed each bath. All non-critical equipment (permanent markers and polypropylene scrapers) remained in a 2% HNO_3 until needed for sampling. Non-critical equipment was rinsed in MQ water after the acid bath. All equipment was then dried in a laminar flow clean bench and double sealed in polyethylene bags.

Polyfluoroalkoxy (PFA) Teflon bottles were used to hold the trace element standard solutions used to calibrate the ICP-MS. Teflon was used to hold samples and standards at room temperature because it adsorbs Ag at the lowest rate relative to other laboratory materials (Wen et al., 2002). Fifteen mL Teflon vials (Savillex, Eden Prairie, MN, USA) were used to hold prepared samples for ICP-MS analysis. Both varieties of Teflon labware were washed twice in 48-hour baths of 1% hydrofluoric acid (HF) and 2% HNO_3[2]. MQ water rinses followed each bath.

[2] http://www.savillex.com/Content.aspx?PageName=Guide%20to%20Cleaning%20PFA%20Labware.

Analyses were performed with a multi-use Thermo Scientific X-Series 2 Inductively Coupled Plasma Mass Spectrometer (ICP-MS) coupled with an Elemental Scientific Inc. SC-FAST Automated Sample Introduction System (hereafter, autosampler). The ICP-MS laboratory was not a Class 100 Clean Room. Therefore, special steps were undertaken to limit contamination sources from airborne particulates in the ICP-MS laboratory and from memory effects within the ICP-MS resulting from other experiments.

Contamination from airborne particulates in the ICP-MS laboratory was mitigated by eliminating direct exposure of samples to the ICP-MS laboratory environment. Contamination potential was reduced by placing the autosampler within a laminar flow clean bench (AirClean AC4000 Workstation, Raleigh, NC, USA). The autosampler encased samples in plastic to further prevent particulate infiltration (*Figure 3*). Likewise, all samples were prepared and thawed in a Class 100 Clean Room.

High background Ag counts in the ICP-MS from unrelated experiments had to be minimized prior to analysis. This instrument was frequently used for laser ablation of geologic materials, resulting in disruptive memory effects from Ag. Ag counts were reduced in two ways. First, a 4% HNO_3 ultra-pure solution was delivered through the ICP-MS until Ag counts stabilized. Counts stabilized to 30 ± 10 counts per second in 1 - 12 hours, depending antecedent conditions. Second, a dedicated set of internal parts for the ICP-MS was used for this analysis. A nickel micro-skimmer cone (Meinhard, Golden, CO, USA), nickel sampler cone (Meinhard), perfluoroalkoxy (PFA) tubing, quartz cyclonic spray chamber (ESI, Omaha, NE, USA), and a quartz nebulizer (ESI) and injector (ESI) were used exclusively for this study.

Samples were acidified as per the EPA Direct Analysis Method 200.8 [27]. This acidification method was chosen primarily because it has been the conventional method for analyzing precipitation and natural waters for decades. Snow was acidified to 2% HNO_3 and stored at room temperature to thaw. Once prepared, samples were stored in the dark for 24 hours within the clean room prior to analysis. Adopting this method allowed for direct comparison with other studies, because element concentrations at these low values can be altered by both acidification duration and strength [28]. However, it should be noted that samples were acidified within their field vials and prior to thawing. When samples were thawed and decanted from the polypropylene field vials to the Teflon test vials prior to acidification, 45% lower Ag concentrations resulted (n = 9, *Figure 4*). This was likely due to adsorption and/or the bonding of solid Ag particulates to the field vial walls. Therefore, previous studies that acidified samples after decanting into analysis vials may have underestimated Ag concentrations in snow.

Samples were prepared in the clean lab prior to being transported to the ICP-MS laboratory. After the 24 hour acidification period, samples were decanted from the 50 mL polypropylene field vials to the 15 mL Teflon test vials in the clean lab. Test vials were sealed with Parafilm, placed in a clean LDPE rack, and sealed again in a clean HDPE tub before being transported to the ICP-MS laboratory. The LDPE sample rack was loaded directly into the autosampler, housed within a laminar flow clean bench.

The ICP-MS was calibrated using three serial dilutions of 1,000 mg/L (1,000 ppm) standards to analyze the following crustal tracers: Na, Al, Cr, Co, Sr, Ba, La, Ce, and Pb. Ag was calibrated using serial dilutions of 1,000 ppm to concentrations to 1,000 parts per trillion (ppt), 100 ppt, 10 ppt, and 1 ppt. The Ag calibration linear regression

lines were re-calibrated a minimum of 3 times per analysis to address drift. Drift was further mitigated by analyzing a 10 ppb indium internal standard throughout the analysis. Blank (2% HNO_3) rinses followed each calibration to reduce memory affects from 100 ppt and 1,000 ppt standards. Blanks were also analyzed every 10 samples to ensure instrument precision. Standard operating conditions for the ICP-MS are listed in *Table 2*.

3. Results

3.1 Is a traditional ICP-MS laboratory suitable for trace chemical analysis of snow?

Our methods produced limits of detection for Ag low enough to identify distinct snow layers that contain elevated Ag concentrations. Detection limit, calculated as three times the standard deviation of Ag in blanks, of 0.4 ppt were obtained. These detection limits were necessary to identify trace Ag seeding signatures as low as 2 ppt (*Figure 5*). However, most Ag-enriched layers identified exhibited greater Ag enhancements, generally ranging from 8 to 25 ppt.

An inter-laboratory comparison was done to test the accuracy of our methods. Eight columns of snow samples were collected in one snow pit. Four columns were analyzed by Boise State University and four by Curtin University's Trace Research Advanced Clean Environment (TRACE) laboratory. Curtin University housed a High Resolution ICP-MS (Thermo Scientific ELEMENT 2), with an Ag detection limit of 0.05 ppt. Profiles analyzed in both laboratories were comparable even though the low Ag concentrations from this site oscillated about Boise State's detection limit (*Figure 5*).

While the ICP-MS used in this study was not in a clean laboratory, the team had access to, and used, a clean lab for cleaning of materials for sampling and analysis as well as preparation of samples and standards. This capacity was considered essential to the

success of the project. Therefore, an ICP-MS housed outside a trace metal clean room can be used to measure Ag concentrations to sub-ppt precision if clean environments are accessible and all relevant equipment is nitric acid washed.

3.2 Are low signal to noise Ag enhancements in field samples replicable and reliable?

Because the anticipated Ag concentrations associated with cloud seeding are almost always less than 50 ppt, natural Ag in the snow or dust within the snow can often exceed Ag contributed to the snow by cloud seeding. Ag enhancements from AgI can be as small as 1 ppt [14]. Minor enhancements due to cloud seeding can be difficult to quantify relative to background Ag concentrations. In the Western United States, background Ag concentrations have been documented to range from 1 ppt in Idaho [15] to 5 ppt in Wyoming [25]. From the current study the background Ag concentration was found to be one ppt in the Payette Basin, in agreement with the most recent trace analysis performed here [15]. The background Ag concentration was established by collecting snow samples (n = 105) at a control site 63 km upwind and North of the nearest ground generator.

Another challenge is to discern the fraction of Ag due to AgI compared with other anthropogenic or naturally occurring contaminants like dust. Ag concentrations greater than 15 ppt due to dust have been observed in remote, non-seeded regions. The primary source of Ag in this region was attributed to dust [25]. Anthropogenic contamination in non-seeded regions can cause Ag concentrations to be as high as 107 ppt, as seen in the Alps [17]. Because the Payette Basin is far from anthropogenic contamination sources, we assumed high background Ag concentrations were primarily derived from dust. The average Ag enriched snow storm layer (corresponding to a known seeding event)

contained Ag concentrations of 14 ppt (n = 14 seeded layers), similar to Ag concentrations observed in non-seeded snow in Wyoming. Therefore, Ag concentrations alone are not necessarily useful in identifying seeded snow layers.

To resolve the cloud seeding signature from Ag in the snow associated with dust, we used a normalizing approach in which we calculate an enrichment factor for Ag relative to the mean concentration of the earth's upper continental crust. This crustal enrichment factor (CEF), computed as in Equation 1, identified where significant Ag enrichments existed relative to elements commonly abundant in dust. A CEF value of 1 or less suggests Ag concentrations the sample are primarily due to dust. The crustal isotopes of the elements used in Equation 1 were ^{27}Al, ^{140}Ce, ^{88}Sr, and ^{137}Ba.

Equation 1: $$CEF = \frac{1}{4}\left(\left(\frac{Ag_i/Ag_{crust}}{Al_i/Al_{crust}}\right)+\left(\frac{Ag_i/Ag_{crust}}{Ce_i/Ce_{crust}}\right)+\left(\frac{Ag_i/Ag_{crust}}{Sr_i/Sr_{crust}}\right)+\left(\frac{Ag_i/Ag_{crust}}{Ba_i/Ba_{crust}}\right)\right)$$

CEF = Crustal enrichment factor [unitless]

Ag_i = Concentration of Ag in sample i [ppt]

X_i = Concentration of element X in sample i [ppt]

X_{crust} = Average concentration of element X in the earth's crust [ppt].

Table 5 shows the values of X_{crust}, computed by Taylor (1995)

Hereafter, "seeding signatures" will refer to snow samples that meet the following three criteria. First, the Ag concentration must exceed the established background in the Payette Basin of one ppt. Second, the CEF factor must exceed 2, indicating Ag

concentrations double of expected concentrations relative to mean crustal averages. Third, Ag enhancements must correspond to some known AgI seeding event.

Seeding signatures from samples with Ag concentrations near background were resolved using the unitless CEF Factor. Ag enhancements due to AgI as low as 1 ppt above background were reliably identified using the CEF. *Figure 6* shows three Ag concentration profiles (dotted lines) where the highest Ag concentrations were located at the base of the storm snow layer. However, Ag enriched samples analyzed at the base of the storm layer contained a visible dust layer (*Figure 6*) and was not likely enriched in Ag by cloud seeding. The corresponding CEF (black lines) indicated the base of the snowpack was not enriched (CEF $\approx$ 1) while the upper half of the storm layer showed CEFs in excess of 4. This trend was seen elsewhere in the Payette Basin in the March 24 storm snow layer. The upper half of the snowpack from this storm resulted in high Ag enrichment factors at all 6 sites (*Figure 9*). Four sites contained high Ag concentrations ranging from 5 to 28 ppt with CEFs greater than 4. However, two sites only had Ag concentrations ranging from 2 to 4 ppt yet the location of the enriched layer in the snowpack corresponded to ground generator seeding times. Also, the minor Ag enrichment at these two sites still resulted in CEFs greater than 4. Because the CEF profile in *Figure 6* correspond to seeding times and produced similar CEF profiles as adjacent sampling sites in the Payette Basin (with Ag concentrations up to 28 ppt), the upper 4 cm in *Figure 6* appears to be affected by AgI. Therefore, the CEF equation may be an effective tool to delineate Ag concentration enhancements as low as 2 ppt.

3.3 Are the identification of Ag cloud seeding signals replicable over a small scale?

A small scale variability test was conducted for two reasons: (1) to validate our field and laboratory methods and (2) to determine how many snow pits were necessary to describe local seeding signature trends. This test was conducted by sampling 1-3 profiles from 8 snow pits within a 0.25 km^2 area (noted as site SM in *Figure 1*). Samples from two seeded storm events (March 24 and April 5) were collected on April 7, 2015 (at the locations shown in *Figure 7*). These two storms were delineated by noting snow stratigraphy and using a nearby high-resolution precipitation gage operated by Idaho Power Company. The snow accumulation rates at these locations differed significantly, so Ag signatures were present at different absolute depths within the profiles (*Table 3*). However, assuming a constant accumulation rate during each storm layer, normalizing each seeded storm snow layer to one depth revealed a consistent Ag signature in the profiles across the area.

The normalized Ag concentration profiles from the snow pits show similar trends. Depth-normalized snow pit showed nearly identical chemical profiles in the April 5th storm (sampled 36 hours following the storm). The March 24th storm layer (sampled 14 days following the storm) showed more variability (*Figure 8*). This may be due to differential melting rates between the 8 pits. The March 24th storm contained a thick ice crust at the top of the storm snow layer and had an average density of 0.34 g cm^{-3} at the SM site, indicating significant melt since deposition. Differences in accumulation due to wind effects could have also contributed to these differences in depth. These two processes resulted in a shallower snow depth for the outlier profile (denoted P5), which only had a total snow depth of 130 cm (*Table 3*). This pit contained 55 cm less snow than

the next lowest pit and had 32% less than the average total snow depth of the 8 pits measured at SM. The Ag seeding signatures at P5 in the upper snowpack of the April 5 and March 24 storm showed identical Ag concentrations and relative locations within the storm snow layer prior to being normalized, but were located at greater depths relative to the other seven snow pits after normalization. Normalizing depths at P5 was therefore unsuccessful due to excessive alteration of snowpack after deposition.

Based on these results, one snow pit was sufficient to identify a representative seeding signature on a small scale in these two storm situations. *Figure 9A* and *Figure 9D* show the average deviation (ε_d) associated with each depth after normalizing snow depths (omitting the outlier profile P5 for *Figure 9A*). The average Ag concentration deviation at a given depth is 1.9 ppt. However, ε_d was lower than 1.9 ppt in 71% of the depth intervals (n = 31). All samples with ε_d lower than the average were also not suspected of AgI enrichment.

Equation 2: $\varepsilon_d = \frac{1}{N}\sum_{i=1}^{N} \mu - x_i$

ε_d = average deviation at depth d [cm]

N = number of snow pits at site SM

i = snow sample number collected at site SM

μ = mean Ag concentration of 8 pits at normalized depth d [ppt]

x_i = Ag concentration at depth d [ppt]

Seeding signals were replicable at SM. This was observed both in snow that had been deposited 2 weeks prior to sampling and that had undergone extensive metamorphism and compaction, and was also observed in freshly deposited snow.

Therefore, one snow pit can identify a seeding signature amid this terrain and storm conditions and despite considerable snow compaction and metamorphism.

3.4 Can the distribution of seeding signals be reliably determined over a basin scale?

A ground generator and aircraft seeded event took place on March 24, 2015 during a two-day storm event (March 23-March 24). At 700 mb, wind speeds and temperature in the Payette Basin averaged 271 at 16 m s^{-1} and -10^0 C, respectively. Ground generators around the Payette Basin started at variable times on March 24 between 03:47 and 07:44 MST (*Table 4*). Based on SNOTEL sites within the basin, 50-66% of the snow-water equivalent from this two-day storm was deposited when the first ground generator was activated. Figure 10 shows one of those SNOTEL stations in the southern target zone. The highlighted regions denote AgI release times and the corresponding snowpack potentially enriched with AgI. These data suggest Ag seeding signatures could only be present in the upper half of this two-day snow storm layer.

Samples from the March 24 storm were collected at six widely separated sites (see *Figure 9*) in the Payette Basin (2,400 km^2) to determine if a seeded layer could be identified at every site. Profiles collected and analyzed from all six sites contained samples with CEFs exceeding 4, denoted by the square points on Figure 9. These enrichments were present in the upper half of every snow storm layer, in agreement with AgI seeding times.

Sites in the eastern Payette Basin had lower Ag concentrations than western sites. Ag enrichments between 1-3 ppt were found at the two eastern-most sites. CEFs were necessary to delineate AgI signatures at these downwind sites (*Figure 9D and 9E*). High CEFs (>2) were found in the upper half of each storm regardless of the Ag concentration

or terrestrial Ag contamination. These observations appear to demonstrate the documentation of a cloud seeding Ag signature within the snowpack across the basin. This suggests that the sampling and analysis method has the potential to constrain Ag enrichment, in both time and space, within the snowpack at the basin scale. However, it needs to be stressed that the results show that Ag from seeding reached the various sites in the basin, and do not help quantify the microphysical impacts of seeding.

Like other studies, Ag enrichments could be identified and replicated in snow several weeks old. *Figure 9A and 9B* were collected 14 and 16 days following the storm event, respectively. Snow densities were greater than 0.34 g cm^{-3} at all depths at both sites, suggesting considerable compaction. Ag signatures were reliably identified at both sites despite these conditions. However, these sites had the most variability between field replicates relative to samples collected within 48 hours, suggesting some degradation of the signal.

4. Conclusions

The purpose of this study was to demonstrate sampling and analysis methods to quantify trace Ag enhancements from cloud seeding using AgI as the nucleation agent. The effectiveness of the developed methods was evaluated in several ways. First, we verified that trace Ag enhancements can be detected using an ICP-MS housed outside of a trace metal clean room. Access to a Class 100 Clean Room for cleaning and sample preparation was essential to detect the 1-28 ppt Ag enhancements above background. Next, we evaluated the reproducibility of snowpack Ag profiles at various spatial scales. Reproducible profiles were evident over a 0.25 km^2 area and across the entire basin targeted for precipitation enhancement. The evidence of Ag from seeding was less

obvious at the furthest downwind sites but use of a CEF ratio suggested Ag enhancements as small as 1-3 ppt could have been present. These results suggest this approach may be suitable to evaluate cloud seeding efforts. These data can be used to validate model predictions of the spatial and temporal presence of AgI over cloud seeding target areas, provide field data to improve the model targeting, and provides a basis for direct quantification of cloud seeding impacts.

5. References

[1] DeMott P. 1995. "Quantitative Descriptions of Ice Formation Mechanisms of Silver Iodide-Type Aerosols." *Atmospheric Research*, no. 38: 63–99.

[2] Breed, D., Rasmussen, R., Weeks, C., Boe, B., and Deshler, T. 2014. "Evaluating Winter Orographic Cloud Seeding: Design of the Wyoming Weather Modification Pilot Project (WWMPP)." *Journal of Applied Meteorology* 53: 282–89.

[3] Manton, M., and Warren, L. 2011. A Confirmatory Snowfall Enhancement Project in the Snowy Mountains of Australia. Part II: Primary and Associated Analyses. *Journal of Applied Meteorology and Climatology* 50: 1448–1458.

[4] WWMPP. 2014. "The Wyoming Weather Modification Pilot Project: Level II Study. Executive Draft Summary."

[5] Super, A., and Heimbach, J. 1983. "Evaluation of the Bridger Range Winter Cloud Seeding Experiment Using Control Gauges." *Journal of Climate and Applied Meteorology* 22 (12): 1989–2011.

[6] Super, A. 1990. "Winter Orographic Cloud Seeding Status in the Intermountain West." *The Journal of Weather Modification* 22 (1): 106–16.

[7] NRC. 2003. *Critical Issues in Weather Modification Research*. National Research Council of the National Academies. Washington, D.C.: The National Academies Press.

[8] Warburton, J., and Young, L. 1968. “Neutron Activation Procedures for Silver Analysis in Precipitation.” *Journal of Applied Meteorology* 7: 433–43.

[9] Boutron, C. 1990. “A Clean Laboratory for Ultralow Concentration Heavy Metal Analysis.” *Fresenius Journal of Analytical Chemistry* 337 (5): 482–91.

[10] Warburton, J., Stone, R., and Marler, B. 1995a. “How the Transport and Dispersion of AgI Aerosols May Affect Detectability of Seeding Effects by Statistical-Methods.” *Journal of Applied Meteorology* 34 (9): 1929–41.

[11] Warburton, J., Young, L., and Stone, R. 1995b. “Assessment of Seeding Effects in the Snowpack Augmentation Programs: Ice Nucleation and Scavenging of Seeding Aerosols.” *Journal of Applied Meteorology* 34: 121–30.

[12] Huggins, A., Edwards, R., and McConnell, J. 2005. “Summary of Trace Chemical and Physical Measurements of Snowfall in Two Nevada Cloud Seeding Target Areas.” *Desert Research Institute (Reno, NV)*, 1–5.

[13] Chai, S., Finnegan, W., and Pitter, R. 1993. “An Interpretation of the Mechanism of Ice-Crystal Formation Operative in the Lake Almanor Cloud-Seeding Program.” *Journal of Applied Meteorology* 32: 1726–32.

[14] Warburton, J. Chai, S., Stone R., and Young, L. “The Assessment of Snowpack Enhancement by Silver Iodide Cloud-Seeding using the Physics and Chemistry of the Snowfall,” *J. Weather Modif.*, vol. 28, no. 1, pp. 19–28, 1996.

[15] Edwards, R., Huggins, A., and McConnell, J. 2004. “Trace Chemistry Evaluation of the IPCo 2003-3004 Cloud Seeding Program”. Desert Research Institute.

[16] Huggins, A., Kenyon, S., Warren, L., Peace, A., Billish, S., and Manton, M. 2008. “The Snowy Precipitation Enhancement Research Project: A Description and Preliminary Results.” *Journal of Weather Modification* 40: 28–53.

[17] Barbante, C., Cozzi, G., Capodaglio, G., Van De Velde, K., Ferrari, C., Boutron, C., and Cescon, P. 1999. “Trace Element Determination in Alpine Snow and Ice by Double Focusing Inductively Coupled Plasma Mass Spectrometry with Microconcentric Nebulization.” *Jounal of Analytical Atomic Spectrometry* 14: 1433–38.

[18] Barbante, C., Schwikowski, M., Doring, T., Gaggler, H. W., Schotterer, U., and Tobler, L. 2004. “Historical Record of European Emissions of Heavy Metals to the Atmosphere since the 1650s from Alpine Snow/Ice Cores Drilled near Monte Rosa.” *Environmental Science Technology* 34: 4085–90.

[19] Planchon, F., Boutron, C., Barbante, C., Cozzi, G., and Gaspari, V. 2001. “Ultrasensitive Determination of Heavy Metals at Teh Sub-Picogram per Gram Level in Ultraclean Antarctic Snow Samples by Inductively Coupled Plasma Sector Field Mass Spectrometry.” *Analytica Chimica Acta*, no. 450: 193–205.

[20] Hong, S, Barbante, C, Bourtron, C, Gabrielli, P, Gaspari, V, and Cescon, P. 2004. “Atmospheric Heavy Metals in Tropical South America during the Past 22,000 Years Recorded in a High Altitude Ice Core from Sajama, Bolivia.” *Journal of Environmental Monitoring* 6: 322–26.

[21] Krachler, M., Zheng, J., Fisher, D., and Shotyk, W. 2008. “Atmospheric Inputs of Ag and Tl to the Arctic: Comparison of High Resolution Snow Pit (AD 1994-2004) with a Firn (AD 1860-1996) and an Ice Core (previous 16,000 Yr).” *Science of the Total Environment*, no. 399: 78–89.

[22] Snyder-Conn, E., Garbarino, J., Hoffman, G., and Oelkers, A. 1997. “Soluble Trace Elements and Total Mercury in Arctic Alaskan Snow.” *Arctic* 50 (3): 201–15.

[23] Boutron, C. 1979. “Reduction of Contamination Problems in Sampling of Antarctic Snows for Trace Element Analysis.” *Analytica Chimica Acta* 106: 127–30.

[24] Rodushkin, I., Engstrom, E., and Baxter, D. 2010. “Sources of Contamination and Remedial Strategies in the Multi-Elemental Trace Analysis Laboratory.” *Anal Bioanal Chem*, no. 396: 365–77.

[25] Edwards, R., and Simeral, D. 2006. “Baseline Silver Concentrations in Freshwater and Snow in the Wyoming Weather Modification Project Target Area”. Desert Research Institute.

[26] Hong, S., Lluberas, A., and Rodriguez, F. 2000. “A Clean Protocol for Determining Ultralow Heavy Metal Concentrations: In Application to the Analysis of Pb, Cd, Cu, Zn, and Mn in Antarctic Snow”. Polar Research Center.

[27] Telliard, W. 2008. “Method 200.8: Determination of Trace Elements in Waters and Wastes by Inductively Coupled Plasma - Mass Spectrometry”. Environmental Protection Agency.

[28] Koffman, B., Handley, M., Osterberg, E., Wells, M., and Kreutz, K. 2014. “Dependence of Ice-Core Relative Trace Element Concentration on Acidification.” *Journal of Glaciology* 60 (219): 103–12.

CHAPTER TWO: AgI TARGETING ASSESSMENT OF GROUND-BASED AND AERIAL CLOUD SEEDING USING TRACE CHEMISTRY

1. Abstract

Glaciogenic cloud seeding is the practice of increasing wintertime precipitation through the addition of artificial ice nuclei. Silver iodide (AgI) is the artificial ice-nucleating agent commonly used for orographic clouds lacking optimal precipitation efficiencies. Recent estimates suggest successful glaciogenic cloud seeding programs increase precipitation between 3 and 15%. However, these estimates remain uncertain. Improper AgI targeting is regarded as the leading obstacle to achieving statistically significant precipitation enhancements in cloud seeding evaluations. To better understand AgI targeting, we (1) assess AgI targeting effectiveness spatially for ground and aerial-based seeding, (2) quantify temporal variability of AgI targeting using real-time snow collection methods, (3) determine the maximum spatial extent AgI signatures can be detected in snow, and (4) compute precipitation enhancements in storms with AgI signatures in snow (accurately targeted storms). We address these issues by analyzing more than 4,000 snow samples in two winter seasons. Snow samples were collected between 6 and 180 km downwind of AgI sources using both real-time and traditional snow pit methods. At sites within 70 km of AgI sources, we found silver enrichments in 93% of cases involving ground generators seeding but in only 11% of aircraft seeding cases. Real-time snow collection methods confirm seeding signatures in snow for the

duration of cloud seeding events. Sites sampled beyond 70 km of AgI sources (n=13) lacked detectable AgI signatures in snow. An analysis comparing modeled natural (unseeded) storms to observed revealed a 8.9% and 14% precipitation increase for storms lacking trace chemical data and storms with AgI signatures in snow, respectively. The methods of this study can be used to increase signal-to-noise ratios in precipitation enhancement methods and to evaluate existing cloud seeding model performances.

2. Introduction

Cloud seeding is a water management tool used to increase precipitation yield from a given storm. Glaciogenic cloud seeding enhances precipitation specifically for cold clouds by providing additional active ice nuclei, using silver iodide (AgI), within a super-cooled liquid water (SLW) layer lacking optimal concentrations of active ice nuclei. AgI is typically targeted at orographic clouds because they are short-lived and are relatively inefficient at producing ice. Seeding orographic clouds encourages storm development sooner as the cloud is lifted. Recent literature suggest seeding orographic clouds typically increases precipitation by 3-15% [14]. However, methodologies of determining apparent precipitation increases has been challenged by many. A literature review of cloud seeding efficacy by the Bureau of Reclamation pointed to the root of these concerns "*As of yet, no rigorous scientific study conducted as a randomized confirmatory seeding experiment with pre-defined primary response variables and requiring an established threshold of statistical significance has demonstrated that seeding winter orographic clouds increases snowfall*" [15].

Some in the weather modification community consider the principal obstacle to assessing cloud seeding efficacy to be AgI targeting [16], [17]. The National Research

Council stated "*The areas affected by cloud seeding remains an open question*" [18]. The clearest example of how AgI targeting uncertainties affect anticipated enrichments come from the Snowy Precipitation Enhancement Research Project (SPERP) project [19]. When all precipitation gauges from 107 randomized seeded events were analyzed *a priori*, target sites had 7% more precipitation at 24% level. However, this calculation assumed AgI targeting was 100% accurate. Filtering analysis of these gages to include events with at least 45 hours of seeding (*a posterior analysis*), ensuring winds delivered seeding agents to the gages dictated by the GUIDE model, and ensuring high Ag/In ratios in snow from trace chemistry (suggestive of active AgI nucleation), the precipitation enhancement estimation increased to 14% at the 3% significance level. Therefore, understanding where AgI goes after it is released, instead of assuming targeting is 100% accurate, has the potential to finally produce a statistically significant result for a randomized study.

Trace chemistry is an indispensable physical validation tool still used today to assess AgI targeting and supplement cloud seeding models. Two recent cloud seeding studies utilize trace chemical results to inform statistical models and parameterize weather model inputs [19], [20]. Precipitation enhancement estimates from these studies ranged between 3-15%, much lower than previous work void of physical data (10-25%). However, the conservative modeled enhancements are not surprising in light of recent trace chemical studies. Several trace chemical studies noted that only about 20% of samples collected in the target zone contain significant silver enrichments in snow[21]–[27] [15]–[17] [13], [18]–[20]. Recent models advanced our ability to predict when and where AgI are active [2], but there are still critical uncertainties in these models regarding

the timing of AgI activity and potential unintended downwind effects [20]. Trace chemical evaluations calibrate and validate these models, bringing the weather modification community one step closer to answering the ultimate question: how much extra snow do we get from cloud seeding.

It is clear that physical data are necessary to address a suite of questions not suitable with modeling and statistics alone. More specifically, the following three areas rely on trace chemistry and are currently among the highest areas of uncertainty: spatial availability of AgI, temporally constraining AgI, and downwind seeding effects.

2.1 Spatial availability of AgI

The spatial availability of AgI in snow is currently poorly constrained. Trace chemical analysis studies typically identify seeding signatures at unintended locations. Edwards identified silver concentrations at an assumed control site to be more than 50 parts per trillion (ppt), almost double that of average silver concentrations in the target zone [6]. Chai identified AgI seeded samples at control sites but not at target sites, suggesting control sites received AgI at the expense of target sites [4]. This resulted in a "negative" precipitation enhancement using classic statistical methods. In reality, this is a positive seeding enhancement at an unintended target. Trace chemical data correct these errors and help ensure AgI plumes are delivered in "*the appropriate cloud volumes at the times and in the concentrations prescribed by the seeding hypothesis over … large target areas*" [28].

2.2 Temporally constraining AgI

The timing of AgI deposition is another area of uncertainty and can be constrained using real-time snow sampling methods. To date, few studies utilized time-

sequential sampling methods [26], [27]. Without real-time snow sample collection, it is unknown precisely when AgI plumes enter and depart a given region. This type of sampling also reduces the possibility of terrestrial contamination and contamination from seeded snow redistributed from upwind sources [6], [19], [29]. Evidence from real-time snow sampling studies indicate that though an entire storm may be seeded, silver signatures tend to be present in only a fraction of the snowpack. Real-time snow sampling allows these AgI signatures to be constrained in the highest possible temporal resolution. These are useful data for model input parameters.

2.3 Spatial extent of seeding effects

Downwind seeding effects are a subject of scientific debate but currently a lack of field data make it difficult to substantiate claims. The argument that cloud seeding increases precipitation in one region and decreases precipitation downwind (the "robbing Peter to pay Paul" argument) is a commonly held public belief [30]. Several studies not only refute the rain shadow effect of cloud seeding, but also suggest precipitation increases extend up to 200 km downwind of the intended target [31]–[37]. Hunter listed dozens more studies that document precipitation increases 100 km or more downwind of the AgI sources [38]. However, many of these studies depended on statistical data with high signal-to-noise ratios. One study did incorporate trace chemical data at sites far downwind [39]. However, these data were collected prior to the acceptance of ultra-clean laboratory techniques and should be interpreted accordingly [40]. Therefore, weather modification studies are in dire need of additional field data regarding areas affected by cloud seeding.

2.4 Estimating precipitation increases using modeling

Two recent publications suggest this clouds seeding program effectively increases precipitation in the seeding basin of interest (Section 3). A Weather Research and Forecasting (WRF) model with a cloud seeding scheme showed precipitation enhancements of 5% and 20% for the Snake River Basin (Idaho) and local target sites, respectively [2]. More recently, Kunkel found precipitation increases of 12% with a double mass-balance analysis, and between 1.2 and 28% (depending on the seeding year) using the target-control regression analysis on high resolution precipitation gauges [41]. However, comparing modeled natural conditions to observed precipitation within the target zone is a method that warrants further investigation. Kunkel's method showed 20% seasonal increases for a single target precipitation gauge relative to a high-resolution Weather Research and Forecasting (WRF) [42] model output. Supplementing Kunkel's analysis with trace chemical data will allow us to compute the precipitation enhancement of a properly targeted storm.

2.5 Challenge statement

The primary objectives of this study are to (1) understand AgI targeting effectiveness spatially for aerial and ground-based seeding, (2) quantify temporal variability of AgI targeting using real-time snow collection methods, (3) determine the maximum distance from AgI sources that seeding signatures in snow exist, and (4) estimate precipitation enhancements comparing modeled natural conditions to observed seeded sites. We addressed these issues by analyzing more than 4,000 snow samples over the course of two winter seasons. Samples collection took place in the target zone and up to 180 km downwind of AgI sources using both real-time and traditional snow pit

methods. The methods described evaluate the overall targeting effectiveness of IPC's cloud seeding program and assess, for the first time, the maximum spatial extent of AgI enrichments in snow using ultra-clean methods. The results of this study both provide controlled observations that can inform cloud seeding operations and can be used to evaluate the performance of existing cloud seeding models.

3. Study area

Idaho Power Company (IPC) has been operationally cloud seeding this region since 2003. IPC specifically targets the Payette River Basin for precipitation enhancement, approximately 50 km NE of Boise, Idaho (Figure 11). This region has elevations ranging from 650 m to 3,110m and annual precipitation ranging from 300 mm to 1,700 mm. IPC seeds this region using remotely controlled ground generators and aircraft.

4. Methods

4.1 Field Sample Collection

Trace chemical analysis of snow provides robust evidence for cloud seeding targeting and effectiveness. One physical evaluation tool is trace chemical analysis of snow, also known as the source-receptor method. The precision and usage of this method increased dramatically in the 1990's, primarily because reliable clean room methods were refined and economically feasible for operational use. The source-receptor method is used to assess AgI plume targeting [4], [13], [43] linking microphysical changes of snow to AgI [21], [43], [44], and model validation [20].

The sampling method employed to understand AgI spatial variability is the 'snow pit method'. This method entails inserting 3-cm diameter 50 mL polypropylene vials

(FisherBrand, Pittsburg, PA, USA) orthogonal to the snow pit face. Two profiles were collected at each snow pit for replication purposes.

Timing and location were key to achieving replicable trace chemical data. Minimizing the time between the seeded storm and sample collection reduced photolytic effects on silver concentrations in snow [45],wind redistribution [3], snow compaction, and migration of trace elements through the snowpack [46]. Therefore, technicians collected samples within 48 hours of a seeded storm from remote, flat clearings that effectively shielded from wind, and were in a shaded area. Technicians strictly adhered to clean field techniques [47] throughout to reduce the potential for anthropogenic contamination.

To reduce contamination potential during real-time sampling, tasks were divided between two personnel based on equipment cleanliness. While one technician collected samples and only handled triple acid-washed equipment (“clean hands”), another technician measured relevant snow properties with less clean equipment (“dirty hands”) [48]. “Dirty hands” measured snow depth, snow temperature, and SWE at each time step 100 m downwind of 669 mL polypropylene containers (Figure 12). One drawback of this method is 100 m is beyond the correlation length of snow. Therefore, precipitation amounts and density measured by “dirty hands” are likely not identical to snow collected in the polypropylene containers upwind. However, this method is effective at mitigating contamination, and resulted in a seasonal average of 0.41 ppt Ag standard deviation between field replicates (n = 86 samples in 28 time intervals).

4.2 Measuring Timing of AgI in snowpack

The sampling method used to constrain timing of AgI signatures in snow was the 'real-time method'. Three triple-cleaned 669 mL polypropylene containers (Rubbermaid, Hoboken, NJ, USA) remained open until about 10 grams of snow collected (visually determined). Setting a minimum mass as the threshold driving sample frequency achieves the highest possible temporal resolution for trace chemistry. Real-time sample collection frequency typically ranged from 15 and 45 minutes, depending on precipitation intensity.

4.3 Laboratory Analysis

Samples were acidified as per the EPA Direct Analysis Method 200.8 [49]. This acidification method was chosen primarily because it has been the conventional method for analyzing precipitation and natural waters for decades. Samples are acidified to 2% HNO_3 (SeaStar Chemicals BASELINE®, Lot No. 1214070) and stored at room temperature to thaw. Once acidified, samples are stored in the dark for 24 hours within the Class 100 clean room and prior to analysis. Adopting this method allowed for direct comparison with other studies, because trace element concentrations are a strong function of acidification strength [50] and time stored at room temperature [12].

Samples are prepared in the clean lab prior to transport to the Thermo Scientific X-Series 2 Inductively Coupled – Plasma Mass Spectrometer (ICP-MS) laboratory (not a Class 100 clean room). After the 24 hour acidification period, samples were decanted from the 50 mL polypropylene field vials to the 15 mL Teflon vials in the clean lab (Savillex, Eden Prairie, MN, USA). Test vials were sealed with Parafilm, placed in a clean polyethylene rack, and sealed again in a clean polyethylene tub before being transported to the ICP-MS laboratory. The polyethylene sample rack was loaded directly

into the Elemental Scientific Inc. SC-FAST Automated Sample Introduction System, housed in an AirClean AC4000 Workstation. The AirClean Workstation substituted for a clean room environment.

The ICP-MS was calibrated using three serial dilutions of 1,000 mg/L (1,000 ppm) standards to analyze the following crustal tracers: Na, Al, Cr, Co, Sr, Ba, La, Ce, and Pb. Ag was calibrated using serial dilutions of 1,000 ppm to concentrations to 100 parts per trillion (ppt), 50 ppt, 10 ppt, and 1 ppt. The Ag calibration linear regression lines were re-calibrated a minimum of 3 times per analysis to address drift. Drift was further mitigated by analyzing a 10 ppb indium internal standard throughout the analysis. Blank (2% HNO_3) rinses followed each calibration to reduce memory effects from 100 ppt and 1,000 ppt standards. Blanks are also analyzed every 10 samples to ensure instrument precision. Standard operating conditions for the ICP-MS are listed in Table 2.

4.4 Distinguishing AgI signature from background silver concentrations

The primary objective of this study was to better understand AgI plume targeting within the Payette Basin using trace chemical analysis in snow. One shortcoming of this method is that a high silver concentration does not always indicate proper targeting because high silver concentrations in snow can come from several other sources [51]. However, silver concentrations near natural, background concentrations is evidence of poor targeting or inactive AgI over the region [26]. Additionally, one can speculate the source of silver using enrichment factors [6].

A crustal enrichment factor was used in this study to filter out the most common source of naturally occurring silver in snow: aluminosilciate dust. The crustal enrichment factor (CEF) was designed to highlight samples with high silver concentrations

irrespective of elements commonly found in terrestrial dust using a normalizing approach. (Equation 1). All elements in Equation 1 are normalized to the mean concentration of the upper crust [52] as listed in Table 5. CEF values greater than two indicate silver concentrations are primarily sourced outside of aluminosilicate dust. CEF values close to one mean all of the silver from a given sample was likely derived from dust.

Two criteria must be met for a sample to have a "seeding signature". First, a sample must have a silver concentration two standard deviations above the mean concentration that naturally occurs in snow (μ=1 ppt, σ = 1 ppt) [53]. Second, a sample must have a CEF greater than two to indicate significant Ag enrichments beyond the Ag concentration that would be expected from dust in snow.

$$Equation\ 1:\ CEF = \text{median}\left(\frac{Ag_i/Ag_{crust}}{Al_i/Al_{crust}}, \frac{Ag_i/Ag_{crust}}{Ce_i/Ce_{crust}}, \frac{Ag_i/Ag_{crust}}{Sr_i/Sr_{crust}}, \frac{Ag_i/Ag_{crust}}{Ba_i/Ba_{crust}} \right)$$

CEF = Crustal Enrichment Factor [unitless]

Agi = Concentration of Ag in sample i [ppt]

Xi = Concentration of element X in sample i [ppt]

Xcrust = Average concentration of element X in the earth's crust [ppt].

4.5 Modeling Timing of AgI in snowpack

We developed a simple empirical model to convert snow depth to the time snow was deposited. Total precipitation in the field was obtained using a 200 cm^3 box density

cutter. Density measurements were recorded at 3 cm intervals in the snow profile. We took density measurements adjacent to column profiles in the snow pit.

$$Equation\ 2: p_i^* = \frac{P_s}{P_f} p_i$$

p_i* = Normalized hourly precipitation increments vector at the SNOTEL site [cm]

P_s = Total precipitation from seeding event measured at SNOTEL station [cm]

P_f = Total precipitation from seeding event measured at snow pit [cm]

p_i = Array of SWE from 3-cm depth density measurements in the field [cm]

Equation 2 normalizes SWE measurements taken adjacent to chemistry samples for direct comparison with a nearby SNOw TELemetry (SNOTEL) precipitation gauge (assuming the ratio of precipitation at the SNOTEL site and sampling site are constant). This approach creates an opportunity to relate SWE measurements in the snow pit to the timing of deposition metrics recorded by SNOTEL. We modeled the approximate time of snow deposition using 1st, 2nd, and 3rd degree polynomials (Figure 13, plot B); chosen on the basis of the most realistic trends and relatively low R^2 values.

Next, we converted snow depth recorded in the sampled pit to time of deposition. We first equated p_i* to depth in the snow profile. Using the time (MST) – p_i relationships at the proximal SNOTEL station, we were able to relate snow depth to time of deposition in the snow pit using a second degree polynomial (13, plot A-C). For this study, we found this method useful only when we collected snow within 48 hours of deposition.

4.6 Downwind spatial extent of seeding effects

It is still unknown the distance downwind of AgI sources that seeding signals are present in snow. To better constrain the furthest distance AgI can be detected in snow, we performed two sampling campaigns (13 sites total) with at least one site >80 km downwind of AgI sources. The first campaign consisted of four sites with the February 18 2016 ground generator storm event. These sites were collected at various distances from the nearest AgI source (13, 16, 19, and 86 km) and all parallel to the mean wind direction of at least one ground generator. The second transect consisted of nine sites roughly orthogonal to the mean wind direction and 180 km from the seeding source. We sampled nine to maximize the chances of seeing a seeding signal and to test whether the seeding signal is continuous.

Hobbs noted changes in microphysical characteristics of snowflakes present on the lee (east) side of the Cascade Range [54], [55] but not on the windward side. Snowflakes on the lee side were smaller, not rimed, and contained higher silver concentrations on the Cascade's lee side. In order to account for such differences in local scale seeding signals, we sampled three aspects of the Lost River Range (LRR): the windward slope, ridge, and lee side of the range. We hypothesize the strongest AgI signals are on the lee side of the LRR.

4.7 Precipitation enhancement estimates with trace chemical data

One of the difficulties of comparing point data (SNOTEL stations) to grid data (WRF-GFS model outputs) is the grid's spatial aggregation can average out point-scale observations [56]). Studies that directly compare SNOTEL points to grid points find SNOTEL precipitation can be higher by a factor of two or more [12], [13] in

mountainous terrain. Moreover, SNOTEL stations are not positioned on the basis of representivity, and actually tend to be positioned in locations higher than local surrounding. This means that SNOTEL stations tend to receive more precipitation than the surrounding area [57]. This study was no exception. Raw point-to-grid comparisons differed up to a factor of two (Figure 14). Most of this can be attributed to spatial aggregation. Spatial aggregation affects environmental variables such as aspect, wind speed, and elevation [15], [16]. But other localized mechanisms can cause precipitation measurement uncertainties as high as 30% such as bridging, under-catch, wind scour, snow capping, change in surrounding landscape, and deposition of foreign material [14].

The benefit of a WRF to SNOTEL comparison is the ability to incorporate more control SNOTEL stations (not just sites climatologically similar to target sites). There are 216 sites in this WRF domain[3], 156 are likely unaffected by cloud seeding (Figure 15). The increased sample size will make the statistics more robust.

In an effort to compare grid points to SNOTEL stations directly, I used a normalizing approach on WRF model outputs to daily precipitation. The relative enrichment between the target SNOTEL sites and control sites are computed below.

$$Equation\ 3: \quad C = \frac{P_{mar31_{obs}} - P_{nov01_{obs}}}{P_{mar31_{mod}} - P_{nov01_{mod}}}$$

C = Coefficient normalizing observed precipitation at SNOTEL stations to WRF models.

P_{mar31_obs}-P_{nov1_obs} = Cumulative precipitation at a SNOTEL site from Nov01-Mar31

P_{mar31_mod}-P_{nov1_mod} = Cumulative precipitation simulated by WRF from Nov01-Mar31

[3] NW corner: 46.2229 -120.0689, SE corner: 40.9928 -109.5833

$$Equation\ 4: \quad \Delta = \frac{1}{P_{mar31\_mod} - P_{nov01\_mod}} \sum_{i=1}^{n=nSEED} (C * P_{i\_obs}) - P_{i\_mod}$$

Δ = difference between normalized SNOTEL and the precipitation gauge

P_{mar31_mod}-P_{nov1_mod} = Cumulative precipitation simulated by WRF from Nov01-Mar31

C = Coefficient used to normalize observed precipitation at SNOTEL stations to WRF models.

P_{i_obs} = Observed daily precipitation for a seeded storm

P_{i_mod} = Modeled daily precipitation for a seeded storm (simulates natural conditions)

nSEED = Number of seeded storms between Nov01-Mar31.

$$Equation\ 5: \quad E = \left(\left(\frac{1}{t_{sites}} \sum_{i=1}^{n=t_{sites}} \Delta \right) - \left(\frac{1}{c_{sites}} \sum_{i=1}^{n=c_{sites}} \Delta \right) \right)$$

t_sites = number of target sites

c_sites = number of control sites

Δ = percent difference between normalized SNOTEL and the precipitation gauge

This method has several advantages. First, this method encourages inclusion of every non-seeded SNOTEL sites in in the WRF domain. This will result in more robust statistics because we are not forced to subset our data to climatologically similar sites. Second, this method analyzes precipitation enhancements on a per-storm basis. Therefore, we are able to quantitatively compare the effectiveness of both AgI release methods (ground generator and aircraft). Third, incorporating trace chemistry into seeded storms ensures we are computing enrichments of properly targeted AgI seeding events.

5. Results

The three primary objectives of this study were to: (1) understand where AgI enriched snow deposition occurs in central Idaho during both ground-based and airborne seeding methods, (2) constrain the temporal duration of AgI signatures, and (3) determine the spatial extent of AgI signatures in snow from seeding sources and (4) compute the precipitation enhancement of well-targeted seeding events.

5.1 Spatial availability of AgI

To determine where AgI enriched snow occurred in Central Idaho (Figure 11), we sampled no fewer than three snow pits, each with two profiles. Our results indicate Ag signals were consistent at every site. All snow pits either possessed a signal, or all did not. A consistent Ag enrichment signal existed up to 60 km downwind of the seeding source (aka "the target zone"). Our data indicate that silver enrichments within the target zone tend to be widespread and replicable (Figure 16).

To establish if seeding method impacted the presence of silver enrichments, seeding events were separated into three categories: ground generator only, aircraft only, and mixed (ground generator and aircraft seeding events). Ag enrichments were found in 90%, 11%, and 100% of sites seeded by ground generators only, aircraft only, and mixed events (Table 6). These results suggest AgI released from aircraft may not be seeding intended sites in the target zone.

5.2 Temporally constraining AgI

In order to constrain the timing and duration Ag enriched snow deposition in the target zone, four storms were analyzed using time-sequential (aka "real-time") sample collection methods (Figure 17). We observed that only 20-75% of the time during ground

generator seeding events do we detect Ag enrichments (Table 7). Based on these observations, static seeding mechanisms may not be the primary precipitation mechanism for half the duration of the storm on average.

For the purpose of constraining the temporal duration of Ag enriched snow using the column method, we constructed a basic empirical model relating snow depth to the time of deposition. Two outcomes were realized. First, when at least three sites are sampled, the AgI plume can be modeled through time and space (Figure 118). The plume in Figure 8 was computed using linear regression of all starting and ending points of modeled Ag enrichment times. Ag signals are constrained from 03:58 – 0740 MST 4.8 km downwind of ground generators but 09:23 – 14:03 MST 38.5 km downwind of ground generators. This does suggest the head of the plume would be moving only 1.8 m s^{-1} while surface winds averaged 16 m s^{-1} that day. These results suggest diffusion is not negligible because trend lines at 38.5 km are 26% than 4.8 km. Second, the model is quite effective at constraining time. The model used only the nearest SNOTEL data and density measurements as inputs. Temporal errors, when compared to observed real-time data were less than an hour (Figure 19). This simple model may temporally constrain Ag enrichments within a given storm event, reducing the need for real-time sampling.

5.3 Downwind seeding effects

We tested for the approximate maximum spatial extent from AgI sources that silver enrichments could be detected downwind in snow. We performed a nine-site sampling transect 180 km downwind of seeding sources. Of the 678 total samples collected in this transect, only 9 samples exceeded 5 ppt. Of those 9 samples, 8 were located in the southern Lost River Range and were deposited during the February 18

ground generator seeded storm event. The other three storm events combined did not contain a single sample containing 5 ppt Ag and an enrichment of at least 2. This observation suggests ground generators have the potential to seed downwind, but aircraft generally do not.

5.4 Statistical analysis

From lowest to highest, precipitation enhancements from each seeding method are aircraft (0.8-7.8%), ground generators (5.9-15.3%), and seeding events with validated an AgI signatures in snow (9.9-33.5%). For the WRF-GFS to SNOTEL comparison, cumulative precipitation curves at target sites were significantly different from control sites at the 1% significance level[4]. Table 8 shows summarizes precipitation enhancements by category. Uncertainty bounds are computed by standard deviations of 200 Monte Carlo simulations, sub-setting 70% of storms for equations 3, 4, and 5.

Precipitation enhancements from SNOTEL sites relative to normalized WRF-NAM (1.8 km resolution) were 69% lower than WRF-GFS enhancements (1.8 km resolution). Precipitation enhancements of each seeding method for the two model outputs were correlated ($R^2 = 0.84$), so the rankings of seeding methods are the same for both models.

6. Discussion

6.1 Spatial availability of AgI

One surprising outcome of this study is that we found AgI in snow for most ground generator seeding events (90%) and rarely for aircraft-only seeding events (11%).

---

[4] using the two-sample Kolmogorov-Smirnov test

We expected to find high concentrations (or pulses) of silver within the snowpack because aircraft burn AgI at a much faster rate relative to ground generators. Each of Idaho Power Company's burn-in-place flares releases 16.2 g of AgI over the course of 3-5 minutes. Aircraft ejectables release 2.2 g AgI. Conversely, ground generators burn 23 g of AgI per hour. When all 30 ground generators in southern Idaho are active, AgI release rates are about 60 g per 5 minutes, almost four times that of aircraft release rates. This is likely the reason aircraft seeding signals were not detectable in snow. The mass of silver released from aircraft were too trace to detect above natural background concentrations. Another potential reason is the efficacy of aircraft seeding is more sensitive to antecedent drop size and ice nucleus concentrations than ground generators [17], it is also possible that ice nuclei concentrations prior to seeding (from dust or pollution) preferentially impeded efficient aircraft seeding.

Our AgI targeting comparison between aircraft and ground generators yielded similar results as a study in the Tahoe Truckee Basin [39]. Warburton's study showed similar silver concentrations at aerial seeded target sites as control sites, suggesting aerial releases of AgI are too trace to detect. Conversely, ground generator events contained relatively higher silver concentrations, often exceeding 20 ppt. Conversely, aircraft-only events only recovered roughly 15% of AgI in snow in the three events, on average.

Our analysis demonstrates that AgI ground generator targeting is observed to at least 60 km of AgI sources. Our data also confirm that AgI signatures are replicable within the basin [47] and silver enrichments are present at all sampled sites in the target zone following a seeding event. We believe that it is highly likely that the observed elevated silver concentrations reflect a seeding signal. It is possible that silver sources

could come from anthropogenic contamination during sampling or analysis, terrestrial contamination, and/or scavenging of AgI. However, we consider these silver enrichments from alternative sources unlikely for several reasons. First, a minimum of two field replicates and three lab replicates were analyzed for each site, these samples did not exhibit evidence of anthropogenic contamination. Second, enrichment factors were employed to account for potential terrestrial contamination; all identified silver signals represent silver concentrations that are high while concentrations of elements that would reflect terrestrial contamination are not. Third, AgI has an extraordinarily low scavenging efficiency [4], [26], [58] so high concentrations of silver (> 3 ppt) are unlikely to result from scavenging alone. Therefore, it is likely that AgI plumes were delivered to the targeted clouds at the desired concentrations and times for optimal nucleation activity.

6.2 Temporally constraining AgI

Our study shows that real-time sampling is an effective method at revealing not only if, but also when, silver enrichments occur. We demonstrated the effectiveness of this method by, for the first time ever, performing field-validation tests. Two previous studies performed real-time sampling [26], [27] but lacked the field replication or method validation testing to corroborate results. This study, however, provided no less than 3 field replicates for each time interval. The season-long standard deviation for each time interval was 0.41 ppt Ag, only 0.02 ppt above our Inductively Coupled Plasma Mass Spectrometer limit of detection. The results from these real-time samples further validate expected results from cloud seeding and also represent a highly constrained (space and time) target for model validation.

Real-time snow collection agreed with activation times of ground generators upwind. We found silver enrichments at all three seeded events. Two events captured the head or tail of the AgI plume. Real-time samples identified silver enrichments within 30 minutes of the plume entering or leaving the region. The 30-minute lag of signals to AgI release corresponds with travel times of the head of the plume from the AgI source to the real-time sampling site. Conversely, real-time samples collected during a natural storm event (unseeded) yielded silver concentrations less than 1 ppt for all 15 samples. This agrees with background silver concentrations previously measured for Payette Basin snow [6], [53]

6.3 Downwind seeding effects

Our study shows that the maximum spatial extent of AgI signatures from ground generators is about 80 km downwind of AgI sources. This is similar to the findings of the only other known downwind trace chemical study [39]. Warburton's research also found background Ag concentrations in snow at downwind sites. However, these were obtained prior to known clean methods, so results should be interpreted cautiously. Although our results agree with Warburton's study [39],it conflicts with prior statistical studies. Hunter lists 26 studies implying AgI seeding increases precipitation beyond 80 km, suggesting the potential for AgI signatures [38]. The only study to test downwind seeding signals was performed in 1971. This is slightly less than estimates from the 26 studies suggesting AgI impacts 100 km or more beyond AgI sources. Aircraft-only events did not yield enrichments within or beyond the target zone.

A variety of factors may explain the lack of physical evidence for AgI seeding downwind. First, photolytic deactivation renders AgI ineffective after a prolonged

exposure to light. Prior studies estimate photolytic deactivation occurs about 90 minutes [59] [45] after release. Assuming 45 km h-1 winds at the super-cooled liquid water level and seeding took place during daylight hours, this would allow for detectable signatures only 45 – 70 km downwind. Second, the deposition of AgI in the target zone, fused with the dispersion of the remaining AgI downwind will likely dilute the available aerosols downwind [60]. This may reduce the AgI signal to near background levels. Lastly, sampling snow more than 48 hours after a storm poses several challenges. Compaction of the snow results in a potential dilution of seeding signal. A column sample may include seeded and unseeded snow. Diffusion of AgI signals throughout the snowpack further lowers the AgI signal. If a signal did exist at great distances from its source, there are several atmospheric and hydrologic processes that will reduce the Ag signal in the snow pit.

In summary, there is limited evidence of downwind seeding effects. Based on these data, the source-receptor approach is not an effective method at detecting targeting of AgI plumes (if they exist). The signal-to-noise appears to be too low to detect these subtle differences.

6.4 Statistical analysis

This calculation shows significantly higher precipitation increases for seeding events with AgI signatures in snow relative to seeding events void of trace chemical validation. If targeting were 100%, we would expect a precipitation enhancements void of trace chemistry to approximate enhancements of storms with AgI signatures in snow. This suggests that AgI may contaminate control sites and/or AgI miss target sites.

Seeded storms with AgI suggest precipitation enhancements in excess of 30%. The 33.5% increase is about twice as much as recent cloud seeding evaluations in the Payette Basin. However, this is not the first time a 30%+ seeding signal in literature when computing enhancements on a *storm-by-storm* basis. For instance, Super found in the Bridger-Range experiment seeded storms with cold ridge temperatures (between -9°C and -13°C) frequently showed 50% increases in precipitation relative to control sites [61]. The result of these calculations collaborate with the trace element chemistry results, aircraft seeding is less effective than ground generator seeding. Aircraft seeding tended to lack significant seeding signals in the snow and have about half the precipitation enhancements of ground generator events.

7. Conclusions

Silver signatures tend to be widespread and replicable within the target zone using trace element chemistry. In almost all instances, silver enrichments were identified and replicated for all sites seeded by a ground generator event. Sampling of aircraft seeding events, conversely, did not reveal physical evidence in snowpack. Only 13 % of seeded snow deposits contained a seeding signature. This is likely due to the fact that the mass of AgI released from aircraft are too trace to detect above natural background concentrations.

We developed and validated a field method for collecting real-time samples of snow suitable for trace element analysis. This method resulted in a seasonal-average replicate standard deviation of 0.41 ppt. Real-time sampling, along with time-reconstructed column sampling, constrained AgI signals within the nearest hour.

Limited evidence of AgI enrichments were found in the Lost River Range, 180 km downwind of AgI sources. Factors limiting Ag detection may have been high wet and dry deposition rates in the target zone, photolytic deactivation, snow compaction, migration of Ag signatures within the snowpack, and limited AgI activity in the target zone (targeting the right cloud, at the right concentration, at the right time).

Comparing SNOTEL to normalized WRF-GFS calculations showed a 10-34% precipitation enhancement for seeded storms with targeting validated by trace chemistry, 6-16% increase for ground generator events, and an 1-8% increase in aircraft seeding events. This suggests targeting is not 100% accurate. Using WRF-NAM models predicted enhancements systematically 69% less than WRF-GFS.

8. Acknowledgements

I would like to thank Matt Masarik, Katelyn Watson, and Miguel Aguayo for sharing useful scripts to analyze WRF data. I would also like to thank Reggie Walters for sharing scripts to automate downloading SNOTEL data. Finally, I would like to thank Rob Florence, Andy Karlson, Clay Roehner, Kerrie Weppner, and Larry Thomas Oltheim ("TomO") for assisting me in sample collection, especially during obscure working hours.

9. References

[1] Breed, D., Rasmussen, R., Weeks, C., Boe, B., and Deshler, T., "Evaluating winter orographic cloud seeding: design of the Wyoming Weather Modification Pilot Project (WWMPP)," *J. Appl. Meteorol.*, vol. 53, pp. 282–289, 2014.

[2] Reynolds, D. W., "Literature review and scientific synthesis on the efficacy of winter orographic cloud seeding," CIRES, Boulder, CO, A report to the U.S. Bureau of Reclamation, 2015.

[3] Silverman, N. L. and Maneta, M. P., “Detectability of change in winter precipitation within mountian landscapes: spatial patterns and uncertainty,” *Water Resour. Res.*, vol. 52, pp. 4301–4320, 2016.

[4] A. Zipori, D. Rosenfeld, J. Shpund, D. M. Steinberg, and Y. Erel, “Targeting and impacts of AgI cloud seeding based on rain chemical composition and cloud top phase characterization,” *Atmospheric Res.*, vol. 114, pp. 119–130, Oct. 2012.

[5] Rasmussen, R. *et al.*, “How well are we measuring snow? The NOAA/FAA/NCAR winter precipitation test bed,” *Bull. Am. Meteorol. Soc.*, vol. 93, pp. 811–829, 2012.

[6] Super, A. B. and Heimbach, J. A., “Feasibility of snowpack enhancement from Colorado winter mountain clouds: emphasis on supercooled liquid water and seeding with silver iodide and propane,” Bureau of Reclaimation, Technical Services Center, Denver, CO, Final Report., 2005.

[7] Reynolds, D. W., “A report on winter snowpack-augmentation,” *Bull. Am. Meteorol. Soc.*, vol. 69, pp. 1435–1456, 1988.

[8] NRC, *Critical Issues in Weather Modification Research*. Washington, D.C.: The National Academies Press, 2003.

[9] Manton, M., Warren, L., Kenyon, S., Peace, A., Bilish, S., and Kemsley, K., “A Confirmatory Snowfall Enhancement Project in the Snowy Mountains of Australia. Part I: Project Design and Response Variables,” *J. Appl. Meteorol. Climatol.*, vol. 50, pp. 1432–1447, 2011.

[10] Chai, S. K., Finnegan, W. G., and Pitter, R. L., “An Interpretation of the Mechanism of Ice-Crystal Formation Operative in the Lake Almanor Cloud-Seeding Program,” *J. Appl. Meteorol.*, vol. 32, pp. 1726–1732, 1993.

[11] McGurty, B., “Turning Silver into Gold: Measuring the Benefits of Cloud Seeding,” *Hydro Rev.*, vol. 18, no. 1, pp. 1–5, 1999.

[12] Warburton, J., Young, L., and Stone, R., “Assessment of seeding effects in the snowpack augmentation programs: ice nucleation and scavenging of seeding aerosols,” *J. Appl. Meteorol.*, vol. 34, pp. 121–130, 1995.

[13] A. B. Super and B. A. Boe, “Microphysical Effects of Wintertime Cloud Seeding with Silver Iodide over the Rocky Mountains. Part III: Observations over the Grand Mesa, Colorado,” *J. Appl. Meteorol.*, vol. 27, no. 10, pp. 1166–1182, Oct. 1988.

[14] Huggins, Arlen W., “Summary of studies that document the effectiveness of cloud seeding for snowfall augmentation,” *J. Weather Modif.*, vol. 41, pp. 127–134, 2009.

[15] WWMPP, “The Wyoming Weather Modification Pilot Project: Level II Study. Executive Draft Summary.” 2014.

[16] Reynolds, D. W., Humphries, J. H., and Stone, R. H., “Evaluation of a 2-month cooperative ground based silver iodide seeding program,” *J. Weather Modif.*, vol. 21, pp. 14–28, 1989.

[17] Long, A. B., “Physical investigations of winter orographic clouds in Utah.,” Desert Research Institute, Reno, NV, Final Report., 1984.

[18] Super, A. B., Woodley, W. L., and McPartland, J. T., “Silver-in-snow evaluation of cloud seeding effectiveness for snwo pack enhancement in Colorado during the 2002/03 season.,” Denver, CO, Final report from Woodley Weather Consultants to the Denver Water Board, 2003.

[19] WMA, “Weather Modification Association (WMA) Position Statement on the Environmental Impact of Using Silver Iodide as a Cloud Seeding Agent,” 2009.

[20] J. Warburton, R. Stone, and B. Marler, “How the Transport and Dispersion of AgI Aerosols May Affect Detectability of Seeding Effects by Statistical-Methods,” *J. Appl. Meteorol.*, vol. 34, no. 9, pp. 1929–1941, Sep. 1995.

[21] Huggins, Arlen W., “Trace Chemical Monitoring for the Wyoming Weather Modification Pilot Project: Tasks for the 2010 Field Project.” Desert Research Institute, 2010.

[22] Xue, L. *et al.*, “Implementation of a Silver Iodide Cloud-Seeding Parameterization in WRF. Part II: 3D Simulations of Actual Seeding Events and

Sensitivity Tests," *J. Appl. Meteorol. Climatol.*, vol. 52, no. 6, pp. 1458–1476, Jun. 2013.

[23] Mielke, P. W., Brier, G. W., Grant, L. O., Mulvey, G. J., and Rozenweig, P. N., "A statistical reanalysis of the replicated Climax I and II wintertime orographic cloud seeding experiments.," *J. Appl. Meteorol.*, vol. 20, pp. 643–659, 1981.

[24] Manton, Michael J. and Warren, Loredana, "A contirmatory snowfall enhancement project in the Snowy Mountains of Australia. Part II: primary and associated analyses," *J. Appl. Meteorol. Climatol.*, vol. 50, pp. 1448–1458, 2011.

[25] Edwards, R., Huggins, A., and McConnell, J., "Trace Chemistry Evaluation of the IPCo 2003-3004 Cloud Seeding Program." Desert Research Institute, 2004.

[26] World Meteorological Organization, "Policty statement on the status of weather modification," *J. Weather Modif.*, vol. 25, pp. 1–6, 1993.

[27] Edwards, R. and Simeral, D., "Baseline Silver Concentrations in Freshwater and Snow in the Wyoming Weather Modification Project Target Area." Desert Research Institute, 2006.

[28] Long, Alexis B., "Review of Downwind Extra-Area Effects of Precipitation Enhancement," *J. Weather Modif.*, vol. 33, no. 1, pp. 24–45, 2001.

[29] Dennis, Arnett S., *Weather Modification by Cloud Seeding*, vol. 24, 25 vols. New York: Academic Press, 1980.

[30] Griffith, D. A., Solak, M. E., and Yorty, D. P., "30 + seasons of operational cloud seeding in Utah," *J. Weather Modif.*, vol. 41, pp. 23–37, 2009.

[31] Grant. L. O., Chappell, C. F., and Mielke, P. W., "The Climax experiment for seeding cold orographic clouds," presented at the Proceedings of International Conference on Weather Modification, Canberra, Australia, 1971, pp. 78–84.

[32] Brown, K. J., Elliont, R. D., and Thompson, J. R., "Seeding convective bands in winter storms and the observed large scale effects.," presented at the Papers presented at teh Second WMO Scientific Conference on Weather Modication., Geneva, Switzerland, 1976, vol. WMO-No. 443., pp. 465–472.

[33] Solak, Mark E., Yorty, David P., and Griffith, Don A., “Estimations of Downwind Cloud Seeding Effects in Utah,” *J. Weather Modif.*, vol. 35, no. 1, pp. 52–58, 2003.

[34] Wise, E. A., “Precipitation evaluation of the North Dakota Cloud Modification Project (NDCMP),” Thesis, University of North Dakota, Grand Forks, ND, 2005.

[35] Griffith, D. A., Solak, M. E., Almy, R., D., and Gibbs, D., “The Santa Barbara Cloud Seeding Project in Southern California, summary of results and their implications,” *J. Weather Modif.*, vol. 37, pp. 21–27, 2005.

[36] DeFelice, T.P *et al.*, “Extra area effects of cloud seeding - An updated assessment,” *Atmospheric Res.*, vol. 135–136, pp. 193–203, 2014.

[37] Hunter, S., “Comprehensive literature survey on teh potential extra-area precipitation effects of winter cloud seeding,” Denver, CO, Final Report submitted to teh Colorado Water Conservation Board, 2009.

[38] Warburton, J. A., “Physical evidence of transport of cloud-seeding materials into areas outside primary targets.,” presented at the Proceedings of International Conference on Weather Modification, Canberra, Australia, 1971, pp. 185–190.

[39] Boutron, C., “A clean laboratory for ultralow concentration heavy metal analysis,” *Fresenius J. Anal. Chem.*, vol. 337, no. 5, pp. 482–491, 1990.

[40] Super, Arlin B. and McPartland, Jack T., “Field Observations of the Persistence of AgI-NH4I-Acetone Ice Nuclei in Daylight,” *J. Appl. Meteorol.*, vol. 14, no. 12, pp. 1572–1577, 1975.

[41] Huggins, A., Edwards, R., and McConnell, J., “Summary of Trace Chemical and Physical Measurements of Snowfall in Two Nevada Cloud Seeding Target Areas,” *Desert Res. Inst. Reno NV*, pp. 1–5, 2005.

[42] Johannessen, M. and Henriksen, A., “Chemistry of Snow Meltwater: Changes in Concentration During Melting,” *Water Resour. Res.*, vol. 14, no. 4, pp. 615–619, 1978.

[43] Fisher, James F., Benner, Shawn G., and Marion Lytle, “Trace chemical evaluation of cloud seeding in the Payette Basin,” Denver, CO, 2015.

[44] Snyder-Conn, E., Garbarino, J., Hoffman, G., and Oelkers, A., “Soluble Trace Elements and Total Mercury in Arctic Alaskan Snow,” *Arctic*, vol. 50, no. 3, pp. 201–215, 1997.

[45] Telliard, W., “Method 200.8: Determination of Trace Elements in Waters and Wastes by Inductively Coupled Plasma - Mass Spectrometry.” Environmental Protection Agency, 2008.

[46] Koffman, B., Handley, M., Osterberg, E., Wells, M., and Kreutz, K., “Dependence of ice-core relative trace element concentration on acidification,” *J. Glaciol.*, vol. 60, no. 219, pp. 103–112, 2014.

[47] Wen, L., Santschi, P. H., Gill, G. A., and Tang, D., “Silver Concentrations in Colorado, USA, Watersheds using Improved Methodology,” *Environ. Toxicol. Chem.*, vol. 21, no. 10, pp. 2040–2051, 2002.

[48] Taylor, Stuart R. and Scott M. McLennan, “The geochemical evolution of the continental crust,” *Rev. Geophys.*, vol. 33, pp. 241–265, 1995.

[49] Hobbs, P.V., “The nature of winter clouds and precipitation in the Cascade Mountains and their modification by artificial seeding. Part I: Natural conditions,” *J. Appl. Meteorol.*, vol. 14, pp. 783–804, 1975.

[50] Hobbs, P.V., “: The nature of winter clouds and precipitation in the Cascade Mountains and their modification by artificial seeding. Part III: Case studies of the effects of seeding,” *J. Appl. Meteorol.*, vol. 14, pp. 819–858, 1975.

[51] Griffith, Don A. and Solak, Mark E., “Economic Feasibility Assessment of Winter Cloud Seeding in the Boise River Drainage, Idaho,” *J. Weather Modif.*, vol. 34, pp. 39–46, Apr. 2002.

[52] Deshler, T. and Reynolds, D. W., “the persistence of seeding effects in a winter orographic cloud seeded with silver iodide burned in acetone,” *J. Appl. Meteorol.*, vol. 29, pp. 477–488, 1990.

[53] Cardno ENTRIX, “Geochemistry and Impacts of Silver Iodide Use in Cloud Seeding.” 2011.

[54] U. S. Senate, “Weather modification: Programs, problems, policy, and potential,” in *Committee on Commerce - Science and Transportation*, Washington, D.C., 1978, pp. 1–645.

CHAPTER THREE: SILVER TOXICITY

I Executive Summary

Silver is a rare metal present at concentrations averaging 50 parts per billion by mass (ppb) in the upper continental crust, 100-1,000 ppb in soil, and 0.002-0.03 ppb in freshwater environments. Localities exceeding these silver concentrations tend to be a result of anthropogenic releases, with exceptionally high sources from photographic industries, urban refuse combustion, and sewage treatment. Silver toxicity varies widely amongst different organisms and silver speciation. Many gilled aquatic organisms are highly sensitive to the free silver ion (Ag+).

Water quality parameters present in the environment such as Cl^-, Ca^+, pH, particulates/colloids, dissolved organic carbon (DOC), and sulfur-bearing species impact the equilibrium concentration of the silver ion and its biological uptake. Equilibrium concentrations of the silver ion are extremely difficult to measure in the aquatic environment. Numerical models have been used to estimate concentrations in place of real-time measurements. Equilibrium concentrations of the silver ion are highly dependent on aquatic chemistry and the presence of suspended solids such as colloids.

The free silver ion (Ag^+) is extremely toxic in aquatic environments. The most sensitive species that experience lethal effects (LC_{50}-96 hr) in waters amended with the free silver ion are the following: fathead minnows (5.3 ppb), juvenile rainbow trout (4.8 ppb), daphnids (5.0 ppb), and amphipods (1.9 ppb). Juvenile fish tend to experience toxic effects at lower concentrations than their adult counterpart. Free silver ion concentrations

are fungicidal and bactericidal at 10 ppb. Algae have bioconcentration factors up to 2.1 x 10^6. Some species of algae experience a unique toxic response to both forms of dissolved silver, the free ion and complexed state. However, there is no evidence of a direct correlation between the amount of accumulated silver within an organism and toxicity.

The free silver ion is much less toxic to humans and terrestrial species relative to species in aquatic environments. Humans can ingest 10 grams of total recoverable silver in a lifetime without experiencing toxic effects or precursors to toxic effects. In excess of 10 grams the risk of developing argyria, a grey discoloration of the skin, increases. Data are sparse on silver ion toxicity to terrestrial animals; most studies examine the effects of the less toxic, insoluble silver species. The most sensitive mammal to the free silver ion found were rats. Rats given water amended with soluble silver experienced sluggishness at 95 ppb after 125 days. Germinating plants experience toxic effects from the free silver ion at 750 ppb. Adult plants have a higher resilience to silver. Toxic silver concentrations in plants range from 14,000-120,000 ppb in soils amended with insoluble silver.

Water quality standards vary at the global, country, and local scales. Aquatic environment guidelines range from 0.05 ppb of the free silver ion and up to 3.4 ppb of total recoverable silver. The EPA and state governments typically assess silver toxicity as a function of hardness. Critical assessments of EPA standards highlight more impactful variables on silver toxicity, such as DOC and chloride. The New South Wales (Australia) EPA set toxicity guidelines as a function of the free silver ion. There is little variability in drinking water standards. Standards set by the World Health Organization, EPA, and most state governments are fixed at 100 ppb of total recoverable silver.

Silver iodide (AgI) is an insoluble salt used in cloud seeding. AgI is present at trace concentrations in seeded snow and adjacent waterbodies (0.001 – 0.05 ppb) and does not dissociate readily in water (K_{sp} = 9.2 x 10^{-9} M). As a worst case scenario, a solution of 0.984 ppb of the free silver ion would result if it were in equilibrium with an infinite amount of AgI, with unlimited time to react, assuming Ag^{+} does not sorb/precipitate/complex. This concentration is below every U.S. silver toxicity guideline. AgI primarily accumulates in the upper soil horizon or streambed sediments in solid form. Bioavailability depends on the bonding of the soluble silver fraction to the sediments and organics present. Environmental assessments of cloud seeding operations have found no detectable increase in total silver concentrations above background levels in soil, streams, or aquatic species in seeded areas. Likewise, there is currently no evidence supporting adverse effects to wildlife in natural settings. In fact, free silver ion concentrations are at least one order of magnitude lower than LC_{50}-96hr concentrations (acute toxicity) to known sensitive freshwater species even using these worst case scenario assumptions: 100% of the snowpack is seeded with AgI, all snow has 0.05 ppb silver, 100% of the AgI dissolves, and the dissolved fraction does not bind to any water constituents (100% of dissolved silver concentrations are the free silver ion).

1. Silver as an Element

1.1 Sources

The relative contributions of anthropogenic releases of silver to the environment are listed below in Table 9. These data were collected and analyzed in 1978, where an estimated 2.5 million kg of silver was released in the environment [1]. Distributions may have changed slightly since 1978 because it became economically viable for industries to

recover trace amounts of silver and environmental regulations have become more stringent. Also, silver usage from the photography industry has decreased sharply since 1978 [2].

Table 9 shows most of the silver released due to anthropogenic practices. Silver in the natural environment is primarily found in sulfide minerals, typically in conjunction with lead, copper, iron, and gold. These sulfides are generally insoluble [1].

Silver sulfides are locally concentrated in ores. Many ore deposits in the Western United States are hydrothermal in origin. These ore deposits yield relatively high amounts of the following common silver minerals: argentite (Ag_2S), horn silver (AgCl), and stephanite (Ag_5S_4Sb) [3]. Outside of these locally concentrated ores, however, silver is present at trace amounts at shallow terrestrial depths. The upper continental crust (mostly sedimentary rocks) and bulk continental crust are generally 0.05 ppm and 0.08 ppm respectively [4].

1.2 Typical Concentrations in the Environment

1.2.1 Crustal Abundances and Occurrences

The upper continental crust (mostly sedimentary rocks) and bulk continental crust are generally 0.05 ppm and 0.08 ppm respectively [4]. However, much higher, naturally occurring, silver concentrations are found in crustal material, especially in mineral ore bodies. Silver is often found in ore deposits associated with sulfide minerals, typically in conjunction with lead, copper, iron, and gold. Silver is also concentrated in some soils [5].

1.2.2 Soils

Silver concentrations in soils typically range between 0.1 to 1 ppm [6]. Organic soils soils usually range from 2 – 5 ppm [7]. Polluted soils (e.g. from excessive dry deposition or sewage sludge) are known to be several times higher than these ranges [7]. Note that these typical soil concentrations are at least one order of magnitude greater than the bulk continental crust., Silver is delivered to soils by wet and dry deposition of atmospheric silver and released from *in-situ* minerals by weathering. Soil serves as a large environmental sink of silver because silver is strongly associated with the solid phase and generally immobile [2].

1.2.3 Water

Silver is typically present in waters at very low concentrations, making it difficult to quantify using standard water analysis techniques. For this reason, silver concentrations in water measured prior to the 1990's should be interpreted with caution because levels of instrumental detection were often not sufficiently precise and sample collection did not commonly follow clean, ultra-trace techniques [8]. More recent studies utilizing ultra-trace techniques have found that common freshwater Ag concentrations are most commonly between 1 ppt and 30 ppt using unfiltered, total recoverable methods [3][9]. Concentrations in excess of 50 ppt are not uncommon in turbid environments. For instance, 0.05 grams of soil with 1 ppm Ag concentration suspended in a one liter water sample would result in a 50 ppt silver concentration (if unfiltered, and total recoverable methods are employed). Riverine and entrained sediments commonly contain 0.2-1.7 ppm silver (same range as the shallow soil horizon) [3]. Hence, an important control of silver concentrations in aquatic systems is the amount of suspended sediment.

Because the turbidity of water has a large impact on the total recoverable silver in a water sample, selecting a proper filter size prior to chemical analysis is paramount. One study found passing river water samples through a 0.45 µm and 0.1 µm filter reduced silver concentrations by roughly 60% and 70% respectively in comparison to direct analysis methods [10]. Colloidal silver is primarily in the 0.25-0.40 µm size range [11]. In other words, the sample passing through 0.45 µm filters does not account for the significant colloidal fraction of the water sample. Since there is uncertainty around what size filters result in "dissolved" silver, the filter size used on water samples should be disclosed in order to interpret reported silver concentrations in aqueous systems.

1.2.4 Air

Eisler reported on typical values of atmospheric loads of silver in the environment [1]. Typical dust Ag concentrations were reported between 0.012-10.5 ng/m^3 in natural environments [1]. Since the average male breathes roughly 20 m^3 per day, about 0.2 µg of silver enters the lungs per day. Air samples taken right next to a smelter in Idaho resulted in dust concentrations as high as 36.5 ng/m^3 [1]. This is still considerably below acceptable standards set for the workplace. The Occupational Health and Safety Administration (OSHA) airborne limit for silver is 0.01 mg/m^3 based on an 8-hour work shift and 40-hour work weeks [12].

1.2.5 Riparian Sediments

Riparian sediments tend to be the same order of magnitude as silver concentrations in soil. Concentrations of these suspended particulates/sediments have been measured to average around 0.2 – 1.7 ppm [3].

1.2.6 Snow

Silver concentrations in snow in the Western United States typically have silver concentrations between 2-4 ppt [13][14][15][16] with a standard deviation of 1-2 ppt [13]. In Idaho, the mean concentration of background concentrations of silver is around 1 ppt based on results from the 1996 (Richard Stone IPC Report), 2004 [6], and 2015 [17] [18][19]. Background Ag concentrations in Wyoming have been measured up to 15 ppt using clean techniques [3]. Snow samples containing more than 20 ppt were most likely caused by AgI or human contamination. For studies prior to 1990, contamination during collection or analysis likely limits validity.

1.3 Chemical Characteristics

1.3.1 Speciation

Silver mobility and toxicity are strongly influenced by chemical speciation and solid-aqueous partitioning. The most commonly occurring forms of Ag are reactive and tend to easily create bonds with other species in solution (complexes), with other elements to form mineral phases, and to reactive surfaces (adsorption).

1.3.2 Chemical Speciation

The silver element has four possible ionic states: 0, 1^+, 2^+, and 3^+, and 20 radioisotopes [20]. However, the most common oxidation state in the natural environment is either uncharged (Ag^0) or the monovalent silver ion (Ag^+, also known as the argentous ion) [1]. Silver is also available in 20 radioisotopes but none occur naturally in the environment [20]. Speciation strongly controls silver toxicity (*described*

below); the free, non-complexed, silver ion (Ag^{+}) is by far the most toxic species [1][20][21]. Hereafter, the monovalent silver ion will be referred to as the "silver ion.[5]"

1.3.3 Complexation and Adsorption

The silver ion (Ag+) has a strong affinity to create aqueous complexes and bind to adsorption sites. Aqueous complexes are dissolved compounds that are typically composed of an anion and a cation. The anion ligand, or adsorption site to which silver will bind to, depends on the environment in which silver resides; Ag behaves differently in oxidizing and reducing environments. Examples of oxic environments include rainwater and snow, rivers, and lakes. The most common species the silver ion bonds to in oxic environments involve chloride (Cl^{-}) and dissolved organic carbon (DOC). In addition to the $AgCl_{(aq)}$ complex and $AgCl_{(s)}$ solid phase, silver can also form similar compounds with bromide and iodide [20]. Examples of reducing (or anoxic) environments are swamps, peat, and deep groundwater reservoirs. Reduced silver sulfur (sulfide) species (either as a solid or complexed) and the dissolved silver concentrations can be higher in these environments [1].

Silver speciation can also change when exposed to light. Many silver salts, such as AgCl and AgBr, photolytically decompose when exposed to ultraviolet light. In this reaction, the Ag+ is reduced to Ag^{0} and the anion is released to the solution. This technology is harnessed in photography but is a hindrance for chemical analysis of water samples, as this reaction causes an under-estimate of the total recoverable silver

[5] In literature, this is called the argentous ion, free silver, free silver ion, or the monovalent silver ion. For simplicity, the toxic Ag^{+} ion will be called the silver ion in this paper (not to be confused with dissolved silver, which contains the free silver ion, complexed dissolved silver, and in some cases colloids).

concentration (mass spectrometers measure concentrations based on mass/charge ratios). Photolytic reduction is partially suppressed if samples are treated with nitric acid [22].

1.3.4 Ag mineral solubility

Silver forms more insoluble mineral phases (often referred to as ‘salts’ when artificially made) than any other trace metal [22]. Silver nitrate ($AgNO_3$) is the only silver mineral phase considered soluble, and will precipitate out as other compounds in aqueous solutions containing common constituents like Cl^-, PO_4^-, and dissolved oxygen. The solubility product (K_{sp}), expressed in terms of molarity of some of the most common silver salts, are listed in Table 10. The maximum dissolved silver concentrations provided in Table 10 assumes the silver species had an unlimited amount of time to react (estimated for calculations, not observed in the environment) and does not re-precipitate with other species in solution. However, these concentrations do not specify what dissolved species will result (toxic or non-toxic), under what conditions the maximum amount of salt dissolves.

1.3.5 Implications for Assessing Silver Concentrations

The strong bonding tendency of silver influences how observed silver concentrations are collected and assessed. Natural waters generally contain both dissolved and suspended fractions. Because silver tends to be associated with the solid phase, a bulk water sample analysis will produce silver concentrations that are dominated by the solid phase fraction. To determine the dissolved fraction the sample must be filtered prior to analysis. The filter size traditionally used is 0.45 µm. However, this size allows small, colloidal sized, particles to pass through into the sample to be analyzed, which will result in exaggerated dissolved Ag concentrations. Therefore, a 0.1 µm filter

must be employed to eliminate silver associated with small solid particles and colloids. In some instances, it is of value to use unfiltered samples; this provides a silver concentration inclusive of the suspended and dissolved phase (total recoverable) fractions.

A second practical consideration is the influence of complex formation. It is important to note that the total dissolved concentration of Ag is not equal to the concentration of the most toxic free silver ion (Ag^+) [23]. In laboratory environments where the highly soluble silver nitrate is used, free silver (Ag^+) concentrations can be quite high. However, these laboratory conditions produce silver ion concentrations not commonly observed in natural environments. In natural environments, dissolved silver is mostly complexed into a much less toxic form, such as a silver-chloride or silver-thiosulfate complex [24]. To determine the 'free' silver ion concentration in solution, geochemical modeling (using programs like MINTEQ+) have been used [21]. Of course, input data for this assessment should be produced with filtered samples.

In practice, the dissolved silver ion concentration will generally be below 0.2 ppb, but this is highly dependent on the environmental conditions [25]. All else equal, dissolved silver ion concentrations will be higher under conditions of lower anion concentrations, lower levels of reactive sulfides and/or sulfur, lower amounts of suspended sediments, lower pH, and lower dissolved organic carbon [2].

1.4 Fate of Silver in the Environment

Silver distribution and transport is dominated by sorption/precipitation processes in freshwater systems (both groundwater and surface water) [20]. Dissolved and colloidal

silver will tend to adsorb to particulates or form insoluble mineral phases and partition into the soils or sediment fraction.

Because gases and sub-micron sized particles can travel thousands of kilometers from their source, the primary source of trace metals in many remote environments (such as ice sheets, lakes, and peat) is from atmospheric transport [26]. Silver, like many trace metals, is largely immobilized in the soil column by either precipitating into an insoluble salt, reacting to form complex molecules, or adsorbing on reactive surfaces associated with organic matter, clays, and manganese and iron oxides in the soil [20].

Industrial wastewaters, from photographic industries for example, first complex their potentially toxic silver into silver into silver thiosulfate. Next, silver is converted into one of the most insoluble silver salts; silver sulfide. Silver that is not economically recoverable can be mixed with sewage sludges and amended to agricultural soils. Approximately 80,000 kg of silver was amended in agricultural soils in 1978 [1]. Silver sulfides do not adversely affect crops at the concentrations found in amended soils (*Section 2.3.3*) nor does it increase the likelihood of toxic forms of silver bioaccumulating in species consuming these crops (*Section 2.3.2*).

2. Silver Toxicity

2.1 Silver Toxicity in Aquatic Environments

2.1.1 Overview: Bioavailability

There are several water quality parameters that dictate the toxicity of the silver ion; the most impactful being dissolved organic carbon (DOC) and chloride in freshwater systems. The subsequent subsections will highlight factors inhibiting a linear

relationship between the silver ion and toxicity. These subsections are largely a summary of Williams (2009) [2] and Eisler (1996) [1].

Recent studies assessing silver toxicity do not focus on total recoverable silver because there is not a direct correlation to toxicity (Figure 20). The Biotic Ligand Model was developed for this reason. In order to determine the potential toxicity to a species, the Biotic Ligand Model estimates the proportions of silver species between dissolved and solid, what fractions of dissolved Ag are complexed[6], and what fraction will be present as the toxic silver ion. This model does have limitations in assessing silver toxicity. First, it is primarily suited for gilled fish. Second, it does not account for the ameliorating effects of sulfide, a known parameter to reduce silver toxicity 24].

Recent studies have shown the silver ion complexed with DOC may be toxic [27]. Additions of DOC always results in higher total recoverable silver concentrations (reducing bioavilability to aquatic life). However, recent geochemical modeling studies suggest silver complexed with DOC may be toxic, but at least several times less toxic than the silver ion.

2.1.2 Overview: Toxicity

The toxicity of silver depends on many factors. This includes, but is not limited to the species and form of silver, the environment in which silver is present (atmosphere, soil, or water body), and if aqueous, the chemical characteristics of the water.

Silver forms insoluble salts with several other species, including arsenate, arsenite, bromide, chloride, iodide, carbonate, chromate, cyanide, iodate, oxalate, oxide,

[6] A complex has an ion at the center (commonly a metal ion) bonded to one or more ligands. Complexes can be of any charge, including neutral, and tend to exude both dissolved and solid behaviors in solution.

phosphate, sulfate, sulfide, tartrate, and thiocyanide, in aqueous media alone [22]. The free silver ion is therefore not as abundant in natural environments as once thought.

The silver ion is extremely toxic, but solid or complexed forms of silver are much less toxic. For example, AgCl, Ag_2S, and $Ag_2O_3S_2$ are 300, 15,000, and 17,500 times less toxic than the silver ion respectively [1].

2.1.3 Dissolved Organic Carbon (DOC)

The World Health Organization states DOC has the highest protective effects of any other water quality parameter on silver toxicity [20]. Erickson's 1998 study showed how important dissolved organic carbon (DOC) was on controlling silver toxicity. This study compared lab water and water from the St. Louis River with similar Cl, sulfur-containing species, and was void of visible suspended sediment. Erickson stated the major difference between lab water and St. Louis River water was the concentration of DOC. The results showed fish (*Daphnia Magna*) in the St. Louis River water had LC_{50} values 60 times higher than in lab water. In other words, controlling for all of the other water quality parameters, *Daphnia Manga* were able to withstand Ag concentrations 60 times more concentrated by using water more representative of environmental conditions. Wood (1999) demonstrated that DOC complexes may be toxic to both fathead minnows and rainbow trout, but noted total recoverable silver LC_{50} values were raised the most (reducing toxicity) with increases in DOC [24].

DOC concentrations change significantly in the watershed through time. Boyer (2000) showed DOC spikes in streams 2-4 weeks prior to peak streamflow in a Rocky Mountain catchment in Colorado [28]. DOC concentrations quadrupled relative the rest of the year because shallow groundwater interacted with the upper-most soil horizon

during this time. The longer residence times of water ("quickflow" snowmelt) has in the upper vadose zone, the more time organic carbon has to dissolve and later be discharged in the stream [28]. It should be noted that DOC concentrations are very complex and these trends do not apply to every watershed.

2.1.4 Influence of Chloride Ion (Cl^-)

Adding the same amount of dissolved silver to freshwater environments is more toxic than when added to saltwater environments. First, there are more cations (namely, Na^+) to compete for organic ligand binding sites in saltwater, preventing the silver ion from interfering with osmoregulatory processes or bioaccumulation. Second, saltwater ameliorates silver ion toxicity effects by forming silver-chloro complexes and precipitates (only in brackish waters are Cl^- concentrations high enough to precipitate AgCl) [1]. Studies have shown Cl^- to have stronger ameliorating effects compared to hardness by binding to the silver ion to form silver-chloro complexes. Silver-chloro complexes commonly formed are $AgCl_2^-$, $AgCl_3^{2-}$, and $AgCl_4^{3-}$ [2]. In fact, one study modeled the ratio of the toxic silver ion to the total recoverable silver reducing from 100% to about 8% with an addition of 5 $^o/_{oo}$ (parts per thousand) Cl^- [29].

High concentration spikes of the silver ion can still be toxic to fish in brackish environments. Strangely, this is true even when the silver ion concentrations are negligible in brackish waters (i.e. nearly all the silver is in some silver-chloro complex). However, the mechanism causing toxicity in salt-water species differs. In fish for instance, higher silver ion spikes will result in increased Na^+ and Cl^- concentrations in the blood plasma under waters of high salinity (as opposed to reduced Na^+ and Cl^- in plasma

in freshwater species). In this case, dehydration is the ultimate cause of death of the fish in saltier conditions. In contrast, death in freshwater is more likely to be suffocation [20].

2.1.5 Influence of Sulfides and Sulfates

Silver forms the strongest complexes with sulfides in reducing environments. Silver has the highest affinity thiols[7], however, these are not common in natural environments. Silver thiosulfate ($Ag_2O_3S_2$) tends to only be the dominant species in industrial wastewater effluents [1]. In the United States, silver concentrations in these effluents are generally in decline as recovery of silver in these waste products are becoming more economically viable and efficient [20].

WHO (2002) found that in environments not anthropogenically altered, silver sulfhydrate (AgHS) or simple sulfur polymer species (HS-Ag-S-Ag-SH) dominate. At higher concentrations, colloidal silver sulfide or silver polysulfide complexes dominate [20]. Under reducing conditions, the silver ion is sometimes released from the sulfur bearing species. Because concentrations of the silver ion are typically extremely low in natural environments relative to the available binding sites of sulfur, the silver ions are quickly combined with other sulfur complexes. Both scenarios result in essentially non-toxic forms of silver [20].

2.1.6 Influence of Hardness

Hardness is also a significant control on Ag toxicity. However, it is not the largest control on toxicity as once thought [30]. Below are the data used to create the Environmental Protection Agency (EPA) Ag toxicity equation as a function of hardness,

[7] Thiols have similar molecular structures and chemical makeup as alcohols (hence the suffix “ol”). The main difference is the sulfur in thiols take the place of hydrogen in alcohols. Thiols give gasoline its characteristic odor.

re-evaluated by Hogstrand (1996) [29]. Clearly, chloride ion concentrations have a much higher correlation on Ag toxicity than hardness, yet the EPA standard was based on the data in the right plot in Figure 21.

While there does remain a correlation between toxicity and water hardness, it is not as impactful as DOC, Cl^-, or sulfates. In fact, Erickson (1998) found that over the range of hardness values between 50 ppm and 250 ppm, Ag toxicity was only reduced by a factor of 2.5 [32]. This same trend was affirmed by several other publications [2][30]. EPA assesses toxicity of total recoverable silver concentrations as a function of hardness. Critical assessments regarding the toxicity of silver in relation to hardness (*Section 3.1*) interpret the EPA silver toxicity relationship to be over-protective and under-protective at lower and higher hardness values respectively [2]. In other words, low buffering capacity of lab waters (low ionic strength) over-estimate the toxicity of silver when applied to natural environments. Conversely, the increasing hardness will not buffer the silver ion toxicity as much as previously thought.

The mechanism by which hardness decreases toxicity is identical to that of DOC and sulfate. Cations (mainly calcium) compete with toxic silver ions at the binding sites of fish gills [32].

2.1.7 Colloids and Larger Particulates

Most available silver is adsorbed to the particulate fraction in stream networks. The fraction of silver adsorbed in the particulate increases as a function of turbidity. One recent study estimated 33-89% of total recoverable silver was present on a particulate phase (anything that could not pass through a 0.1 µm filter) [10] whereas some studies have shown 98% of total recoverable silver bound to particulates [2]. The high affinity of

silver to sediments is most clearly seen in the nearly 6-orders of magnitude reduction of silver concentration in sediments and river water. River water samples rarely exceed 30 ppt of silver (when passed through a 0.45 µm filter) while river sediments typically range between 200,000 ppt and 1,700,000 ppt [10].

2.1.8 pH

Generally, as pH decreases, silver toxicity increases. One study showed silver toxicity decreasing by a factor of 3 when increasing the pH from 7.17 to 8.58 when testing juvenile fathead minnows [32]. However, increasing concentrations of humic acid[8] have been shown to decrease silver toxicity [2]. The two competing effects tend to result in a net bioavailability reduction with increased pH.

The precise mechanism of how pH influences silver toxicity is less obvious and more research is needed in this area [32]. Decreasing pH would increase the competition of H^+ ions and the silver ion at gill sites; reducing toxicity. Increasing pH within realistic environmental ranges are not sufficient to result in significant silver speciation with the hydroxide ion. On the other hand, decreasing pH releases the adsorbed silver in soils or particulates, increasing the amount of dissolved silver and making the silver ion more bioavailable. These observations may suggest that the two effects cancel out and result in a net decrease in toxicity with increased pH.

2.2 Toxicity to Aquatic Species

2.2.1 Overview: Early Research

The validity of results from prior to the 1990's may have been compromised by a number of factors [7]. First, the importance of ultra-clean lab methods is not globally

[8] Humic acid is produced from decomposition of organics, often abundant in soils.

recognized. Thus, samples containing extremely low silver concentrations were reported with higher values either because of anthropogenic contamination in the field or lab, or because samples were at or below instrument detection limits. Second, laboratory conditions did not realistically simulate the natural environment. Laboratory water was often used instead of natural waters for aquatic toxicity tests [32]. Laboratory waters often lack natural concentrations of DOC, sulfides, H^+, trace metals, and suspended sediments. Many studies did not report these other water quality metrics, making their applicability to standards questionable [32]. Likewise, the most bioavailable form of silver was used in laboratory procedures instead of silver compounds common in the environment. For instance, silver nitrate ($AgNO_3$) was used in many studies. This is by far the most soluble silver compound and can produce environmentally irrelevant silver ion concentrations (especially when laboratory waters lack natural toxicity buffers) [29]. $AgNO_3$ is rarely found in the natural environment. Recent research is focused on more common silver species in the environment, such as silver salts formed with bromide, iodide, and chloride, which are much less soluble and produce lower free Ag ion concentrations [1].

Much of the historical (pre-clean techniques), as well as recent studies, were plotted in Figure 22 in the 2002 WHO literature review [20]. The lethal concentrations vary by 2 orders of magnitude or more when replicating toxicity tests. This is likely a product of not normalizing for the toxicity buffers and lack of clean techniques.

2.2.2 Toxicity to Fish

The silver ion is especially toxic to fish because Ag^+ disrupts the gas exchanges and acid-base regulatory functions. This inhibited ability to maintain a state of

homeostasis can result in a number of fatal consequences as seen in Figure 23 [29]. Fortunately, mitigating silver toxicity in fish is reversible because it is mostly caused from water interaction at the gill surface. Additions of ameliorating factors in water lower the concentration of the silver ion and immediately restore the ability for fish to osmoregulate normally [1]. Frogs respond differently to lethal concentrations of the silver ion. Silver concentrations (primarily as silver nitrate) in excess of 10 ppb interfered with frogs' calcium metabolism [1].

Importantly, the reason silver is toxic is not because of accumulations in internal organs, but because of the disruptive gas exchanges at the gill surfaces of fish and respiratory processes of other aquatic species. This was verified in several studies. Wood (1996) compared 10 ppb silver nitrate solution (yielding relatively high amounts of the silver ion) and 30,000 ppb of silver thiosulfate (negligible silver ion concentrations). The silver thiosulfate solution caused accumulations in the plasma and internal organs to be more than 3 times greater than the rainbow trout in the silver nitrate solution. The rainbow trout exposed to the silver thiosulfate solution did not experience any of the osmoregulatory stresses while the rainbow trout in the silver nitrate solution experienced lethal effects, despite silver nitrate additions resulted in total recoverable silver concentrations 3,000 times less than the silver thiosulfate group. Bioaccumulation factors of silver in the blood plasma were higher in the fish exposed to silver thiosulfate, but only the fish exposed to silver nitrates experienced toxic effects [33].

There are several fish species that are especially sensitive to silver nitrate toxicity tests. Four of the most sensitive are fathead minnows (5.3 ppb Ag), speckled dace (4.9 ppb Ag), mottled sculpin (5.3 ppb Ag), and rainbow trout (4.8 and 10.2 ppb Ag for

juvenile and adult fish respectively). All metrics for toxicity were 96-hour LC_{50} tests [20]. These values and values reported in subsequent toxicity sections cannot be compared directly because lab waters spiked with silver nitrate have differing amounts of hardness, pH, DOC, salinity, and alkalinity. Therefore, it is difficult to determine the single most sensitive species.

Juvenile fish are the most sensitive to the silver ion (Ag^+). Developing trout and phytoplankton experience adverse toxic effects at concentrations as low as 170 ppt. Lowest Observed Effect Concentrations (tests usually 60 days) for larvae and embryos have been measured as low as 100 ppt of the silver ion; experiencing stunted growth [20].

2.2.3 Microorganisms and Invertebrates

Ionic silver is fungicidal, algicidal, and bactericidal at concentrations as low as 10 ppb [2]. The silver ion is still occasionally used as an antibiotic today. The most sensitive microorganism (besides algae) is the protozoan (8.8 ppb Ag). This test used silver nitrate as well but the test was a 24 hour LC_{50} test.

The most sensitive invertebrate species studies were mayflies (6.8 ppb Ag), daphnids (5 ppb Ag), and amphipods (1.9 ppb Ag). All of the following were 96 hour LC_{50} tests using silver nitrate as the environmental stressor [20].

Hirsch (1998) investigated how extremely high total recoverable silver concentrations would affect perhaps the most sensitive invertebrate, the amphipod. These amphipods were subjected to Ag concentrations of 753 ppm Ag in natural stream sediments using Ag_2S (one of the most insoluble silver salts). The study showed no adverse effects over the 10 day period even though amphipods burrow in these sediments [34]. This reinforces the necessity of quantifying toxic species of silver and not just total

recoverable silver. Field data alone does not adequately address toxicity. To fully address toxicity, field data should be input data into a model estimating silver speciation. The precise mechanism causing silver toxicity should be interpreted based on these speciation values.

2.2.4 Algae and Clams

There are two ways silver can accumulate in high, and potentially toxic, concentrations within a species relative to the surrounding environment. The first is bioconcentration, where uptake, adsorption or absorption rate of a toxic species is higher than the excretion rate. The bioconcentration factor is the ratio of concentrations of the chemical species within an organism to the surrounding environment. The second is biomagnification, where silver is accumulated from an organism's diet. The sum of bioconcentration and biomagnifications is called bioaccumulation [23].

Bioaccumulation factors are highest in algae and clams of all other studied freshwater species, especially algae. Marine and freshwater algae accumulate Ag from adsorption rather than uptake, so bioaccumulation factors as high as 66,000 have been recorded [1]. Lee (2005) suggested some types of algae accumulate via intracellular accumulation, meaning even silver-chloro complexes could be toxic [35]. Other marine species with notably high bioaccumulation rates are diatoms (210), brown algae (240), mussels (330), scallops (2,300), and oysters (18,700). Freshwater species studies have much lower bioconcentration factors than marine organisms, ranging from negligible (in bluegills) to 60 (in daphnids) [1].

Green algae have bioconcentration factors as high as 2.5×10^6, the highest recorded of any other algae in published literature reviews. However, bioconcentration

factors are rarely this high in nature. This is because bioconcentration factors are again correlated most to the toxic silver ion [23].

Another toxicity concern was raised if the algae with high bioaccumulations were consumed by higher order species in the food chain. This effect has not been witnessed in literature either [23]. However, the silver absorbed to the algae remains in the absorbed (virtually non-toxic) state even when pH is reduced to 2, when the cell walls of the algae break down, and when digestive enzymes react with algae [23]. Therefore, biomagnification to other species is unlikely.

Some forms of algae showed signs of acute toxicity at silver ion concentrations as low as 0.3 – 0.6 ppb, and caused blue-green algal mats to disappear from an experimental ecosystem at Ag concentrations between 2- 7 ppb [20].

2.3 Terrestrial Species

2.3.1. Humans

Silver is generally considered non-toxic to humans and animals. Humans are exposed to large amounts of silver every day. Silver is abundant in our tooth fillings, silverware, jewelry, and many electronics [36]. In addition, humans consume an estimated 70-88 µg of silver per day [37], mostly through water, although more recent estimates of total silver intake by humans are 7.1 µg per day [38]. Humans can consume up to 10 grams of silver throughout their lifetime without any adverse effects or precursors to adverse effects [38]. Assuming the high estimate of 88 µg per day for 70 years, total human intake of Ag would be only 2.2 grams.

The EPA standard of 100 ppb (total recoverable silver) is a secondary maximum contaminant level. This means it is not toxic at this concentration, it is developed to

reduce nuisance conditions. This value is based on historical (accidental) exposures of humans to silver. Doctors prescribed nasal sprays containing extremely high concentrations of silver in the 1930's; 4% silver iodide [7]. There were no reported physiological adverse effects. However, prolonged ingestion of high concentrations of either colloidal silver or the silver ion leads to a skin condition known as argyria. Like animals, there are no adverse effects known but a graying discoloration of the skin [39].

2.3.2 Animals

There are few studies looking at the toxicity of silver to mammals. This is because there is little evidence of silver toxicity in natural aquatic systems, which accumulate silver via bioconcentration (Ag via body surface uptake) and biomagnification (Ag via food). Animals can only accumulate silver through the latter mechanism while aquatic organisms accumulate silver through both [23]. The few studies on silver toxicity studies pertaining to mammals reveal biomagnification is unlikely. However, high silver concentrations in the liver will inhibit the absorption of vitamin E, copper and selenium [1]. Toxic effects in animals often manifest themselves in vitamin deficiency symptoms.

Once the silver ion is ingested or inserted in the bloodstream, most is removed by the gastrointestinal tract and the liver [40]. The silver ion binds to RNA, DNA, or proteins, subsequently accumulating in the liver [23].

In one study turkeys were fed a diet of 900 ppm silver nitrate for 4 weeks – roughly 1,000 times the concentration typically found in soil. Turkeys experienced growth depression, enlarged heart, increased mortality, and a copper deficiency. The enlarged heart and mortality levels were corrected once turkeys were fed copper

supplements in addition to the silver spiked food [37]. The copper supplements ameliorated the deficiency related symptoms in turkeys.

A few studies pertaining to rats and silver nitrate have been conducted as well. Lethal concentrations of silver nitrate for rats are 13.9 ppm silver to body weight. Rats experienced lethal effects via drinking water with 1586 ppm Ag for 37 weeks. Rats also experienced sluggishness when drinking water was 95 ppb and kidney failure when drinking water was 400 ppb for 100 and 125 days respectively [20].

To evaluate the effects of cloud seeding on livestock, 1-year old sheep were fed up to 10 mg silver iodide per kilogram of body weight per day[9]. After 86 days, none of the health metrics differed significantly from control group, despite accumulating silver in the liver at concentrations of 17 ppm [41].

2.3.3 Plants

There have been a few studies performed concerning the effect of insoluble silver compounds on crops. One study was performed for wastewater treatment sludge applications to crops. This study evaluated whether high silver amounts from photo-processing facilities would adversely affect plants. This study investigated corn, lettuce, oats, turnips, iceberg lettuce, spinach, and Chinese cabbage. Sewage sludges were added to one set of crops (mean Ag = 13.5 ppm) while the other set was spiked with silver up to 155 ppm. The results showed that no crops, except for lettuce, showed large increases of silver in edible crop portions. Soybeans subjected to concentrations above about 100 ppm experienced decreased yield. Lettuce, Chinese cabbage, and spinach experienced

[9] 1-year old sheep are typically 60 kg. This would result in 600 g of AgI per sheep per day. 1,000 generator hours from cloud seeding (typical of a given winter season) would release 23 kg of AgI, resulting in ~10 g of AgI deposited per km^2.

decreased yield at 14 ppm soils and toxicity threshold values at 26 ppm and 43 ppm for lettuce and Chinese cabbage respectively [42]. Because most natural soils have silver concentrations between 0.1 and 1 ppm, toxicity threats to plants is unlikely.

This study also showed that silver concentrations increased roughly 0.25 ppm (dry weight) in control plants. In both sets of crops, the lower stem, upper stem, and leaf portions (except for lettuce) accumulated trace amounts of silver from the silver-spiked soils [42].

Ratte (1999) showed two species of plants that have significant bioaccumulation potential [23]. First, mushrooms have bioconcentration factors up to 150 when grown on silver enhanced sewage [23]. Silver was concentrated in the stalk and stem, with bioconcentration factors of up to 230. There was no impairment in growth or fruit given these bioconcentration factors. No conclusion was drawn on the bonding of silver to the mushrooms or the potential susceptibility to biomagnifications. The second species listed was a type of grass grown on an Ontario silver mine tailing pile. Bioconcentration factors of grass blades relative to water in the tailings were up to 124,000 [23]. Strangely, the highest bioconcentration factor of grass roots was only 3 even though the roots had higher Ag concentrations than the grass blades.

It is also worth noting that, as with animals and fish, species are much more susceptible to silver toxicity in the very early stages of life [1]. The most sensitive phase of a plant is during germination. Concentrations of just 750 ppb from soluble silver nitrate induced negative effects on some plant species [20].

3. Standards

The environmental standards for evaluating silver concentrations vary with the application (human vs. aquatic species impact) and between jurisdictions (state, federal, international).

Because silver is considered essentially non-toxic to humans, the EPA lists silver in the "secondary drinking water standards" for potable water. These standards are in terms of total recoverable silver (how much silver is dissolved after strong acid digestion) and is set orders of magnitude higher than normally present in natural conditions. WHO, U.S. EPA, and the Australian EPA have established drinking water standards at 100 ppb. Two states, Arizona and Hawaii, have set more stringent standards on drinking water at 50 ppb [43].

These agencies are aware that the silver ion is the primary control to toxicity of aquatic species, but differ in how they estimate the concentration of the silver ion. State and federal agencies enforce acute silver toxicity standards in terms of dissolved silver concentrations, estimated empirically as a function of total recoverable silver. The Australian EPA on the other hand, regulates the toxic silver ion specifically, as seen in Table 11.

3.1 U.S. EPA Standards

The EPA has two water quality standards for toxic substances: Criteria Maximum Concentration (CMC) and Criterion Continuous Concentrations (CCC). The EPA did not establish a CCC standard for silver, there is only a CMC standard. The EPA defines CMC standards as "an estimate of the highest concentration of a material surface to which an aquatic community can be exposed briefly without resulting in an unacceptable

effect" [48]. The EPA derived these standards using empirical equations estimating the percent dissolved silver (includes complexed silver, ionic silver, and sometimes colloidal silver depending on definition of "dissolved") and its effect on aquatic species in a laboratory setting. Standards and equations are based on of total recoverable silver measurements.

It is important to understand how these standards were calculated in order to interpret the toxicity of silver values in the environment relative to these standards. The EPA is aware that silver speciation is the largest control on toxicity, but is also aware that water quality tests generally quantify total recoverable silver instead of the concentration of the silver ion in solution [49]. Therefore, the EPA created two empirical formulas to estimate toxicity given the water hardness and total recoverable silver concentrations. The first empirical equation calculates permissible total recoverable silver concentrations in freshwater environments as a function of hardness. To create this formula, six laboratories conducted both static and flow-through tests of silver toxicity; resulting in relationships of LC_{50}-96 hour and hardness values at various concentrations for the following sensitive aquatic species: *Daphnia magna*, rainbow trout, and fathead minnows [31]. The relationships for these 3 species EPA were averaged to compute *Equation 3* below [37]; and is plotted against hardness in Figure 23.

Equation 3 $$Ag = (WER) * e^{(1.72 * \ln(hardness)) - 6.59}$$

Ag = Concentration of total recoverable silver [ppb]

$hardness$ = Concentration of calcium and magnesium salts [ppm]

WER = water-effect ratio, fixed at 0.85 [unitless]

Equation 3 has been critically discussed in literature [27] [29][30]. Williams (2009) stated *Equation 3* is under-protective at high hardness and over-protective at low hardness [2]. In other words, the relationship between hardness and Ag toxicity does not possess as much curvature in this relationship as Figure 21 shows and may have a more linear trend (*Section 2.1.6*). Hogstrand (1998) stated "The U.S. EPA hardness equation currently used for regulating acute toxicity is faulty, and research is urgently needed to replace it with a relationship that includes… …more important geochemical modifying factors" [25]. The influential geochemical modifying factors referenced here are explained in greater detail in *Section 2.1*.

Erickson (1998) criticized the data used for the EPA Ag toxicity equation because they did not hold all water quality variables constant (such as pH and alkalinity) when measuring the effect of hardness and silver toxicity. Erickson accounted for those variables and found hardness to be 10 times less impactful than the EPA data when methods were replicated. In this same study, when total organic carbon (not specifically DOC, which is the impactful variable in total organic carbon) was increased by 17 ppm, toxicity values decreased by factors ranging between 10 and 60 [32].

The water-effect ratio (WER) is another coefficient developed by the EPA to estimate the proportion of dissolved silver to total recoverable silver (again, this includes complexed silver, the silver ion, and in some cases colloidal silver) [50]. WER was calculated based on three studies mentioned in the 1993 EPA memorandum, which revealed the primary control on toxicity was the silver ion, not total recoverable silver [49]. The studies used in designing the WER are listed in the Table 12 below (Table modified from 1993 EPA memorandum). Every study was a static water test. The CMC

toxicity concentrations were adjusted using the WER coefficient, fixed at 0.85 based on the results from Table 12, and applied to both freshwater and saltwater standards. After 1993, CMC toxicity values were calculated as an empirical function of "dissolved" using *Equation 3* multiplied the WER of 0.85.

The WER was established so the EPA could give states discretion to adjust standard values to more site-specific conditions. The EPA is aware that many factors ameliorate silver toxicity, so states are given the right to adjust the WER in order to estimate the concentration of the toxic silver ion (relative to the total recoverable fraction) likely present in that environment.

3.2 Idaho Department of Environmental Quality Standards

The Idaho Department of Environmental Quality applies the same formula for the EPA except the two coefficients are altered slightly. First, the Y-intercept is changed from -6.59 to -6.52. Second, the WER is fixed at 1 (assuming total recoverable silver is equal to total dissolved silver) and hardness is assumed to be 100 if actual hardness measurements are unavailable. Idaho's adjustments to the calculation increase the contaminant threshold level. This allows a wider range of permissible total recoverable silver concentrations, especially at high hardness values (Figure 23). Associated tables in descriptions are available in IDAPA 58, section 210 [55]. Expressed mathematically:

$$Equation\ 4 \quad Ag = (WER) * e^{(1.72 * \ln(hardness)) - 6.52} = (1) * e^{(1.72 * \ln(100)) - 6.52} = 3.4\ ppb$$

3.3 Australian EPA Standards

Australia applies guidelines called 'trigger values', and have a different definition compared to the EPA standards in the United States. Trigger values are generally not fixed, but are permissible values relative to natural background concentrations.

Generally, local guideline levels are established to be most applicable to the region of study. However, if no background information is available, the conservative value in Table 11 is assigned to the region. Silver ion concentrations of 0.05 ppb are trigger values in highly protected environments. Should sources go above this trigger value, environmental authorities are required to investigate the sources of the contaminants and discern whether these values are tolerable/typical in the local setting and what proportion of these values are anthropogenic [47]. In other words, these are not "pass or fail" standards, but rather guidelines revealing where research and/or mitigation efforts should be focused.

3.4 World Health Organization (WHO) Standards

WHO ceased to provide world-wide standards of toxic chemicals starting in 1982. Instead, WHO establishes water quality 'guidelines'. Guidelines allow each nation to judge the water quality criteria based on their circumstances and culture. WHO found essentially no risk of silver toxicity to humans due to the low natural levels of silver present in drinking water relative to safe lifetime oral intake of silver. A human can safely intake up to 10 grams of silver orally in their lifetime based on the no-observed-acute-effect-level (NOAEL) and experience no adverse effects or precursors to adverse effects [38]. In other words, a person would have to drink 4 L of water with 100 ppb Ag for 70 years to obtain this value. Even in polluted areas, silver concentrations are generally at least 2 orders of magnitude less concentrated than the 100 ppb WHO drinking water guideline.

4. Concerns of AgI Cloud Seeding and the Environment

4.1 AgI Effects of Cloud Seeding

The effects of cloud seeding on the environment have been studied extensively; especially with respect to freshwater ecosystems [2] [3][15][56]. All studies found sub-ppb total recoverable silver enrichments in precipitation silver due to cloud seeding. These concentrations are low because the total silver flux from cloud seeding can be considered small; it comprises 0.1% of the total silver released to the environment globally [1]. The enriched silver is largely immobilized in soil or absorbs/complexes to aqueous chemical species [7].

More publications on the potential effects of AgI seeding on soils, streams, and organisms are anticipated from the Snowy Hydro Limited cloud seeding project in Australia. Snowy Hydro collected nearly 7,000 samples of stream sediments, stream water, moss, peat, and soils. Published results will be expected to be published soon. However, preliminary statements regarding these data note no significant changes in silver concentrations and “mean concentrations for all locations and sample types are well below relevant environmental guidelines” [57].

4.2 AgI Abundance in Snowpack

AgI is present in only trace amounts in snow because AgI ice nuclei are small. Between 10^{14} - 10^{16} ice nuclei are produced by combusting one gram of silver iodide, yielding 0.06 μm diameter AgI nuclei. Cooler temperatures (up to -15^{o}C) and higher wind speeds generally produce more AgI nuclei per gram [1]. Due to the small size of these nuclei, generators burn roughly 21 grams per hour to seed a storm. The average

release of AgI via ground generators from 2003-2012 is 18.6 kg. These nuclei are dispersed throughout the 2,400 km^2 Payette Basin per snow season.

This results in part per trillion enhancements in seeded snow above background concentrations. These concentrations have considerable spatial variability because seeding rates do not have a linear relationship with total recoverable silver concentration in snow. For example, a seeded snowflake may accrete more water during fallout and secondary ice forming processes such as ice multiplication produce snowflakes void of AgI. These scenarios would both reduce the silver concentrations in the snow.

Field studies in the Western United States investigating silver concentrations in snow Ag from seeding are likely range from 2-20 ppt, rarely exceed 25 ppt [59], and almost never exceed 50 ppt [3]. The layer(s) containing these elevated concentrations tend to occupy a thin layer (1-10 cm scale) in the snowpack. In most instances, vertical sampling at the 1-5 cm scale across multiple sites in a seeded snowpack will produce AgI seeding signatures in roughly 20% of the samples [15][60][16][10][18] with two exceptions having roughly 80% [26][71].

4.3 Cloud Seeding Byproducts

The potential impact of other chemicals used to create ice nuclei through AgI combustion have also been assessed. Aircraft AgI flares are composed of ammonium perchlorate, zinc powder, aluminum powder, silver iodide, and copper iodide. None of these chemicals are listed as hazardous materials by the EPA. Flares burn 150 g of silver

[10] Huggins' 2009 study in the Snowy Mountains study arbitrarily displayed statistics of % of samples greater than 1 ppt. This study stated ~50% of samples from a seeded storm had Ag concentrations greater than 1 ppt. This is not a useful statistic because background Ag concentrations were predicted around 3 ppt here.

iodide in conjunction with the rest of these compounds [64]. These flares likely disperse 200 km down-wind [65], so concentrations will be at trace levels in snow. Additionally, there is only a very limited fire risk from aircraft seeding activities because it is conducted at high altitude under snow covered conditions. Also, ground generators are at limited risk because at least a 9.1 m (30 ft) radius of trees is cleared surrounding ground generators [64].

4.4 AgI Toxicity

4.4.1 Overview

AgI is extremely insoluble (only a small fraction of the solid is dissolved before the solution becomes saturated and no longer dissolves the solid). This means the maximum dissolved Ag concentration, assuming unlimited AgI, is approximately 1 ppb. However, a large fraction of this dissolved Ag would adsorb to particulate matter such as manganese and iron compounds or clay particulates [7]. Once absorbed to particulates, Ag^+ is no longer bioavailable (toxic) to alter the osmoregulatory processes of fish and related species.

A number of studies demonstrated that the total Ag loading from AgI cloud seeding is low in soils, water bodies, and the atmosphere. The Australian EPA found no significant difference in silver concentrations in aquatic, soil, stream sediments, and sensitive aquatic species that bioaccumulate trace metals with the area targeted for cloud seeding [63]. Huggins (2009) found that the average Ag concentrations in seeded snowpack were actually lower in seeded than unseeded years. This was attributed to the relatively large fluctuations of background concentrations year to year, varying from 3 to 9 ppt [61]. These large fluctuations are attributed primarily to dry deposition of

aluminosilicate dust. Lastly, stream samples taken from the Wyoming Weather Modification Pilot Program did not find a correlation between AgI seeded watersheds and stream Ag concentrations. The largest control on Ag concentrations in these streams were suspended sediments [3].

4.4.2 Nano-Silver (Ag^0)

Nano-silver particles are manufactured for use as an antimicrobial agent in consumer products (i.e. long underwear, paint, plastics, and paper). These products are specifically designed to release the silver ion [11]. "Nano-silver species" are defined as being smaller than 100 nm in its longest dimension [36]. Nano-silver has not been well understood until recent years and has been the subject of many recent toxicity studies. The silver ion is toxic not only to bacteria, but every other aquatic species at small concentrations. Nano-silver has an extremely high surface area/volume ratio, increasing the risk of the solid particles being dissolved in solution. Finally, these consumer products tend to be manufactured to prevent bonding of these nano-silver particles [11]. Again, this encourages anti-microbial activity and resists natural processes that would otherwise mitigate Ag toxicity (via DOC, agglomeration, chloride, sorption, etc.).

An AgI nucleus is usually 60 nm in its widest dimension [58] and is classified as a nano-silver particle. However, AgI is not an engineered nano-particle (it is formed by combustion) and it is highly insoluble [36]. Likewise, AgI nuclei are not manufactured to resist bonding, so AgI tends to accumulate in the upper 2 cm of the soil horizon via adsorption [66]. AgI was not identified as a serious source of concern in the EPA's 2010 literature review of nano-silver [66].

Reidy (2013) distinguishes between how the silver ion and nano-silver are bioavailable, and thus toxic to aquatic species. The silver ion enters organisms via diffusion across some biologic membrane (gill, skin cell, etc). Silver ion concentrations tend fluctuate in an organism until some equilibrium is reached. The silver ion has essentially no surface area and reacts primarily with organics, mineral surfaces, and forms complexes. Nano-silver, on the other hand, is actively taken up by an organism. The nano-silver particle then dissociates within the organism resulting in very high, local concentrations of dissolved silver. Nano-silver particles dissociate readily within the species due to their extremely high surface area-to-volume ratio. Nano-silver tends to bind to biomolecules [67].

Newton (2011) investigated the difference in toxicity of nano-silver particles and ionic silver to *Dapnia magna*. Results showed nano-silver toxicity were a function of dissolution into the toxic silver ion, implying nano-silver had no effect in solid form to *Daphnia magna*. Therefore, the toxicity of nano-silver can be estimated in the Biotic Ligand model once dissolution estimates become reliable [68].

4.4.3 An Assessment of Cloud Seeding-Derived AgI Toxicity to Freshwater Environments

We present here a ‘worst case scenario’ calculation for assessing the impact of cloud seeding. In this calculation we make assumptions about the amount of Ag delivered to the snowpack, the behavior of that Ag once deposited, and the delivery of that Ag to a water body. A summary of these calculations and discussion are presented by Edwards (2006) [3]. Table 14 shows two classes of assumptions, maximum and likely.

If 15% of the snowpack contained the enriched Ag concentrations of 50 ppt, then cloud seeding would raise the average silver concentration of the snowpack from the 2 ppt Ag background concentration to 9.2 ppt. This AgI enhancement is still within typical concentrations in natural freshwaters of 1-30 ppt Ag. The trace amounts of dissolved silver will likely complex or will not be bioavailable to aquatic species due sorption processes, where the majority of naturally occurring silver is already present. Wen (2002) found river sediments typically have between 0.2 to 1 ppm of silver, almost 6 orders of magnitude higher than the overlying water [10]. Therefore, the majority of the AgI will become immobilized in a non-toxic form at ultra-trace amounts in stream sediments.

One final hypothetical scenario was proposed by Edwards (2006). If 100% of the snow was at 50 ppt and all other assumptions from Table 13 remained the same. The resulting total recoverable silver concentrations in snowmelt entering the stream would still be more than 10 times lower than the LC_{50} concentration (from Biotic Ligand Model) of the most sensitive aquatic species studied [3]. The LC_{50} values were computed by the EPA using silver nitrate ($AgNO_3$) (*Section 2.1.1).* AgI is approximately 10,000 times less toxic than the $AgNO_3$ salts used in many other toxicity studies [23]. The LC_{50} concentration would be even higher using AgI alone versus the $AgNO_3$ used to derive the standard. Therefore, AgI based LC_{50} values would likely allow much higher total recoverable silver concentrations before these sensitive species experience toxic effects.

4.4.4. AgI Accumulation in Soils

A variable, but significant, contribution of AgI released from cloud seeding is expected to accumulate in the shallow soils where it is deposited. Two studies have been

conducted to evaluate if that accumulation results in significant increase in Ag concentrations in the soil.

One study in Greece collected 2,500 samples after 13 years of hail suppression cloud seeding. More than 800 kg of AgI was burned over the two target areas during that time period. They found no difference in silver concentrations between soils in the 2 target areas and the 3 control sites. In fact, one of those control sites had an average Ag concentration roughly 20% higher than the highest average target area concentration [6].

In another study, 1,464 soils samples were collected in the upper 2 cm in 200 m intervals from a ground generator. Samples were collected the year before cloud seeding began and every subsequent year where cloud seeding was practiced. The results showed no soils exceeded 1 ppm of Ag except for one site, which had equally high concentrations in pre-seeding conditions. There was also no statistically significant increase of silver between target/control sites and no observed accumulation of silver through time [66].

There was no correlation between increases in silver concentration in soil strata and cloud seeding activities practiced by Snowy Hydro Limited. Stromsoe (2011) estimated annual 19-fold increase in AgI usage (assuming every AgI particle landed in target zone) in order to produce a statistically significant silver increase [26].

4.4.5 Iodine Concentrations from AgI

The iodine associated with AgI could be considered another potential impact. However, the iodine contribution from cloud seeding is negligible compared to its naturally occurring abundance. Total recoverable iodine concentrations in precipitation are typically between 0.1 and 15 ppb [70]; at least 1 order of magnitude higher than the iodine present from AgI in rain water. Cooper [40] elaborated on this poin, calculating

130 gallons of cloud seeded rainwater is necessary to obtain as much total recoverable iodine as one serving of iodized table salt

5. Conclusions

The toxicity of silver depends primarily on concentration, speciation, and bioavailability. Natural silver compounds and complexes are not soluble nor bioavailable. The silver ion (Ag+) is the bioavailable (and thus toxic) form of silver. The silver ion was typically the dominant species in laboratory toxicity studies quantifying the toxicity of silver. For the gilled organisms, toxicity is related to Ag+ gill interactions leading to an osmotic imbalance. The conditions necessary to convert solid silver to toxic concentrations of the silver ion are seldom present in the natural environment. Silver can accumulate in organisms several orders of magnitude higher than its surrounding environment without experiencing adverse effects. Currently, there are no direct correlations between accumulated silver and toxic effects in all species studied except algae. Likewise, silver compounds do not dissociate in the digestive systems of organism studied, so silver toxicity to terrestrial species is also highly unlikely.

Silver iodide has been used in weather modification programs for over sixty years. In modern programs extremely small amounts of AgI are dispersed in the atmosphere over relatively large areas. It is insoluble with a low bioavailbility. As a result, toxic effects are highly unlikely. Environmental sampling has found no evidence of adverse effects on wildlife or silver accumulating at detectable levels above background in soils, streams, or aquatic species in seeded areas. There are no documented cases of silver toxicity in the environment from any source of anthropogenic silver release.

6. References

[1] R. Eisler, “Silver hazards to fish, wildlife, and invertebrates: A synoptic review,” Environmental Protection Agency, Contaminant Hazard Biological Report 32, 1996.

[2] B. D. Williams and J. A. Denholm, “An assessment of the environmental toxicity of silver iodide - with reference to a cloud seeding trial in the snowy mountains of Australia,” J. Weather Modif., vol. 41, no. 1, pp. 75–96, Apr. 2009.

[3] P. R. Edwards and D. A. Simeral, “Baseline silver concentrations in freshwater and snow in the Wyoming weather modification project target area.” Desert Research Institute, 2006.

[4] S. R. Taylor and S. M. McLennan, “The geochemical evolution of the continental crust,” Rev. Geophys., vol. 33, pp. 241–265, 1995.

[5] T. W. Purcell and J. J. Peters, “Sources of silver in the environment,” Environ. Toxicol. Chem., vol. 17, no. 4, pp. 539–546, 1998.

[6] S. E. Tsiouris, F. A. Aravanopoulous, I. N. Papadoyannis, M. K. Sofoniou, N. Polyzopoulos, M. Christodoulou, V. F. Samanidou , G. A. Zachariadis and H. A. Constantinidou, “Soil silver content of agricultural areas subjected to cloud seeding with silver iodide,” Fresenius Environ. Bull., vol. 11, pp. 697–702, 2002.

[7] Cardno ENTRIX, “Geochemistry and impacts of silver iodide use in cloud seeding,” 2011.

[8] C. Boutron, “A clean laboratory for ultralow concentration heavy metal analysis,” Fresenius J. Anal. Chem., vol. 337, no. 5, pp. 482–491, 1990.

[9] G. A. Gill, L. S. Wen, D. Tang and P. Santschi, “Silver in Colorado watersheds,” Transport, fate, and effects of silver in the environment. Proceedings of the 5th international conference, September 28 - October 1, 1997, Hamilton, Ontario, Canada. 1997.

[10] L. S. Wen, P. H. Santschi, G. A. Gill and D. Tang, “Silver concentrations in Colorado, USA, watersheds using improved methodology,” Environ. Toxicol. Chem., vol. 21, no. 10, pp. 2040–2051, 2002.

[11] EPA, “State of the Science literature review: everything nanosilver and more,” Environmental Protection Agency (EPA), Washington, D.C., Task Order 95, 2010.

[12] US Department of Labor, “Limits for air contaminants,” Occupational Safety and Health Standards, Washington, D.C., Toxic and Hazardous Substances 1910.1000, Table Z-1, 2006.

[13] J. A. Warburton, S. K. Chai, R. H. Stone and L. G. Young, “The assessment of snowpack enhancement by silver iodide cloud-seeding using the physics and chemistry of the snowfall,” J. Weather Modif., vol. 28, no. 1, pp. 19–28, 1996.

[14] A. W. Huggins, S. L. Kenyon, L. Warren, A. D. Peace, S. P. Billish and M. J. Manton, “The snowy precipitation enhancement research project: a description and preliminary results,” J. Weather Modif., vol. 40, pp. 28–53, 2008.

[15] A. W. Huggins, “Trace chemical monitoring for the Wyoming weather modification pilot project: tasks for the 2010 field project,” Desert Research Institute, 2010.

[16] WMA, “Weather Modification Association (WMA) position statement on the environmental impact of using silver iodide as a cloud seeding agent,” 2009.

[17] P. R. Edwards, A. W. Huggins and J. McConnell, “Trace chemistry evaluation of the IPCo 2003-3004 cloud seeding program,” Desert Research Institute, 2004.

[18] J. M. Fisher, P. Golden, S. G. Benner and M. Lytle, “Trace chemical evaluation of cloud seeding in the Payette Basin,” Heritage Environmental Consultants, Denver, CO, 2015.

[19] S. G. Benner, M. Kohn and P. Golden, “Payette Basin Exploratory Snow Sampling: Final Report,” Heritage Environmental Consultants, Denver, CO, 2014.

[20] P. D. Howe and S. Dobson, “Silver and silver compounds: environmental aspects,” World Health Organization (WHO), Geneva, Switzerland, CICAD 44, 2002.

[21] N. R. Bury, J. C. McGeer and C. M. Wood, “Effects of altering freshwater chemistry on physiological responses of rainbow trout to silver exposure,” Environ. Toxicol. Chem., vol. 18, no. 1, pp. 49–55, Jan. 1999.

[22] P. Gaines, “Chemical stability: silver,” Inorganic Ventures, Christiansburg, VA, 2014.

[23] H. T. Ratte, “Bioaccumulation and toxicity of silver compounds: a review,” Environ. Toxicol. Chem., vol. 18, no. 1, pp. 89–108, 1999.

[24] C. M. Wood, R. C. Playle and C. Hogstrand, “Physiology and modeling of mechanism of silver uptake and toxicity in fish,” Environ. Toxicol. Chem., vol. 18, pp. 71–83, 1999.

[25] C. Hogstrand and C. M. Wood, “Toward a better understanding of the bioavailability, physiology, and toxicity of silver in fish: implications for water quality criteria,” Environ. Toxicol. Chem., vol. 17, pp. 547–561, 1998.

[26] N. Stromsoe, J. N. Callow, H. A. McGowan and S. A. Marx, “Attribution of sources to metal accumulation in an alpine tarn, Snowy Mountains, Australia,” Environ. Pollut., vol. 181, pp. 133–143, 2013.

[27] D. Karen, D. Ownby, B. Forsythe, T. Bills, T. W. La Point, G. Cobb and S. Klaine, “Influence of water quality on silver toxicity to rainbow trout (oncorhynchus mykiss), fathead minnows (pimephales promelas), and water fleas (daphnia magna),” Environ. Toxicol. Chem., vol. 18, pp. 63–70, 1999.

[28] E. W. Boyer, G. M. Hornberger, K. E. Bencala and D.M. McKnight, “Effects of asynchronous snowmelt on flushing of dissolved organic carbon: a mixing model approach,” Hydrol. Process., vol. 14, pp. 3291–3308, 2000.

[29] C. Hogstrand, F. Galvez and C. M. Wood, “Toxicity, silver accumulation, and metallothionein induction in freshwater rainbow trout during exposure to different silver salts,” Environ. Toxicol. Chem., vol. 15, pp. 1102–1108, 1996.

[30] N. R. Bury, F. Galvez and C. M. Wood, “Effects of chloride, calcium, and dissolved organic carbon on silver toxicity: comparison between rainbow trout and fathead minnows,” Environ. Toxicol. Chem., vol. 18, no. 1, pp. 56–62, Jan. 1999.

[31] A. E. Lemke, “Interlaboratory comparison: acute testing set,” Environmental Protection Agency (EPA), Washington, D.C., EPA 600/3-81-005, 1981.

[32] R. J. Erickson, L. T. Brooke, M. D. Kahl, F. V. Venter, S. L. Harting, T. P. Markee and R. L. Sephar, “Effects of laboratory test conditions on the toxicity of silver to aquatic organisms,” Environ. Toxicol. Chem., vol. 17, pp. 572–578, 1998.

[33] C. M. Wood, C. Hogstrand, F. Galvez and R.S. Munger, “The physiology of waterborne silver toxicity in freshwater rainbow trout (oncorhynchus mykiss). The effects of silver thiosulfate,” Aquat. Toxicol., vol. 35, pp. 111–125, 1996.

[34] M. P. Hirsch, “Toxicity of silver sulfide-spiked sediments to the freshwater amphipod (hyalella azteca),” Environ. Toxicol. Chem., vol. 17, pp. 601–604, 1998.

[35] D. Y. Lee, C. Fortine and P. Campbell, “Contrasting effects of chloride on the toxicity of silver to two green algae, pseudokirchneriella subcapitata and chlamydomonas reinhardtii,” Aquat. Toxicol., vol. 75, pp. 127–135, 2005.

[36] Pacific Gas & Electric, “Responses to questions regarding cloud seeding in the Lake Almanor Basin,” Pacific Gas and Electric, San Francisco, CA, 2011.

[37] EPA, “Ambient water quality criteria for silver,” Environmental Protection Agency (EPA), Washington, D.C., 440/5-80-071, 1980.

[38] WHO, “Silver in drinking water,” World Health Organization (WHO), Geneva, Switzerland, 2003.

[39] US Public Health Service, “Toxicological profile for silver,” Agency for Toxic Services and Disease Registry TP*90-24, 1990.

[40] C. F. Cooper and W.C Jolly, “Ecological effects of silver iodide and other weather modification agents: a review,” Water Resour. Res., vol. 6, no. 1, pp. 88–98, 1970.

[41] R. L. Younger and H. R. Crookshank, “Chronic exposure of sheep to silver iodide,” Water. Air. Soil Pollut., vol. 9, pp. 281–287, 1977.

[42] M. P. Hirsch, “Availability of sludge-borne silver to agricultural crops,” Environ. Toxicol. Chem., vol. 17, pp. 610–616, 1998.

[43] EPA, “Drinking water standards and health advisories table,” Environmental Protection Agency (EPA), San Francisco, CA, 2007.

[44] Arizona DEQ, “water quality standards for surface waters,” Arizona Department of Environmental Quality (DEQ), Pheonix, AZ, title 18, ch. 11, article 1, 2009.

[45] Hawaii Department of Health, “Hawaii administrative rules: water quality standards.” Honolulu, HI, title 11, ch. 54. 2013.

[46] Idaho DEQ, “Water quality standards,” Idaho Department of Environmental Quality (DEQ), Boise, ID, title 1, ch. 2, IDAPA 58, 2014.

[47] NSW EPA, “Using the ANZECC guidelines and water quality objectives in NSW,” New South Wales (NSW) Environmental Protection Authorities, Armidale NSW, Austalia, 2013.

[48] EPA, “National recommended water quality criteria,” Environmental Protection Agency (EPA), Washington, D.C., 2015.

[49] M. Prothro, “Office of water policy and technical guidance on interpretation and implementation of aquatic life metals criteria,” Environmental Protection Agency (EPA), Washington, D.C., Memorandum to water management division managers, Oct 1., 1993.

[50] EPA, “Interim guidance on determination and use of water-effect ratios for metals,” Environmental Protection Agency (EPA), Washington, D.C., EPA-823-B-94-001, 1994.

[51] G. A. Chapman, “Memorandum to C. Stephan June 4,” 1993.

[52] A. V. Nebaker, R. McAulittle, R. Mshar and D. G. Stevens, “Toxicity of silver to steelhead and rainbow trout, fathead minnows, and daphnia magna,” Environ. Toxicol. Chem., vol. 2, pp. 95–104, 1983.

[53] UWS, “Preliminary data from work assignment 1-10,” University of Winsconsin - Superior (UWS), Contract 68-C1-0034, 1993.

[54] J. C. Briggs and J. F. Ficke, “Quality of rivers of the United States, 1975 water year -- based on the National Stream Quality Accounting Network (NASQAN),” United States Geological Survey (USGS), Report 78-200, 1977.

[55] IDEQ, “Water quality standards: Rules of the Department of Environmental Quality (DEQ) title 2, ch. 1, IDAPA 58, 2007.

[56] USBR, “Environmental assessment for the Walker River Basin cloud seeding project,” United States Bureau of Reclamation (USBR), Westminster, CO, 2010.

[57] Snowy Hydro Limited, “Cloud seeding program: environmental management,” Cooma, New South Wales, Australia, 2013.

[58] D. M. Garvey, “Testing of cloud seeding materials at the cloud simulation and aerosol laboratory, 1971–1973,” J. Appl. Meteorol., vol. 14, no. 5, pp. 883–890, 1975.

[59] A. W. Huggins, “Brief summary of findings related to trace chemical monitoring for the Wyoming Weather Modification Pilot Project (WWMPP),” Desert Research Institute (DRI), Reno, NV, 2013.

[60] J. A. Warburton, R. H. Stone and B. Marler, “How the transport and dispersion of AgI aerosols may affect detectability of seeding effects by statistical-methods,” J. Appl. Meteorol., vol. 34, no. 9, pp. 1929–1941, 1995.

[61] A. W. Huggins, “Summary of studies that document the effectiveness of cloud seeding for snowfall augmentation,” J. Weather Modif., vol. 41, pp. 127–134, 2009.

[62] J. A. Warburton, L. G. Young and R. H. Stone, “Assessment of seeding effects in the snowpack augmentation programs: ice nucleation and scavenging of seeding aerosols,” J. Appl. Meteorol., vol. 34, pp. 121–130, 1995.

[63] NSW EPA, “Review of the Snowy Hydro limited cloud seeding program 2013 annual compliance report,” New South Wales Environmental Protection Authority (NWS EPA), Armidale NSW, Austalia, 2013.

[64] D. Gibbs, and T. Fayram, “Santa Barbara County and Twitchell Reservoir cloud seeding program: CEQA final mitigated negative declaration,” County of Santa Barbara, Report 13NGD-00000-00011, 2013.

[65] T. P. DeFelice, J. Golden, D. Griffith, W. Woodley, D. Rosenfeld, D. Breed, M. Solak and B. Boe, “Extra area effects of cloud seeding - An updated assessment,” Atmospheric Res., vol. 135–136, pp. 193–203, 2014.

[66] M. Lincoln-Smith, A. Dye, K. Kemsley and J. Denholm, “Environmental monitoring and assessment: A statistical analysis on concentrations of silver and indium at generator locations,” J. Weather Modif., vol. 43, pp. 1–8, 2011.

[67] B. Reidy, A. Haase, A. Luch, K. Dawson and I. Lynch, “Mechanisms of silver nanoparticle release, transformation and toxicity: A critical review of current knowledge and recommendations for future studies and applications,” Materials, vol. 6, pp. 2295–2350, 2013.

[68] K. Newton, “The influence of dissolved organic carbon and surface chemistry on the toxicity of silver nanoparticles in daphnia magna,” Clemson Univ., Thesis, 2011.

[69] WWDC, “The Wyoming Weather Modification Pilot Project: level ii study. executive draft summary,” Wyoming Water Development Commission. Cheyenne, WY, 2014.

[70] J. Risher and L. S. Keith, "Iodine and inorganic iodides: human health aspects," World Health Organization (WHO), Geneva, Switzerland, 2009.

[71] B. M. McGurty, "Turning silver into gold: measuring the benefits of cloud seeding". Hydro Review, vol. 6. pp. 53-57. 1999.

APPENDIX A

Tables

Table A.1. Sampling locations in the 2015 field campaign

Date Collected [2015]	Site Name	Location	Elevation [m]	Samples Analyzed	Ag Enhancement?
09 January[a]	SY-1	44° 1'28.45"N 115°37'53.22"W	1,890	110	No
09 February[b]	GL	45° 0'57.14"N 116°11'31.15"W	1,931	105	No
24 March	SY-2	44° 1'16.03"N 115°37'52.06"W	1,946	30	Yes
24 March[c]	BS	44°18'13.68"N 115°13'51.42"W	2,137	124	Yes
25 March	MC	43°56'56.74"N 115°40'44.43"W	2,303	24	Yes
25 March	AM	44° 3'29.43"N 115°28'22.39"W	2,092	18	Yes
07 April[c]	SM	44°10'41.03"N 115°43'15.95"W	2,256	248	Yes
11 April	JP	44° 0'10.45"N 115°45'6.22"W	2,185	70	Yes

[a] *Interlab comparison was performed on these samples*
[b] *Control site to determine background Ag concentrations*
[c] *Multiple snow pits were constructed at one site to understand hillslope-scale Ag variability*

Table A.2. Operating ICP-MS conditions and data acquisition parameters for select elements in snow

Forward power	1400 W
Cooling	13 L/min
Expansion Pressure	$2.0 * 10^{0}$ mbar
Analyzer Pressure	$4.0\text{-}4.2 * 10^{-7}$ mbar
Turbo Pump Speed	1000 Hz
Vacuum Pump Load	0.8 - 1.2 A
Pole Bias	1.0
Hex Bias	4.0
Sample Cone	Ni, 1.1 mm aperture inner diameter
Micro-Skimmer Cone	Ni, 0.8 mm aperture inner diameter
Sample Depth	Adjusted daily[1]
Lens settings	Adjusted when appropriate
Nebulizer back pressure	~ 2.0 bar, optimized daily[1]
Nebulizer Flow Rate	400 µL/min
Sample Uptake Time	20 s
Rinse Time between Samples	20 s
Elements Measured	Na, Al, Cr, Co, Sr, Ag, Ba, La, Ce, Pb
Dwell Time per Element	Ag: 200 ms; Na, Al, Cr, Co, Sr, Ba, La, Ce, Pb: 10 ms

[1]Optimized to obtain a stable and high 115In signal (>500,000 cps for 10ppb) and lowest possible oxide formation rate

Table A.3. SM - Total snow depth at each snow pit

Snow Pit ID	Total Snow Depth [cm]
P1	191
P2	219
P3	210
P4	195
P5	130
P6	185
P7	202
P8	220

Table A.4. AgI seeding times for the March 24, 2015 storm

Ground Generator ID	Duration of AgI Seeding Time [MST]	Time Active [hr]
Aircraft	04:56 - 06:32	1.4
1	04:08 - 07:26	3.3
2	03:48 - 07:26	3.6
3	03:50 - 07:26	3.6
4	03:47 - 07:27	3.7
5	03:50 - 08:31	4.7
6	03:48 - 08:31	4.7
7	04:46 - 08:52	4.1
8	04:25 - 08:52	4.4
9	04:25 - 08:52	4.5
10	03:49 - 08:52	5.0
11	03:50 - 08:50	5.0
12	03:49 - 08:55	5.1
13	03:48 - 08:54	5.1
14	04:52 - 09:12	4.3
15	04:50 - 09:13	4.4
16	06:25 - 10:58	4.6

Table A.5. Mean crustal concentration (X_{crust}) to compute CEF

Element	**Ag**	**Al**	**Ce**	**Sr**	**Ba**
X_{crust} [g g^{-1}]	50 X 10^{-9}	80 X 10^{-3}	64 X 10^{-6}	350 X 10^{-6}	550 X 10^{-6}

Table A.6. Summary of AgI targeting from WY2015 - WY2016

	G	A	A + G
Snow storm layers sampled	21*	9	6
Snow storm layers with seeding signal	19	1	6
% Snow storm layers with seeding signal	90%	11%	100%

** One site is > 80 km downwind and lacked a signature. Omitting this site increased accuracy to 19/20 (95%).*

Table A.7. Summary of trace chemical sampling after clean field methods were established

Seeded storm sampled	# Sites sampled	Seeding method	Seeding signal* [%]	Peak Ag [ppt]	Wind speed [m s^{-1}]	Wind direction	Min/max temperature [C]
Mar 24, 2015	6	G	44	21	16	W	-14/-5
Apr 06, 2015	2	G	47	19	10	W	-10/-1
Nov 19, 2015	3	A	0	2.8	7	W	-11/-1
Dec 04, 2015	3	G	62	37	5	W	-12/1
Dec 07, 2015	1	A	20	14	9	W	1/3
Dec 08, 2015	1	G	60	13	9	W	-1/4
Dec 10, 2015	1	A	0	3.0	13	W	-9/1
Dec 11, 2015	1	A	0	1.7	4	SW	-8/-3
Dec 13, 2015	1	A + G	13	3.1	9	S	-6/0
Dec 19, 2015	4	G	75	9.5	5	SW	-11/-1
Dec 21, 2015	4	A + G	73	80	13	SW	-8/-3
Jan 29, 2016	3	A	0	2.6	8	SW	-9/1
Feb 18, 2016	4	G	58	14	8	SW	-4/2
Apr 14, 2016	1	A + G	93	7.3	5	SW	-7/2

A: Aircraft only
G: Ground generator only
** 'Seeding signal' is defined as replicated Ag concentrations greater than 3 ppt and an enrichment factor of 2.*

Table A.8. WY2016 results of precipitation increase by seeding method.

Grouping of storms	SNOTEL WRF-GFS [%]	SNOTEL WRF-NAM [%]
Ground generators – only	(15.3 ± 1.4)	(5.9 ± 1.1)
Aircraft – only	(7.8 ± 1.8)	(0.8 ± 1.3)
Ground generators & aircraft	(15.9 ± 2.1)	(3.1 ± 1.7)
Ground generators or aircraft	(10.4 ± 1.2)	(4.1 ± 0.9)
Seeded storms with sampled AgI signatures in snow	(33.5 ± 2.3)	(9.9 ± 2.1)

Table A.9. Global releases of silver in the environment

Reservoir	Source	Mass [tons]	Contribution [%]
Atmosphere	Metals production	30	1.2%
	Urban refuse combustion	10	0.4%
	Coal and petroleum combustion	9	0.4%
	Iron and steel production	7	0.3%
	Cloud seeding	3	0.1%
	Cement manufacture	2	0.1%
	Other	30	1.2%
	Total Atmosphere	91	3.7%
Aquatic	Soil erosion (natural)	428	17%
	Urban runoff	72	2.9%
	Sewage treatment plants	70	2.8%
	Photographic developing	65	2.6%
	Photographic manufacture	54	2.2%
	Other	6	0.2%
	Total Aquatic	695	28%
Terrestrial	Photographic industry	630	26%
	Urban refuse combustion	445	18%
	Sewage treatment	220	8.9%
	Metals production	165	6.7%
	Electrical contacts and conductors	150	6.1%
	Alloys and solders	60	2.4%
	Other	5	0.2%
	Total Terrestrial	1675	68%

*Table modified from [15] based on data from 1978.

Table A.10. Solubility product of common silver minerals (salts)

Silver Salt	Solubility Product (K_{sp}) [M]	Maximum Dissolved Silver Concentration [‰]
Silver nitrate ($AgNO_3$)	11	1.2×10^{3}
Silver chloride (AgCl)	8.3×10^{-6}	8.9×10^{-4}
Silver iodide (AgI)	9.2×10^{-9}	9.9×10^{-7}
Silver sulfide (Ag_2S)	2.6×10^{-17}	5.6×10^{-15}

[a]*Table modified from Williams* [2].

Table A.11. Drinking water and freshwater standards/guidelines

Standard	Potable Water Total Recoverable Ag [ppb]	Acute Toxicity of Dissolved Ag in Freshwater [ppb]	Source
Arizona DEQ	50	1+ [a,b,d]	[44]
Hawaii DEQ	50	3.2[b,d]	[45]
Idaho DEQ	100	3.4[b,c]	[46]
Wyoming DEQ	100	1.7[b,c]	[37]
U.S. EPA	100	3.2[b,d]	[47]
Australian EPA	100	0.05[e]	[38]
WHO	100	No standard	

a) 1 ppb is the minimum standard, standard increases with increased water hardness b) These standards are based on hardness values and Water Effective Ratios. Hardness is assumed 100 ppm for regulatory purposes; c) Coefficient multiplying total recoverable silver, used to estimate dissolved silver: water–effect ratio (WER) equals 1; d) Coefficient multiplying total recoverable silver, used to estimate dissolved silver: water–effect ratio (WER) equals 0.85; e) This standard is the 95% species protection level. This concentration is just the silver ion.

Table A.12. EPA data used to derive the water effect ratio (WER)

Concentration Ag (ppb)	Dissolved[a] Fraction (%)	Species[b]	Food[c]	Hardness [ppm]	Alkalinity [ppm]	Reference
0.19	74	DM	NO	47	37	[51]
9.98	13	DM	YES	47	37	[51]
4	41	DM	NO	36	25	[52]
4	11	DM	YES	36	25	[52]
3	79	FM	NO	51	49	[53]
2-54	79	FM	YES	49	49	[53]
2-32	73	FM	NO	50	49	[53]
4-32	91	FM	NO	48	49	[53]
5-89	90	FM	NO	120	49	[53]
6-401	93	FM	NO	249	49	[53]

a: "Dissolved" was defined as whatever passed through a 45 μm filter.
b: Two species were analyzed. DM = daphnia magna, FM = fathead minnow.
*c: The EPA memorandum stated the studies that included food probably reflected more realistic toxicity valu*e

Table A.13. Recent freshwater samples collected at AgI seeded areas

Project Location	Highest Ag (Mean Ag) [ppt]	Samples Collected	Date(s) Sampled	Source
Wyoming (pre-seeded)	192 (21)	40	October (23-25)-2005	[3]
Wyoming (seeded)	2 (< 1)	39	July (20-21)-2010	[15]
Idaho (2010-2012, seeded)	32 (9)	112	August 2010 – June 2012 (Highest sample collected June 24-2011)	2012 IPC Freshwater Sampling Report
Idaho (2015)11	45 (7)	24	March 20-2015	2015 IPC Freshwater Sampling Data Sheet

[11] Unlike other campaigns listed in this table, all samples were collected in one basin on the same day. Therefore, these data cannot offer insight on seasonal variations in flow rates known to modify the sediment loading – the speculated primary source of total recoverable silver in these samples.

Table A.14. Hypothetical scenario evaluating AgI environmental impacts

Primary Controls on Toxicity	Hypothetical (maximum) Values	Likely Values
% AgI dissolving into Ag+	100%	<<1% (Ksp = 9.2x10-9M) [2]
% increase in precipitation due to AgI	15%	3-15% [69]
Concentration of seeded snow	50 ppt	3-48 ppt [15][61] [18]b
% of AgI in snow reaching water bodies	100%a	Variable, but <100%

a: This assumes no sorption to soil particles in the upper horizon or uptake by vegetation.
b: 1 sample out of 1,300 had a concentration exceeding 48 ppt Ag.

APPENDIX B

Figures

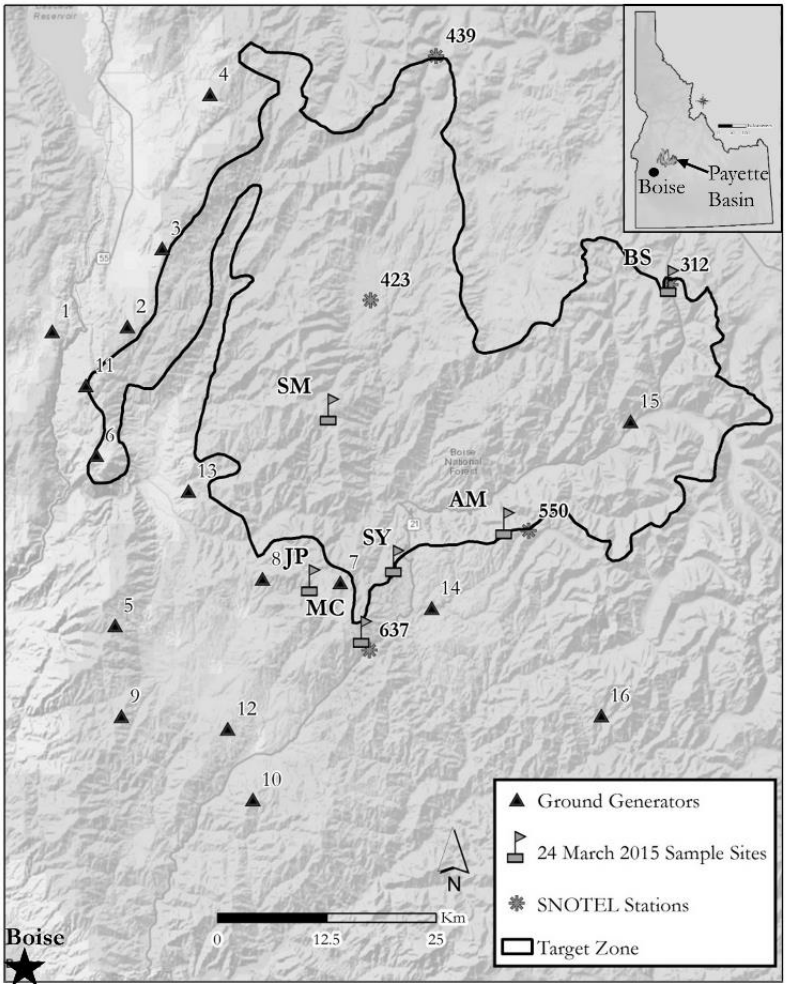

Figure B.1. The black outline delineates the Payette Basin. Above there are five SNOTEL sites, six sampling sites, and 16 ground generators near the Payette Basin. Three-digit identification numbers are listed above SNOTEL sites.

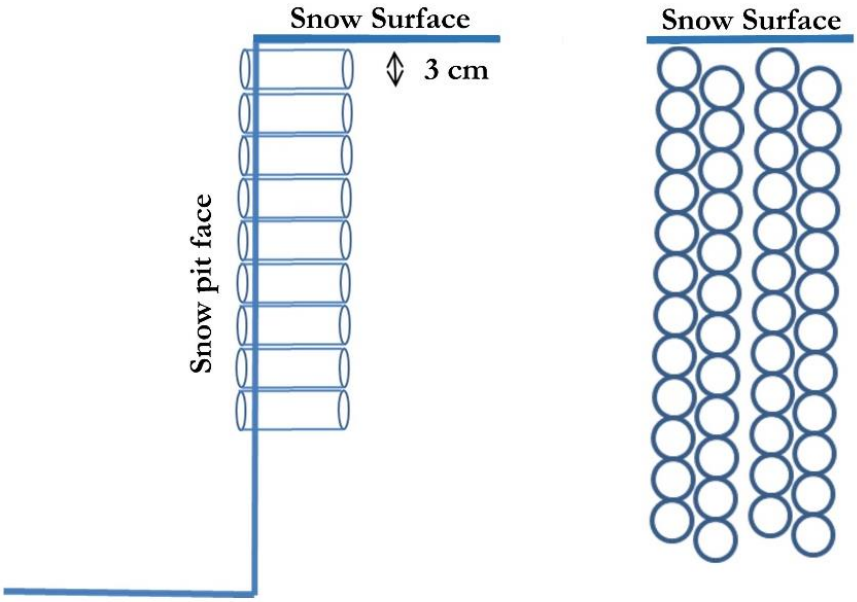

Figure B.2. Diagram illustrating the snow sample collection method. A) 3-cm diameter vials were inserted perpendicular to the snow pit face. B) Four columns of vials were used to collect samples from each snow pit. Vials in each two-column set were are staggered by 1.5 cm.

Figure B.3. A) 4% HNO_3 rinse solution B) Autosampler C) Plastic cover surrounding the autosampler D) Tubing delivering sample from the autosampler to the ICP-MS.

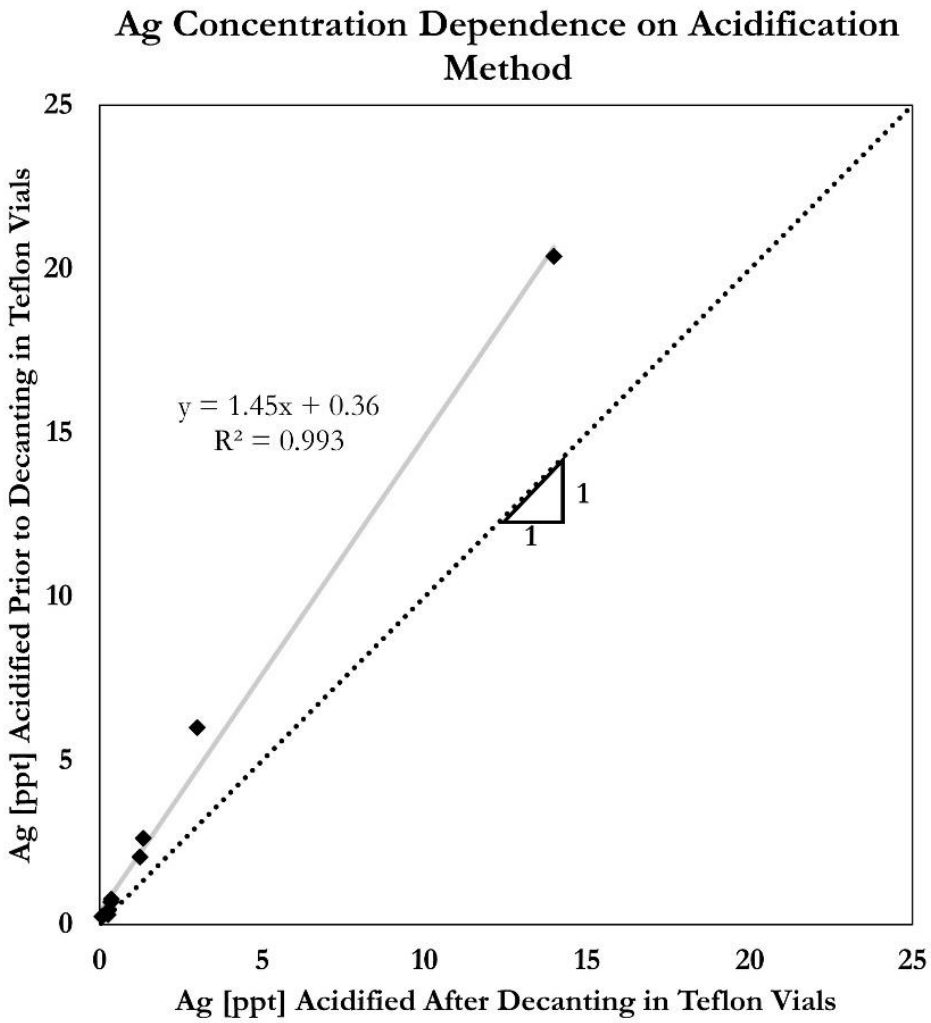

Figure B.4. Ag concentrations depend on the acidification method. Each point represents a lab replicate analyzed two ways: acidifying prior to decanting to Teflon vials (y-axis) and after decanting to Teflon vials (x-axis).

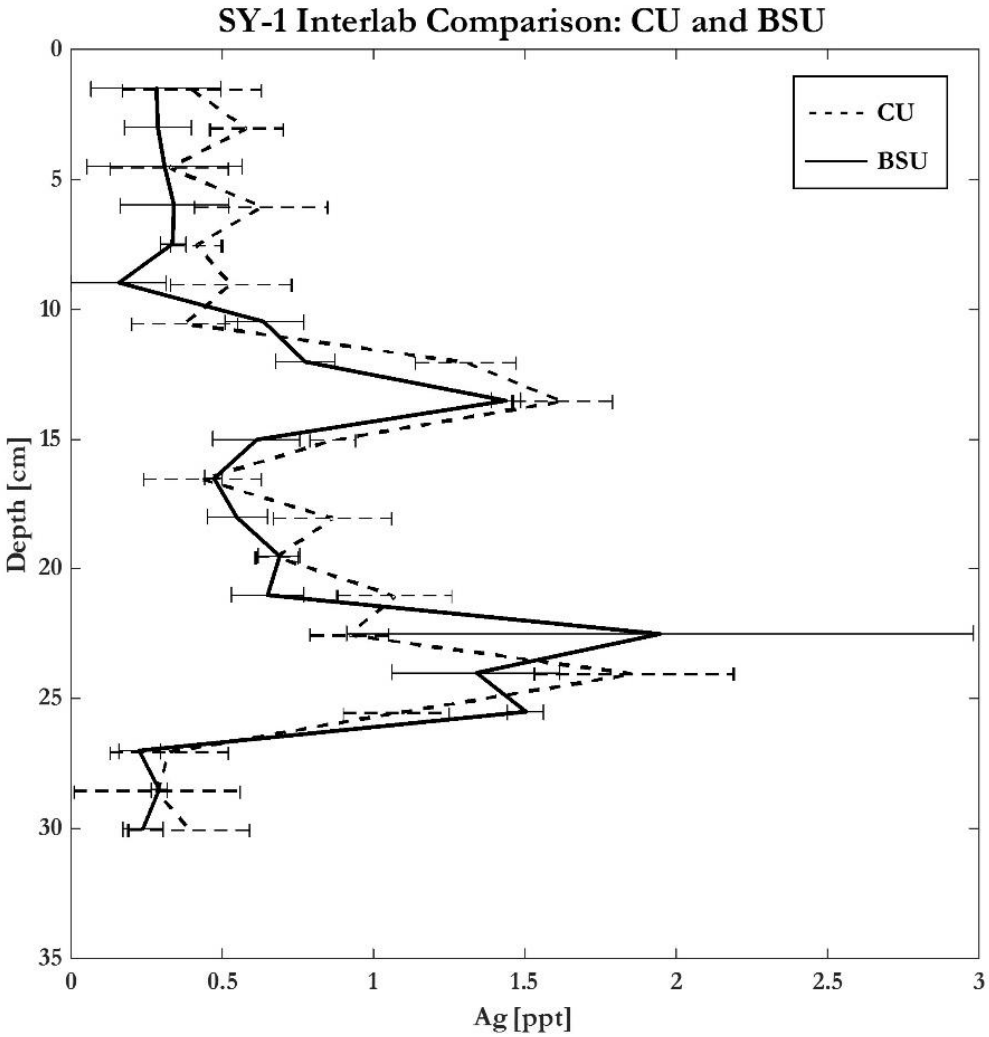

Figure B.5. Boise State University's (black) Ag profile was comparable to the profile analyzed at Curtin University's TRACE laboratory (grey). Error bars denote the range of values obtained from the replicate profiles analyzed.

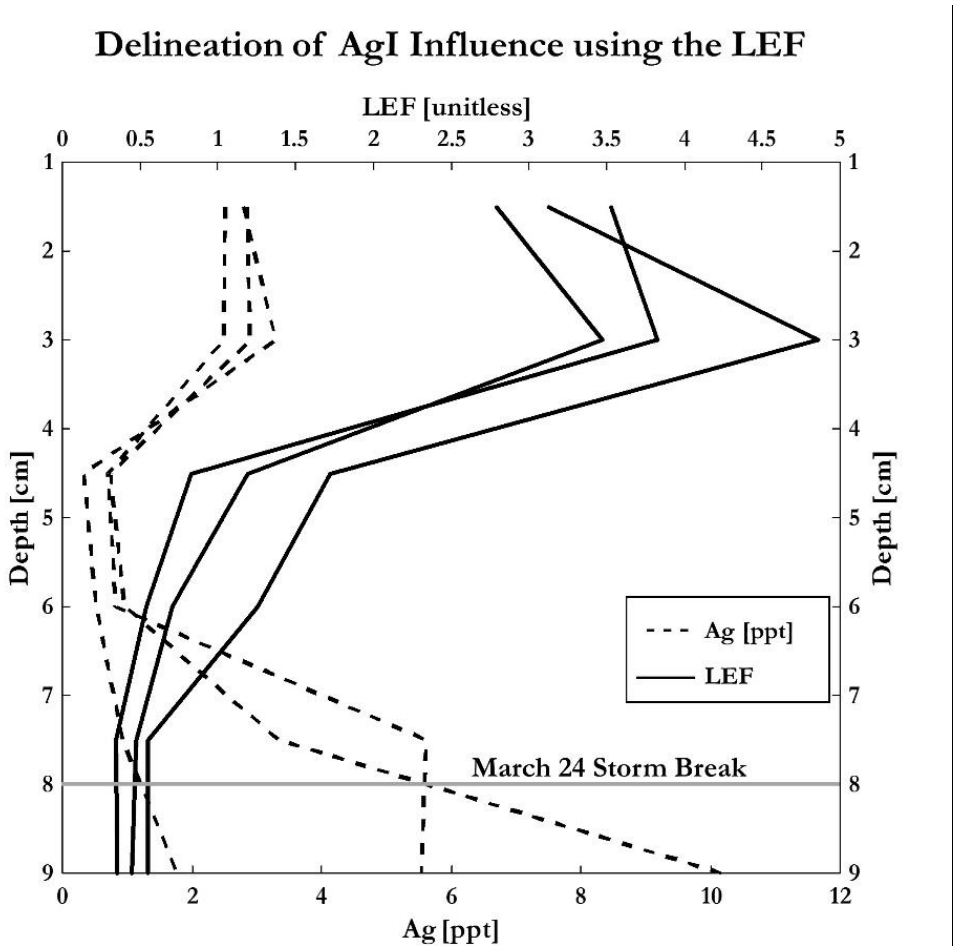

Figure B.6. Three replicate profiles of Ag concentrations (grey) were analyzed at site AM. The corresponding LEF values (black) normalize silver concentrations to 4 other trace elements commonly associated with dust.

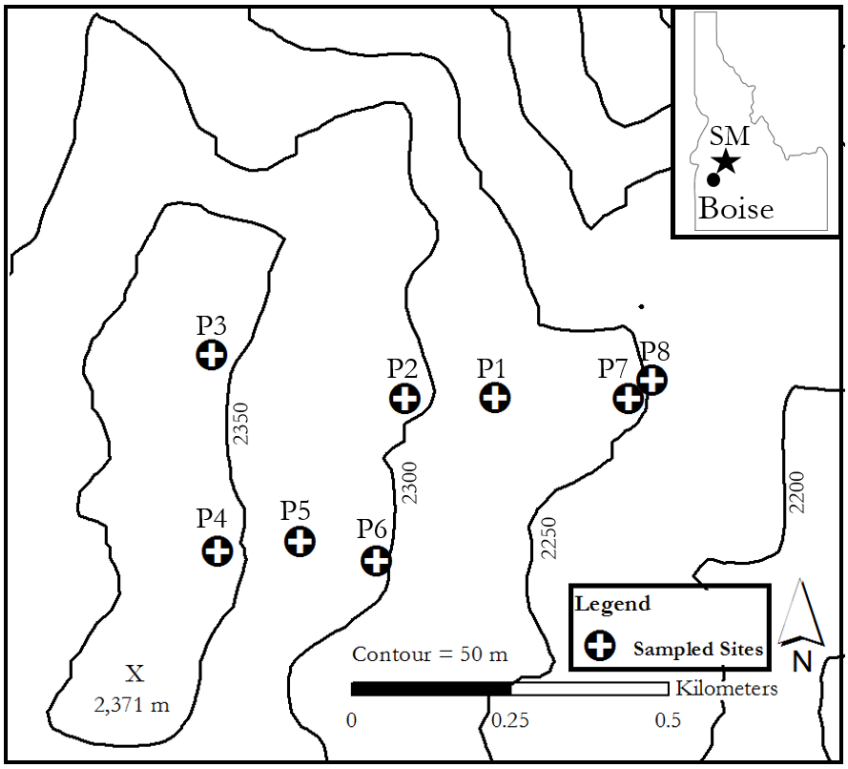

Figure B.7. A small-scale variability test was conducted within this 0.25 km^2 area where sampling sites were as indicated.

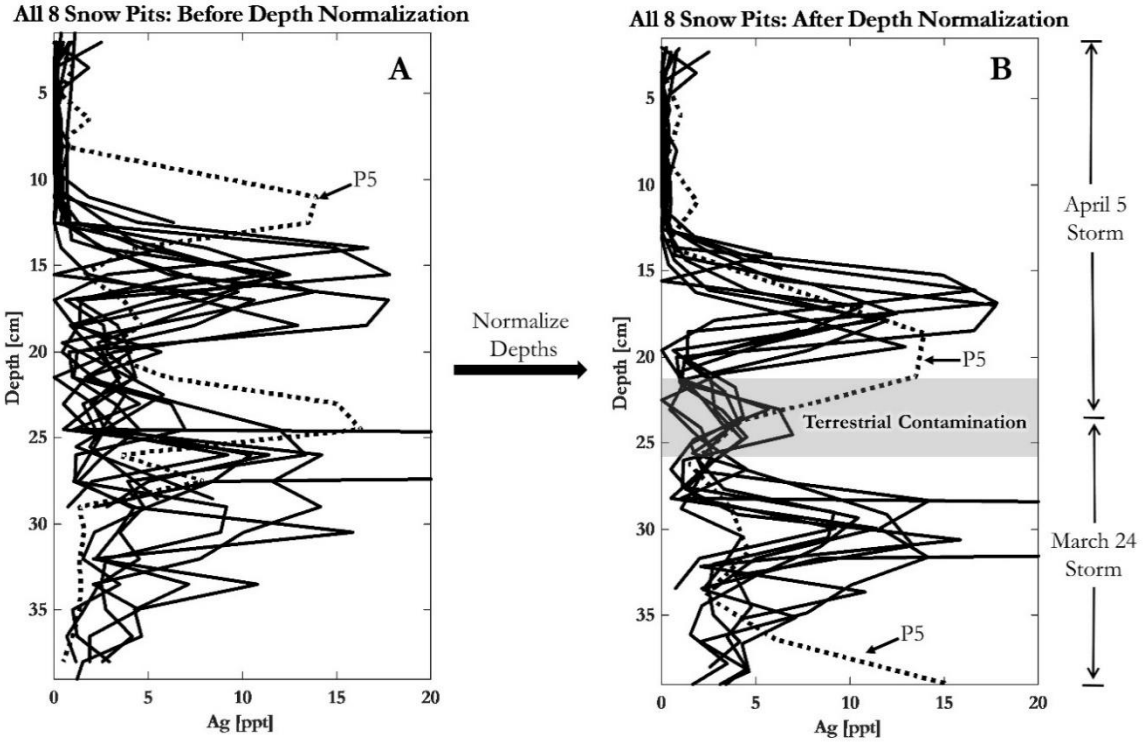

Figure B.8. Plots of Ag concentration from all eight snow profiles used in the small-scale study. A: Ag concentration profiles using the actual snow depths at each site. B: Ag concentrations using profile depths normalized to the site (SM) with the greatest depth. Storm delineations are shown to the right of Plot B. The shaded region in Plot B shows the storm break with a visible dust layer. The outlier Ag profile, P5, was plotted as a dotted line.

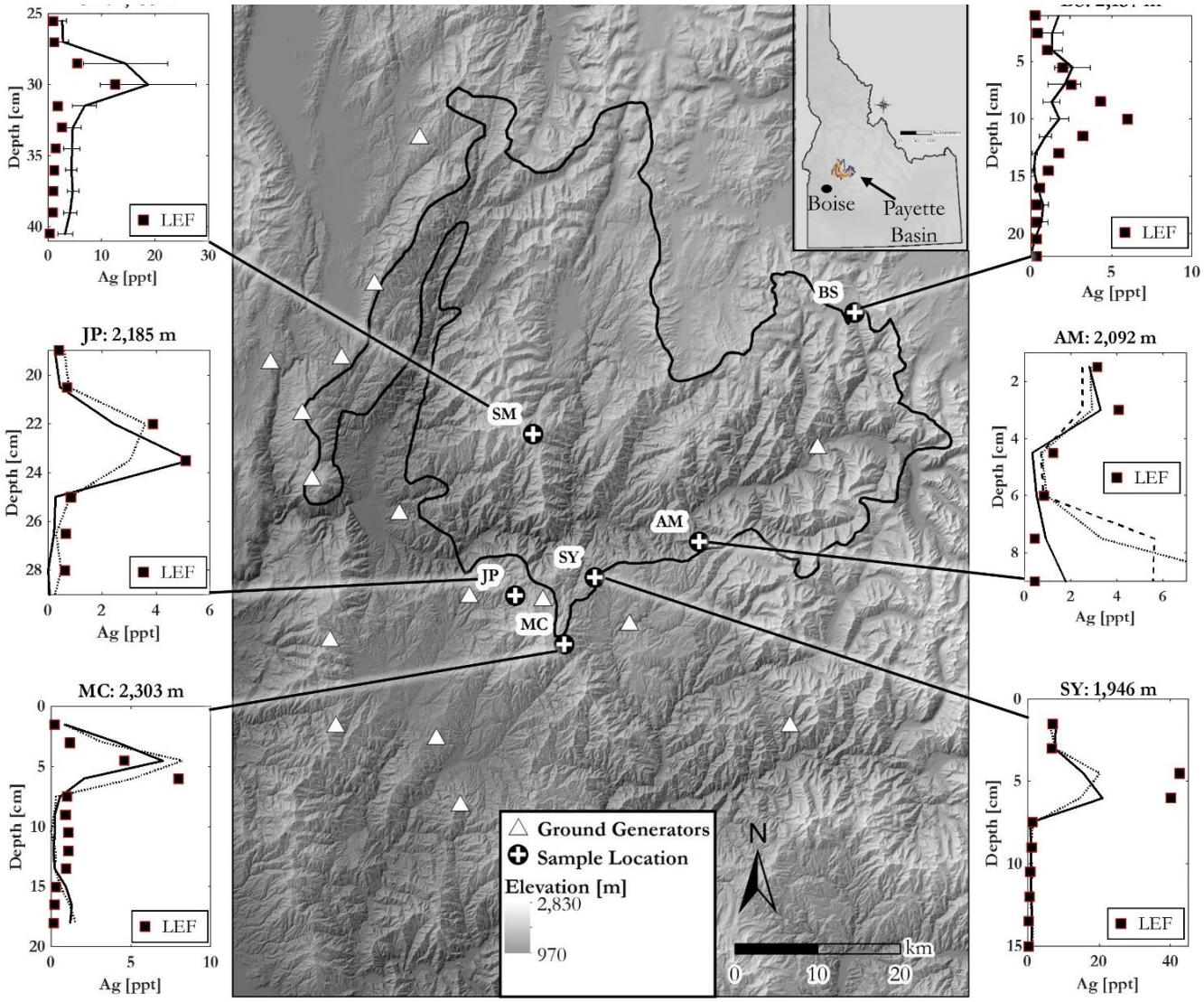

Figure B.9. Six sites were sampled for the March 24 seeded storm event. Multiple pits sampled were constructed at plots A (n = 8 pits) and D (n = 4 pits). Plots A and D display the mean Ag concentration and average error for each snow pit layer (Equation 4) computed using 1.5 cm moving window. Ag profile depths in plots A and D were normalized relative to the total snow depth of the deepest snow profile.

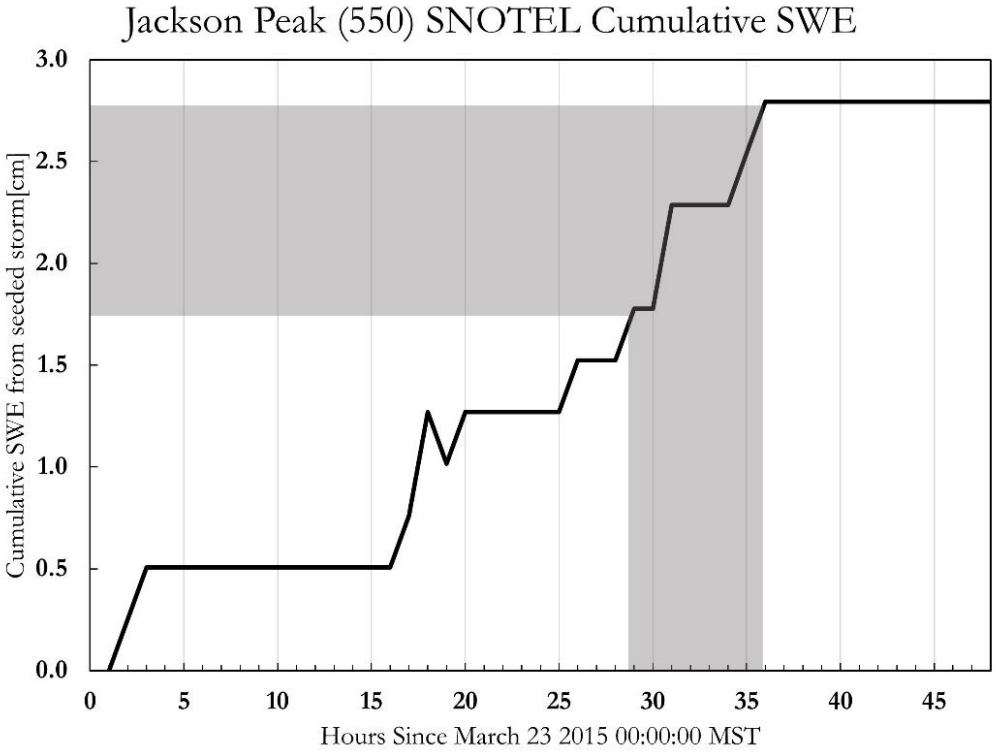

Figure B.10. Cumulative SWE of a SNOTEL site within the Payette Basin. Shaded region covers the duration of AgI seeding and corresponding snow potentially enriched with AgI. Note that 0-24 on the x-axis is the snow deposited from March 23 (unseeded).

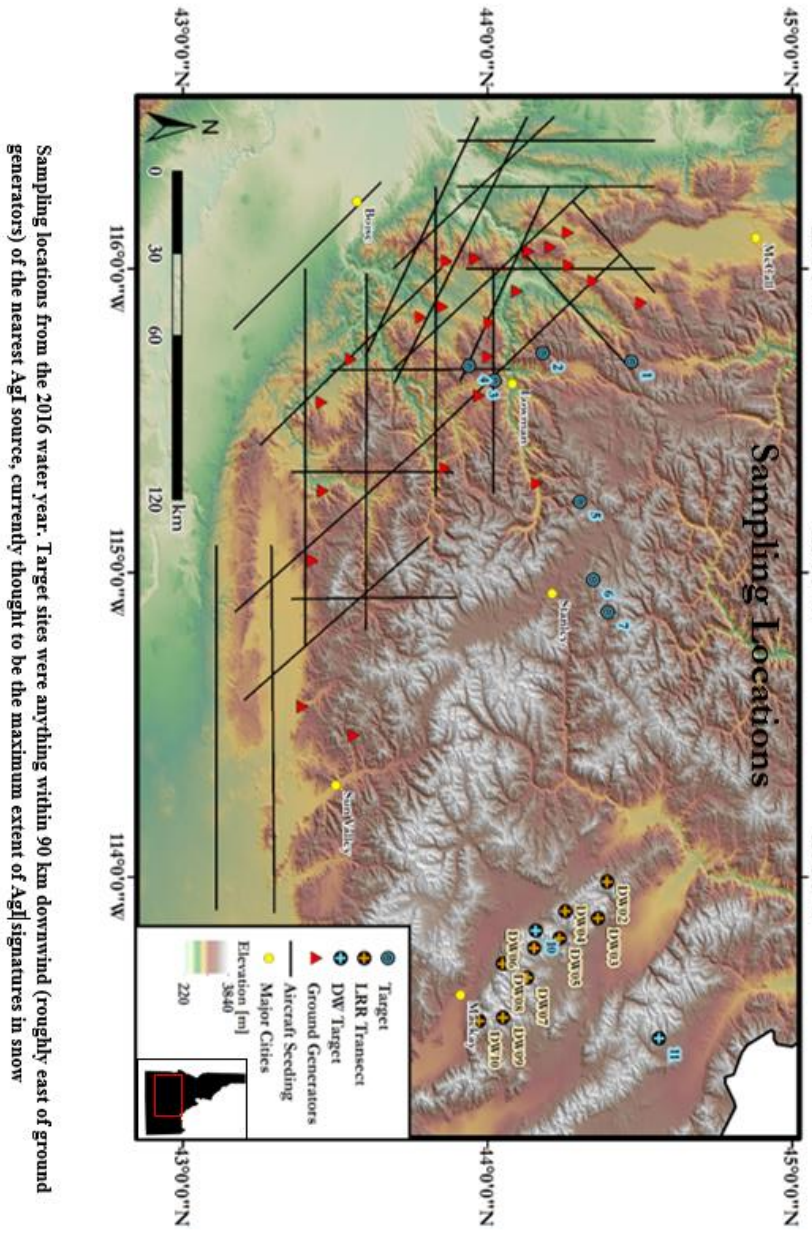

Sampling locations from the 2016 water year. Target sites were anything within 90 km downwind (roughly east of ground generators) of the nearest AgI source, currently thought to be the maximum extent of AgI signatures in snow

Figure B.11 Sampling Locations

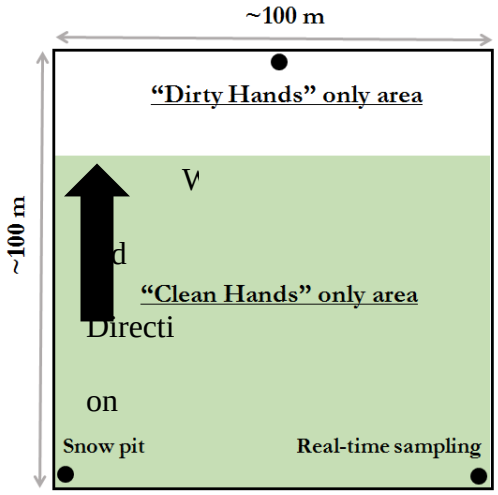

Figure B.12. Sampling sites were divided into two areas. "Clean hands" and acid washed equipment were permitted in upwind areas, where snow pit method and real-time method sample collection took place. "Dirty hands" operated in regions downwind of sample collection and handled equipment not acid washed (snow thermometers, density cutters, field books, etc.).

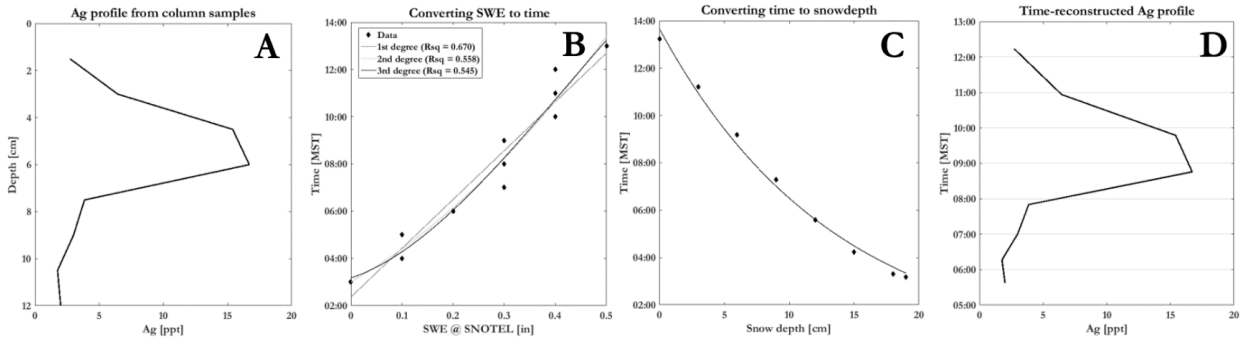

Figure B.13. A) Typical column sample profile, collected at 1.5 cm resolution. B) Time and SWE from a SNOTEL station nearest to the snow pit collected in plot A. 1st, 2nd, and 3rd degree polynomials model these relationships. C) Depth in the snow pit related to time from plot B. D) Reconstructed Ag profile in terms of time.

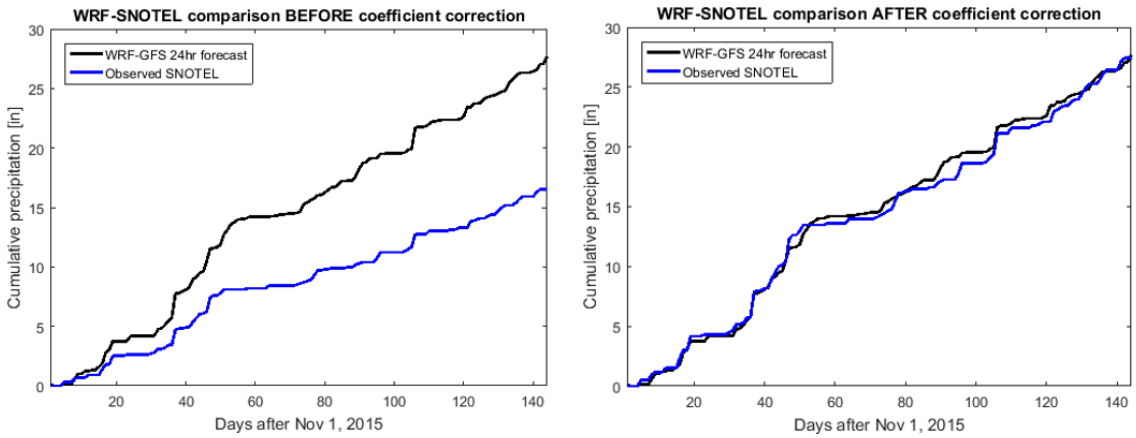

Figure B.14. Normalizing approach for the WRF-SNOTEL comparison. Cumulative wintertime precipitation before normalizing data (left) and after (right) for a SNOTEL station drastically under-predicted by a model.

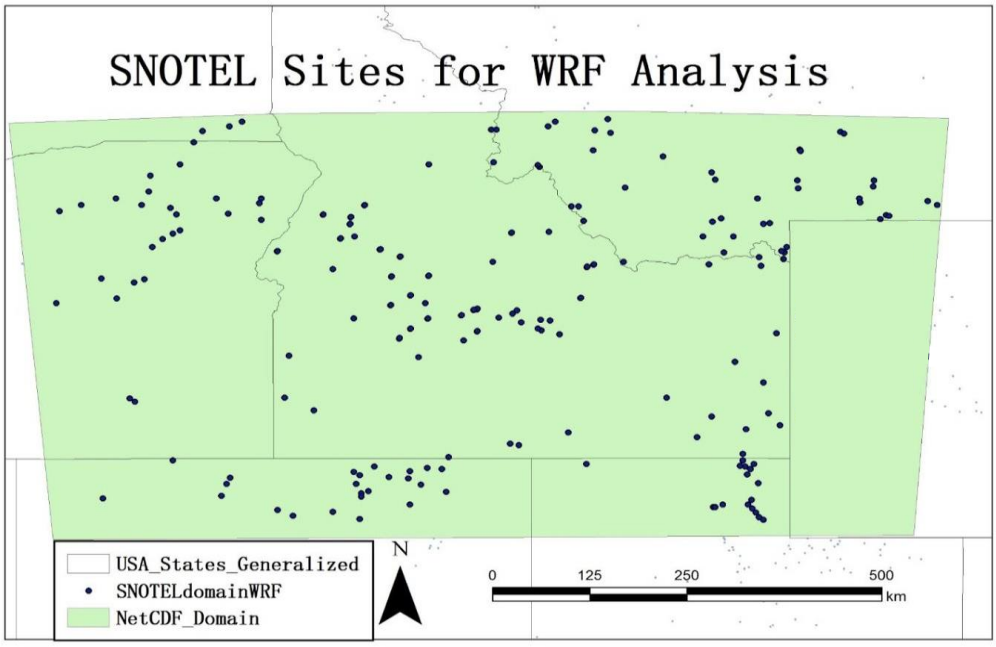

Figure B.15. WRF Domain (green shading). There are 171 SNOTEL sites considered in this study (blue dots). Wyoming was not considered due to an adjacent cloud seeding project outside or region of interest.

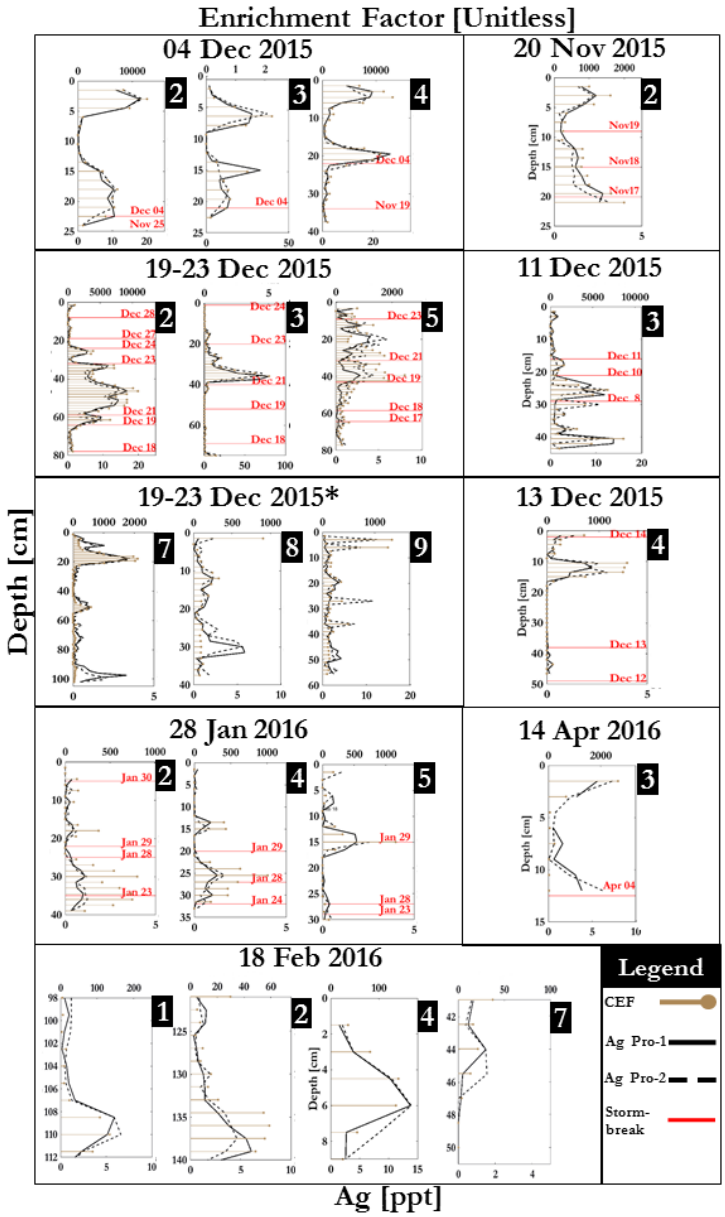

Figure B.16. Solid and dotted black lines are two profiles of samples collected using the column method. Silver concentrations in ppt and values are the bottom x-axis. Gold ball and sticks are enrichment factors (values are the upper x-axis). Black numbers in the upper right corner correspond to Figure 1. Red lines delineate snow from different storms.

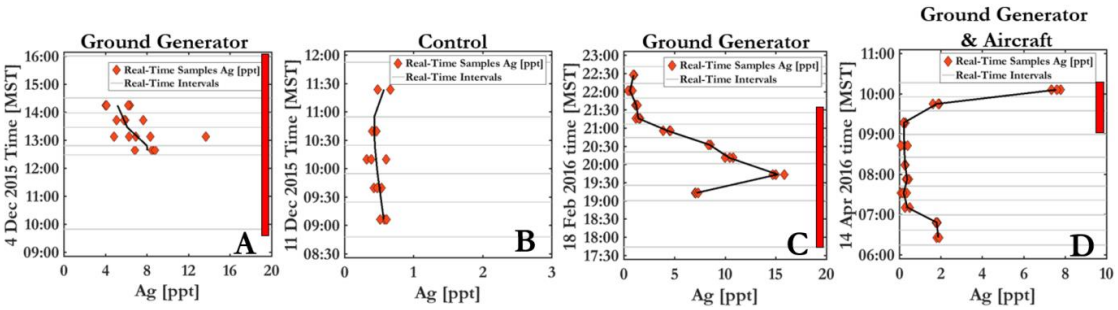

Figure B.17. All 4 real-time sampling results from the season. Red bars denote times of ground generator seeding. Light grey lines delineate sampling intervals. Orange diamonds denote silver concentrations of samples collected at times between the grey lines. Subplots were sampled from sites 2, 5, 4, and 5 respectively.

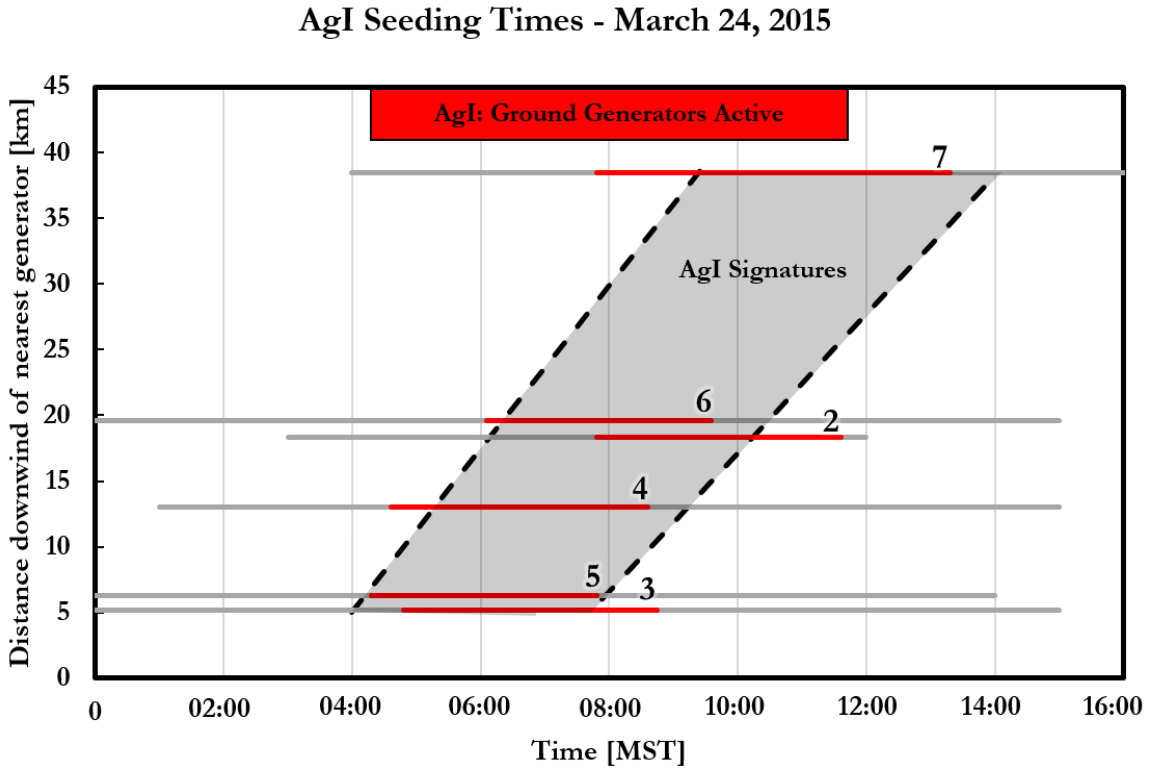

Figure B.18. The time-delineation methods constrained the timing of AgI signatures in snow for the March 24, 2015 storm (ground generator only). Red lines denote modeled times with replicated AgI signals. Grey lines denote portions of the snowstorm void of AgI signatures. Black numbers on plot are site ID's corresponding to Figure 1.

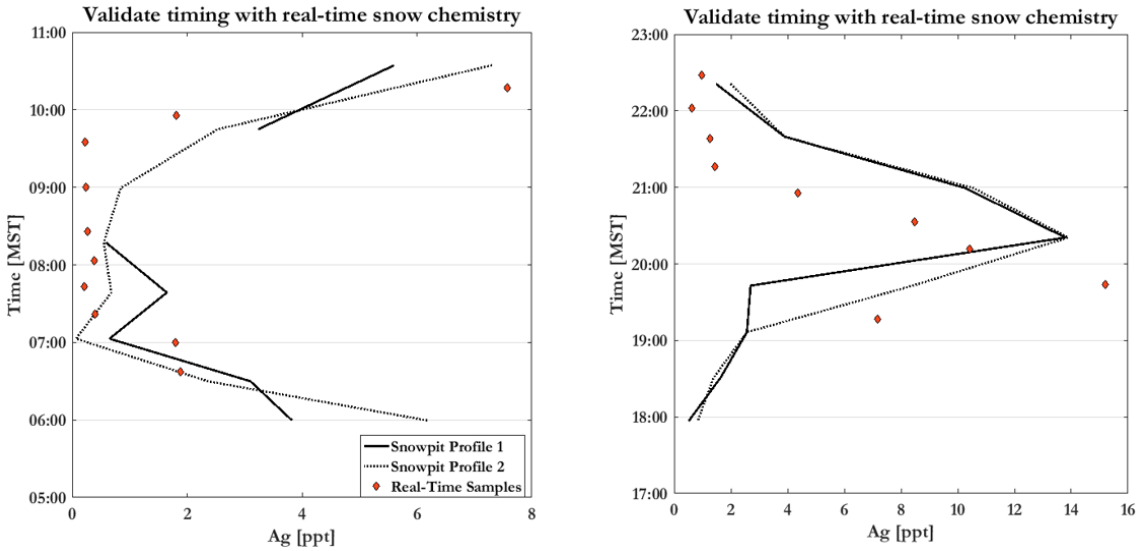

Figure B.19. Validation of time-delineation methods. We compare real-time samples (orange diamonds) with time-delineated column samples (each black line is a profile of column samples). These data are from sites 5 and 4, respectively.

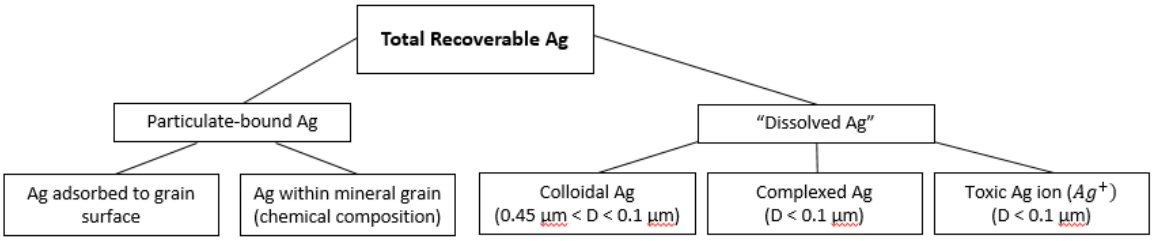

Figure B.20. The form of silver is important when assessing toxicity. Quantifying total recoverable silver does not adequately address the threat of that silver level to the environment. The most toxic silver species, the silver ion, is essentially the non-complexed quantity of silver passed through a 0.1 µm filter (to eliminate colloids). D is the maximum diameter of the silver bearing species. D < 0.1 µg are silver species smaller than colloids (loosely defined as particulates sizes between 0.45 µg and 0.10 µg).

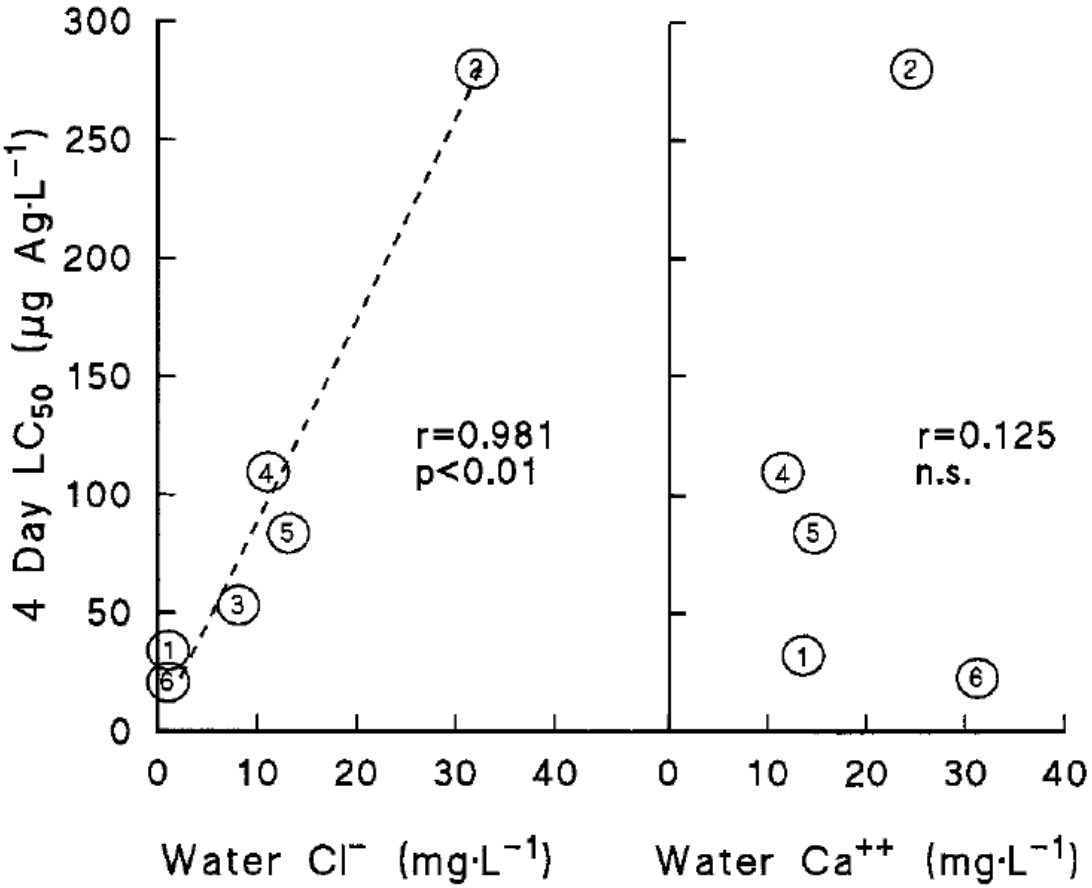

Figure B.21. This figure and caption are from Hogstrand (1996) [29]. Plot of data published by Lemke [31] on the toxicity of $AgNO_3$ to juvenile rainbow trout, indicating the close correlation between toxicity and water [Cl^-], and the lack of importance of water [Ca^+] in modifying 96-hour LC50. Numbers refer to the coded laboratories in the original report [of the inter-laboratory comparison].

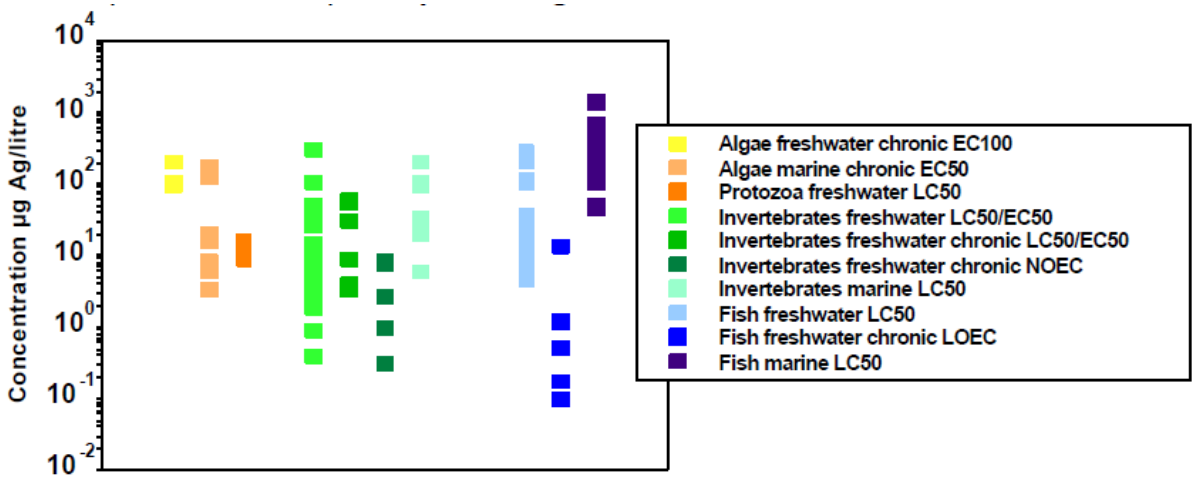

Figure B.22. "Plotted values are from studies where silver was added to the medium as silver nitrate and the silver was likely to be present as the free ion (a scenario unlikely in the environment)." [20].

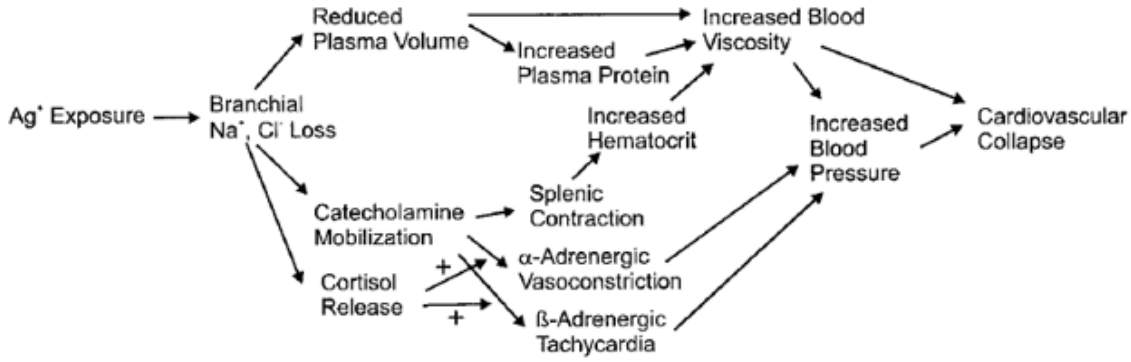

Figure B.23. "Suggested etiology of acute silver toxicity in freshwater fish. Exposure to the free silver ion, Ag^+, results in a net loss of Na^+ and Cl^- from the blood plasma. This osmolyte loss causes a sequence of events that eventually leads to a fatally increased blood viscosity and blood pressure. Cardiovascular collapse is likely to be the final cause of death". Figure and caption directly from [29].

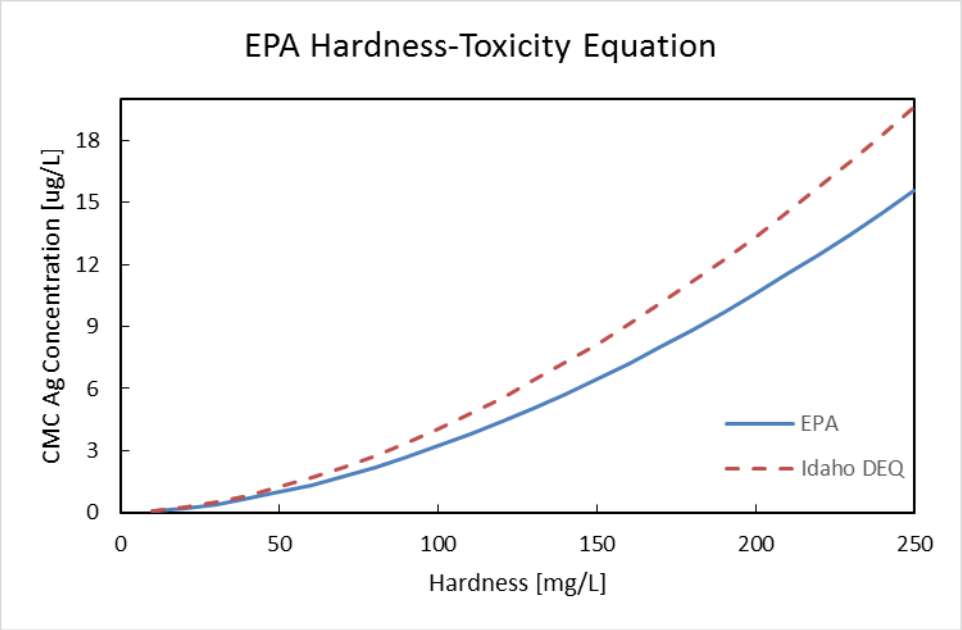

Figure B.24: EPA standards applied as a function of hardness. Generally, hardness values in natural environments in Idaho typically reside between 60 and 120 ppm [54]. Idaho DEQ standards are slightly less stringent.

APPENDIX C

Pictures

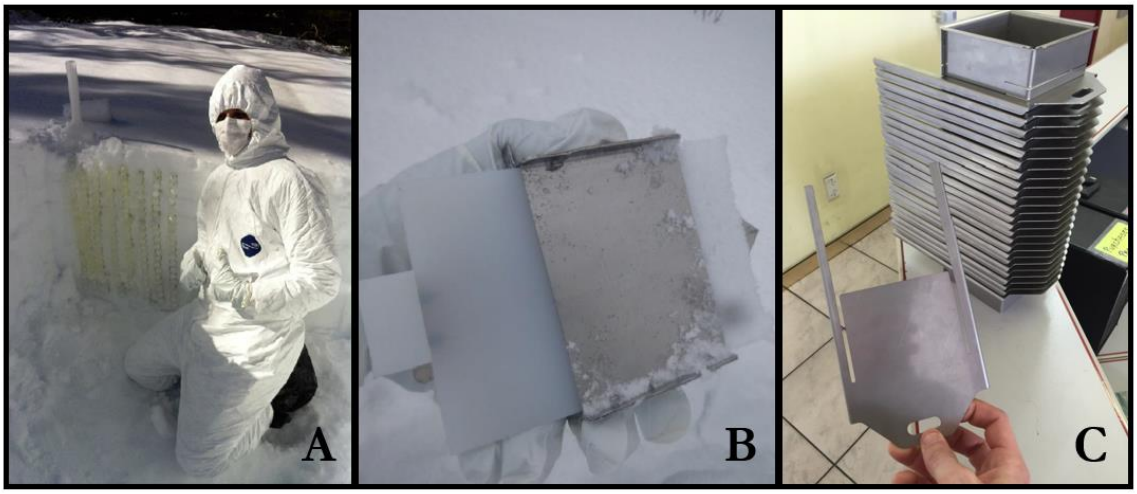

C.1. The three sampling methods tested in season one (2015 Water Year). A) Column sampling method with 3 cm diameter, 50 mL polypropylene vials. Collected samples at 1.5 cm resolution. B) Stainless Steel Sampler (aka "S3"). An all-304 stainless steel density cutter, triple acid washed with a Teflon 'plunger' to liberate all snow inside. Collected samples at 1.5 cm resolution. C) The High Resolution Silver Sampler (aka "HRSS") developed by Ross Edwards at Curtin University. Samples collected at 1 cm resolution.

C.2. Snow pit methods. “Dirty hands” is performing duties that are more susceptible to causing contamination downwind and out of the pit (labeling, opening and closing plastic bags, and taking notes). “Clean hands” only touches triple acid washed vials and in the snow pit.

APPENDIX D

D.1. How much Ag accumulates in snow adjacent to a ground generator?

D.1.1 Goal

The purpose of this calculation is to predict how much silver is coagulating about the ground generator. These results are based on the 32 samples collected on April 15, 2015, adjacent to the Packer John generator. AgI coagulation is a known problem that reduces the amount of active ice nuclei, and ultimately reduces cloud seeding efficiency.

The subsequent outcome of this study is to identify whether Ag concentrations in snow are high enough to adversely affect the environment. This calculation merely sums the mass. Appendix C.1. addresses the environmental impacts.

D.1.2 Assumptions

1. Assume all snow within 5 meters of the generator has a concentration of 2735 ppt (g g-12) (equation 1 assuming x=5 for all x less than or equal to 5).
2. Concentrations of silver (Ag) decrease with distance from the generator according to the best-fit equation sampled.
3. Ag concentrations are computed every meter using Equation 1. The Riemann sum of these meter intervals Ag concentrations multiplied by area rings (AR) approximates the total silver mass in snow surrounding the Packer John generator.
4. Natural, background Ag concentrations are assumed to be 2 ppt. Silver due to the generator is calculated as any silver concentrations exceeding 2 ppt.
5. The Packer John generator site is assumed to have identical SWE values as a nearby SNOTEL site of equal elevation and climate - Bear Creek Summit (338).
    a. Bear Creek Summit SNOTEL averages 61.2 cm of cumulative SWE from snow between Nov10 to Apr 10.
6. Assume the silver did not concentrate while melting (we sampled April 15, so Ag concentrations were likely higher than would be expected in fresh snow).

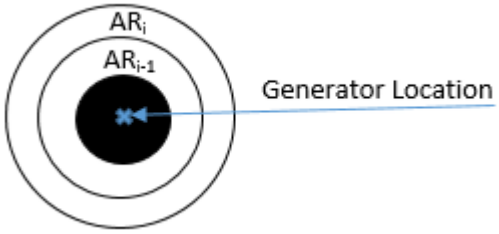

Figure D.1. Total mass of silver in snow was calculated by discretizing the snowpack into 1 meter wide Area Rings (denoted AR). Each ring is assumed to have a uniform Ag concentration using based on *Equation 1*.

D.1.3 Calculation

[1] $Ag_i = 35614.69x^{-1.59472}$

Ag_i = Concentration of Ag [ppt]

X = distance from the generator [m]

[2] $Ag = \sum_{i=1}^{460}((Ag_i - Ag_{nat}) * (AR_i) * (SWE))$

Ag = total mass of silver in snow sourced from the ground generator [g]

Agi = Concentration of silver in area AR^i, estimated using *Equation 1* [ppt]

Ag_{nat} = Natural background concentrations of Ag = 2 parts per trillion [ppt]

AR_i = Area of ring [dm^2]

SWE = Total wintertime SWE at the Packer John generator site [dm]

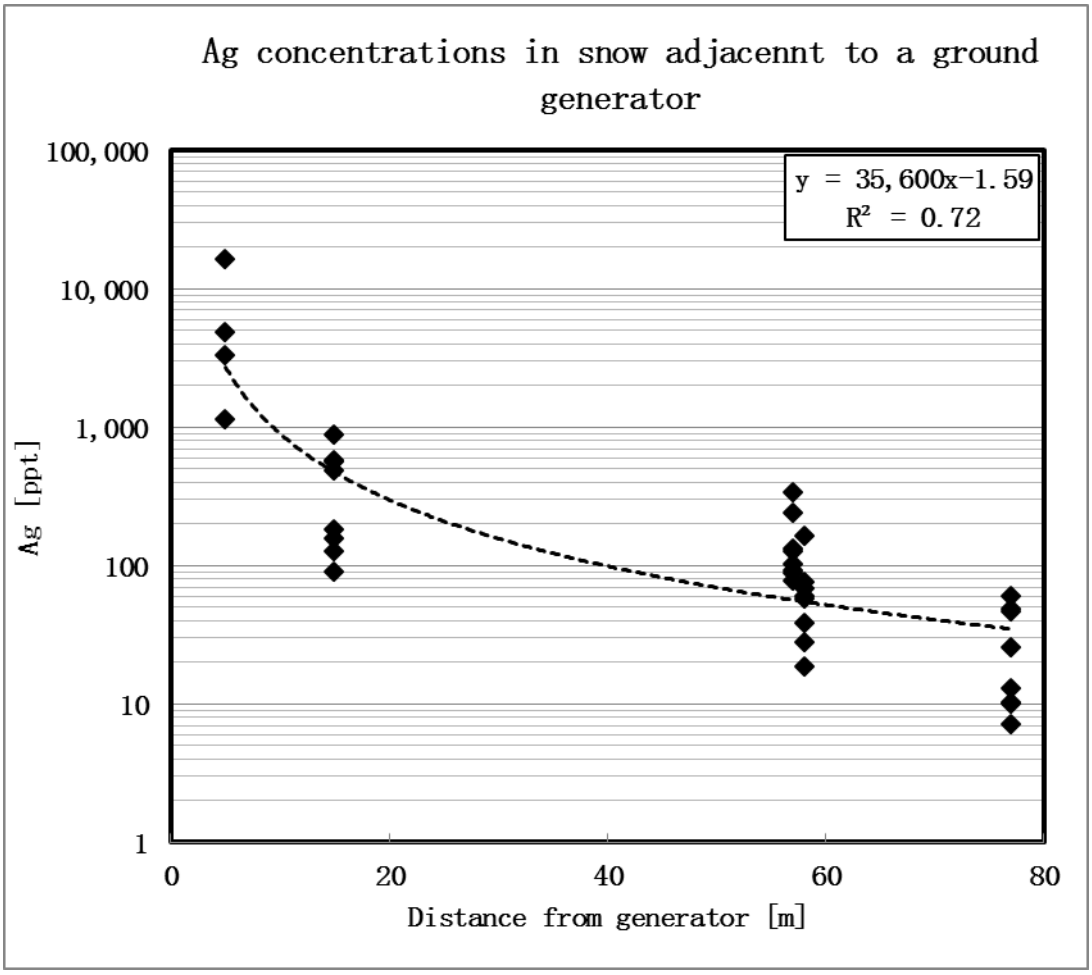

Figure D.2. Equation used to estimate silver concentrations in snow as a function of distance from the generator

D.1.4 Results

Equation 1 resulted in 0.7 g of silver deposited in the 0.26 mi^2 area of snowpack surrounding the generator. This is insignificant relative to the amount of silver released in a typical winter season. For instance, assuming the Packer John generator ran for 20 hours for a winter season (below average) with burn rates of 23 g/hr, then the total silver leaving the generator would be

$$Ag = (burn\ rate) * (time\ seeding) * \left(\frac{Mass\ of\ Ag}{Mass\ of\ AgI}\right) = 23\ \frac{g}{hr} * 20\ hr * \left(\frac{107.8\ g}{234.8\ g}\right)$$

$$= 211\ g$$

In summary, 0.7 grams of silver is concentrated in snow surrounding a generator releasing approximately 211 grams of silver per winter season. In other words, only 0.3% of annual AgI released in the winter are concentrate in the 0.26 mi^2 area surrounding the ground generator. This neither causes concerns for excessive coagulation nor would these concentrations trigger known adverse environmental impacts.

D.2. Bioaccumulation of AgI in soils adjacent to ground generators

D.2.1 Goal

This section computes the 'worst case scenario' of silver accumulation in soil after 50 years of cloud seeding. The 'worst case scenario' snow concentrations would occur adjacent to a ground generator, where AgI aerosols tend to coagulate and accumulate adjacent to the release point. In this calculation, we estimate the total silver accumulation in the upper soil horizon on a 1 cm x 1 cm square of surface area. The main assumption in this study is all silver for 50 years will accumulate in the upper 10 cm. This 'worst case scenario' calculation will determine whether any known adverse environmental impacts will occur long-term adjacent to a ground generator.

D.2.2 Variables

Variable	Value	Source
Soil bulk density [mg/cm^3]	1300	[1,2]
Depth of soil profile [cm]	10	-
Ag concentration in soil [ppt]	550,000	[2-4]
Ag concentration in snow [ppt]	2,735	2015 Field data next to a ground generator
Wintertime cumulative SWE [cm]	61	SNOTEL site 321

D.2.3 Assumptions

1. Snow silver concentrations adjacent to the ground generator are a function of 32 snow samples collected on April 15, 2015. Silver concentrations were interpolated to a two-dimensional surface using a weighted distance function.
2. Assume all snow within 5 m radius of the generator has Ag concentrations of 2,735 ppt every year (based on the average of the 4 snow samples closest to the ground generator)
3. Assume 100% of wintertime precipitation is seeded adjacent to the ground generator
4. Soil Ag concentration of 0.55 mg/kg (this is the average of the 0.1 to 1 mg/kg Ag concentrations typically found in natural soils.
5. Assume lateral migration of meltwater is negligible and silver is adsorbed exclusively in the upper 10 cm of the soil.

D.2.4 Calculation

Mass of soil in a 1 cm by 1 cm surface area, 10 cm deep sample

$$m_s = \rho_s * A * d = 1{,}300 \frac{mg}{cm^3} * (1\ cm^2) * (10\ cm) = 13{,}000\ mg$$

m_s = mass of soil in a 1cm x 1cm x 10cm deep soil profile [mg]

ρ_s = bulk density of soil [mg/cm^3]

A = Area of ground surface [cm^2]

d = depth of soil accumulating all silver [cm]

Amount of silver in the upper 10cm naturally abundant

$$Ag_m = m_s * (Ag_{soil}) = (13{,}000\ mg) * \left(5.5\ x\ 10^{-7}\frac{mg\ Ag}{mg\ Soil}\right) = 0.00715\ mg$$

Ag_m = mass of naturally occurring silver in a 1cm x 1cm x 10cm soil profile

m_s = mass of soil in a 1cm x 1cm x 10cm deep soil profile [mg]

Ag_{soil} = concentration of silver in natural (unseeded) soils [mg/mg]

Ag contribution to the upper 10cm of soil per year

$$Ag_{SWE} = (Ag_{AgI}) * (SWE_w) * A * \rho$$

$$= \left(2.73\ x\ 10^{-9}\frac{mg}{mg}\right) * \left(61\frac{cm}{yr}\right) * (1\ cm^2) * \left(1{,}000\ \frac{mg}{cm^3}\right)$$

$$= 0.000167\frac{mg}{yr}$$

Ag_{SWE} = Mass of silver in snow due to AgI per winter season [mg/yr]

Ag_{AgI} = Concentration of snow within 5 m of the ground generator [mg/mg]

SWE_w = Cumulative wintertime SWE at Bear Creek Summit SNOTEL [cm/yr]

A = Surface area if interest [cm^2]

ρ = water density [mg/cm^3]

Change in Ag concentration in upper 10cm after 50 years of cloud seeding assuming all AgI accumulates in upper 10cm of soil

$$Ag_{snow} = Ag_{soil} + (Ag_{SWE} * t) = (0.00715\ mg) + \left(0.000167\ \frac{mg}{yr}\right) * (50\ yrs)$$

$$= 0.0155\ mg$$

Ag_{snow} = mass of Ag in a $1cm^2$ x 10cm soil column after 50yrs of seeding [mg]

Ag_{soil} = mass of Ag in 1cm x 1cm x 10cm soil column [mg]

Ag_{SWE} = annual silver mass accumulation rate due to AgI [mg/yr]

t = time actively cloud seeding [yr]

The new soil concentration after 50 years of AgI accumulating in the soil

$$Ag_s = \frac{Ag_{snow} + Ag_{soil}}{m_a} = \frac{(0.00715mg + 0.00835)\ mg}{13{,}000\ mg} = 1.19\ x\ 10^{-6}\frac{mg}{mg} = 1.19\ ppm$$

Ag_s = Ag soil concentration after 50 years of cloud seeding [mg/mg]

Ag_{snow} = Ag accumulations from 50 years of AgI seeded snow [mg]

Ag_{soil} = concentration of silver in natural (unseeded) soils [mg/mg]

m_s = mass of soil in a 1cm x 1cm x 10cm deep soil profile [mg]

D.2.5 Brief Discussion

An increase from (an estimated) 0.55 mg/kg to 1.19 mg/kg in the upper 10 cm of the soil profile adjacent to the ground generator. After 50 years of cloud seeding, soil silver concentrations are still within the range of natural concentrations in many environments [2].

This calculation assumed the worst case scenario. Only the 4 highest concentrations of silver in snow were used (all collected 5 m from the generator) and we assumed the entire snowpack every year for 50 years was entirely seeded. Finally, we assumed 100% of silver was adsorbed in the upper 10 cm of soil, leaving silver-free water to percolate below the upper-most 10 cm of soil. Obviously, each one of these assumptions are extremely conservative, resulting in the absolute maximum possible AgI accumulation adjacent to a ground generator. In nature, observed values adjacent to a ground generator are likely less than 25% of these results.

Soil concentrations have to be several mg/kg of insoluble silver in order for acute toxicity symptoms to occur in the most sensitive terrestrial species (mushrooms, leafy plants) [3 - 7]. Leafy plants and mushrooms have the highest capacity to bioaccumulate through silver uptake. The 0.64 mg/kg (‘worst case scenario’) addition of silver due to AgI is unlikely going to affect even the most sensitive plants.

D.2.6 References

[1] K. Froese, “Bulk density, soil strength, and soil disturbance impacts from a cut-to-length harvest operation in north central Idaho”. University of Idaho Thesis, Moscow, ID, pp. 1-81, 2004.

[2] S. E. Tsiouris, F. A. Aravanopoulous, I. N. Papadoyannis, M. K. Sofoniou, N. Polyzopoulos, M. Christodoulou, V. F. Samanidou , G. A. Zachariadis and H. A. Constantinidou, “Soil silver content of agricultural areas subjected to cloud seeding with silver iodide,” *Fresenius Environ. Bull.*, vol. 11, pp. 697–702, 2002.

[3] M. Lincoln-Smith, A. Dye, K. Kemsley and J. Denholm, “Environmental monitoring and assessment: A statistical analysis on concentrations of silver and indium at generator locations,” *J. Weather Modif.*, vol. 43, pp. 1–8, 2011.

[4] Cardno ENTRIX, “Geochemistry and impacts of silver iodide use in cloud seeding,” 2011.

[5] H. T. Ratte, “Bioaccumulation and toxicity of silver compounds: a review,” *Environ. Toxicol. Chem.*, vol. 18, no. 1, pp. 89–108, 1999.

[6] M. P. Hirsch (a), “Toxicity of silver sulfide-spiked sediments to the freshwater amphipod (hyalella azteca),” *Environ. Toxicol. Chem.*, vol. 17, pp. 601–604, 1998.

[7] M. P. Hirsch (b), “Availability of sludge-borne silver to agricultural crops,” *Environ. Toxicol. Chem.*, vol. 17, pp. 610–616, 1998.

D.3. Calculation of silver mass recovery

We wanted to compute the recovery of silver throughout the basin. Therefore, we could estimate how much of the AgI burned actually nucleated snow

EXAMPLE CALCULATION 1.

The Supreme Court literature review of cloud seeding research (1978) reported that AgI affects about 3,600 km^2. Here, I perform of what typical silver concentrations in

snow should be using metrics from an average seeding storm. Assuming a constant concentration of snow in with 25 ppt (typical of seeded snow in WY15-WY16), we computed the approximate area affected before 100% of Ag nucleated a snowflake. The result show that a storm with the following assumptions will affect 3,380 km^2, similar to the Supreme Court study. Of course, concentrations of 25 ppt were not always measured in the snowpack, however this is likely due to the fact that not every AgI particle nucleates a snowflake within the target zone. Potential reasons for this are: snowpack is affected downwind of the target site, coagulation at the ground generator, AgI are photolytically deactivated, and improper targeting (vertically or laterally) of AgI plume.

Table D.1.Assumptions for AgI

AgI burn rate	# Ground Generators	Duration of seeding	Total AgI released	% weight Ag in AgI	Ag released in storm
[g/hr]	[unitless]	[hr]	[g]	[unitless]	[g]
23	20	4	1840	45.9	845.13

Table D.2.Assumptions for snowpack

Water density	Density in snow	Depth of seeded snow	Concentration Ag in snow	AgI affected area	km^2/cm^2 conversion	**AgI affected area**
[g/cm^3]	[unitless]	[cm]	[$g\ g^{-12}$] ([ppt])	[cm^2]	[unitless]	**[km^2]**
1	0.1	10	25	3.38×10^{13}	1×10^{10}	**3380**

EXAMPLE CALCULATION 2.

For another calculation, we assume just one ground generator. Based on our studies, the maximum spatial extent of AgI signatures in snow is approximately 60 km. Assuming an average seeded storm (2 cm of SWE, 4 hours of AgI seeding) we obtain the following conservation of mass equation.

$$m = P * \frac{d}{360} * (\pi r^2) * \rho$$

V = 6.5 x 10^{12} g = mass of snow water equivalent within AgI plume path

P = 2 cm = precipitation (snow water equivalent) from a snow storm (average seeded storm)

d = 15 degrees = dispersion of AgI plume from a ground generator (Holroyd, 1988)

r = 6,000,000 cm (60 km) = radius of AgI signatures in snow (Fisher, 2017)

ρ = 1.0 g cm^{-3} = density of water

$$AgI = BR * R * T$$

AgI = 36.8 g = mass of AgI from a single ground generator

R = 0.45946 = ratio of Ag mass to In mass in AgI

T = 4 hr = average duration of AgI generator activity during a seeded storm

$$C = \frac{m}{AgI} * 10^{12}$$

C = 5.6 ppt = average silver concentration in seeded snow in AgI plume path

m = 6.5 x 10^{12} g = mass of snow from seeded storm within plume path [g]

AgI = 36.8 g = mass of AgI deposited along plume path (assuming 100% nucleation)

This calculation highlights the difficulty of detecting AgI signals in snow. A single generator seeding a 15 degree radius sector 60 km long has a 5.6 ppt silver concentration. Fortunately, our field study area (the Payette Basin) has a consistent 1 ppt background concentration of silver in snow, so trace AgI signals in snow are easily detected. However, regions with higher background concentrations such as Wyoming (Edwards, 2006), need to carefully address the low signal-to-noise ratios in snow when employing trace chemical analysis methods.

D.4. Pulses of AgI seeded snow

One puzzling trend in the WY2015 – WY2016 trace chemical analysis of Idaho Power's cloud seeding program is the nature of seeding signals. Ag concentration profiles tended to represent a pulse shape (*Figure B.25.A)* as opposed to a constant source shape. To determine why this behavior might be the way it is, I compared Ag enrichments with meteorologic variables available at SNOTEL sites adjacent to sampled snow pits.

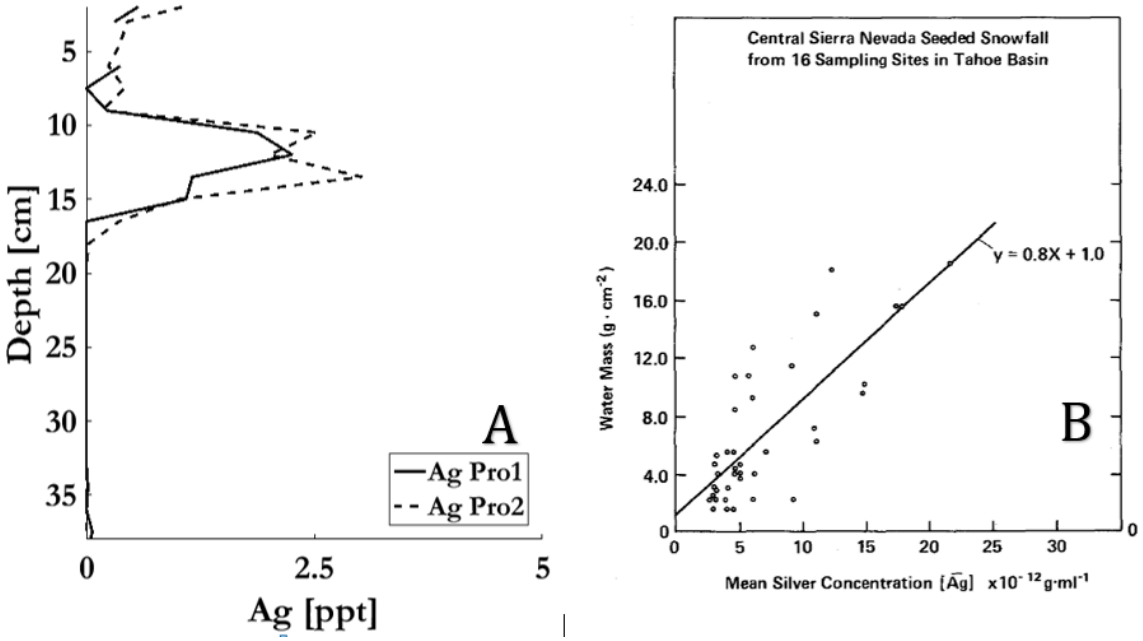

Figure D.3. A). Although AgI was released for the entire duration of the December 13 storm (from 2 – 38 cm depths in the plot above), there is only one 'pulse' detected in this snow storm layer. B). Warburton found a linear correlation between the amount of snow at a site and the mean silver concentration in snow. His study took place in the Sierra Nevada Mountains.

I hypothesize that precipitation intensity will be the most impactful variable on silver concentrations. My hypothesis is based on the conclusion drawn by Warburton's 1995 study. He found a strong linear relationship between total precipitation and silver concentrations (*Figure B.25.B*).

D.4.1. Methods

Two storms are analyzed this study. First, the March 24, 2015 storm. This ground generator seeded storm is ideal because this storm has the highest resolution spatial results – six sites were sampled (as opposed the usual 3-4 sites per storm). Second, I analyzed the Dec 21 ground generator and aircraft seeded storm. This storm is unique because there are three distinct AgI peaks *within* this single storm system. Ground generators were active throughout the entire precipitation period.

The methods to find the timing of each silver concentration peak and precipitation intensity are as follows:

1. **Determine timing of AgI signals**. Using the time series of precipitation accumulations from a SNOTEL site nearest to the sampling pit, timing of seeded snow deposition is modeled. See *Section 4.5* in Chapter 3 for methods on time-reconstruction.
2. **Compute continuous time series of precipitation intensity.** SNOTEL measures SWE to the nearest 0.1 inches, which can be the sum of several hours of precipitation. This gives cumulative precipitation curves (*Figure B.26*) a blocky appearance. Therefore, there were two steps involved in developing a continuous time series of precipitation.
    a. **Step 1. Choose a best fit line to interpolate cumulative precipitation at every minute interval.** I chose a smoothing spline with an R^2 at least 0.90, but often >0.97.
    b. **Step 2. Take the derivative of the cumulative curve to achieve precipitation intensity at every minute interval.** Using data from the spline, the derivatives of the cumulative precipitation curve are plotted at minute intervals.
3. **Compare peak silver concentrations with meteorologic variables.** Peak silver concentrations are compared to temperature, precipitation intensity, and wind speed.

D.4.2. Results

March 24, 2015 storm

BSU sampled six sites for the March 24, 2015 seeding event – the most sites sampled of any storm with a significant seeding signal. Four SNOTEL sites were in the vicinity of these sampled sites. In Figure 2 you can see the raw cumulative precipitation for the 24-hour period of this seeding event. Regions highlighted in yellow are times that significant seeding signals were found in snow.

Cumulative precipitation plots of 4 targeted SNOTEL sites on March 24.

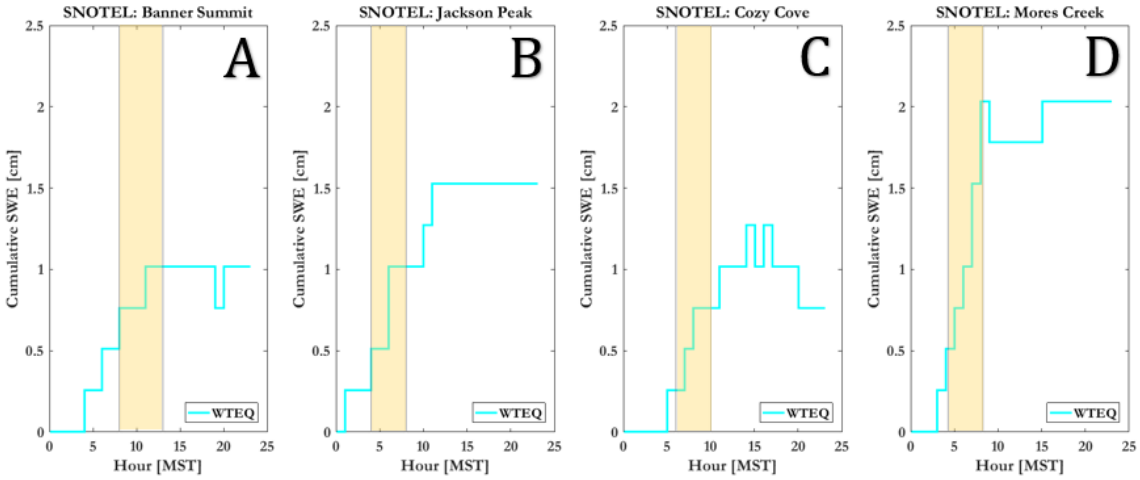

Figure D.4. Cumulative precipitation time series tend to have a 'blocky' look owing to the coarse temporal (hourly) and precipitation measurement method (0.1 inches of SWE). Yellow shading highlights region of the March 24 storm that AgI signals were the highest.

Precipitation intensity may be difficult to visualize in *Figure B.26*. Therefore, these curves underwent a smoothing spline (evaluated at every minute interval), and the derivative of that spline can be seen in *Figure B.27*. The results in *Figure B.27* suggest that seeding signals occurred at the highest precipitation intensities.

Silver enrichments occurred in the upper 1/3 to ½ of the snowpack deposited on March 24. Seeding signals (yellow) occurred at the highest precipitation intensities on March 24.

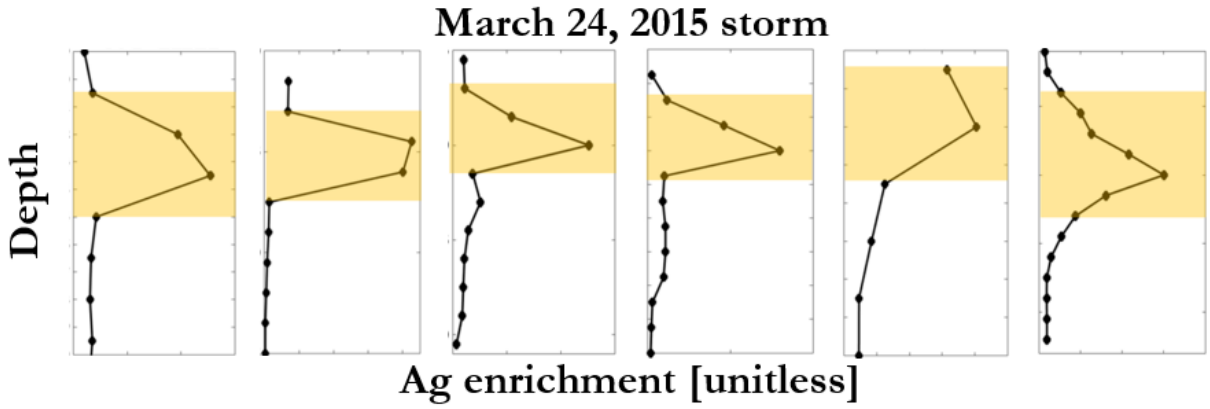

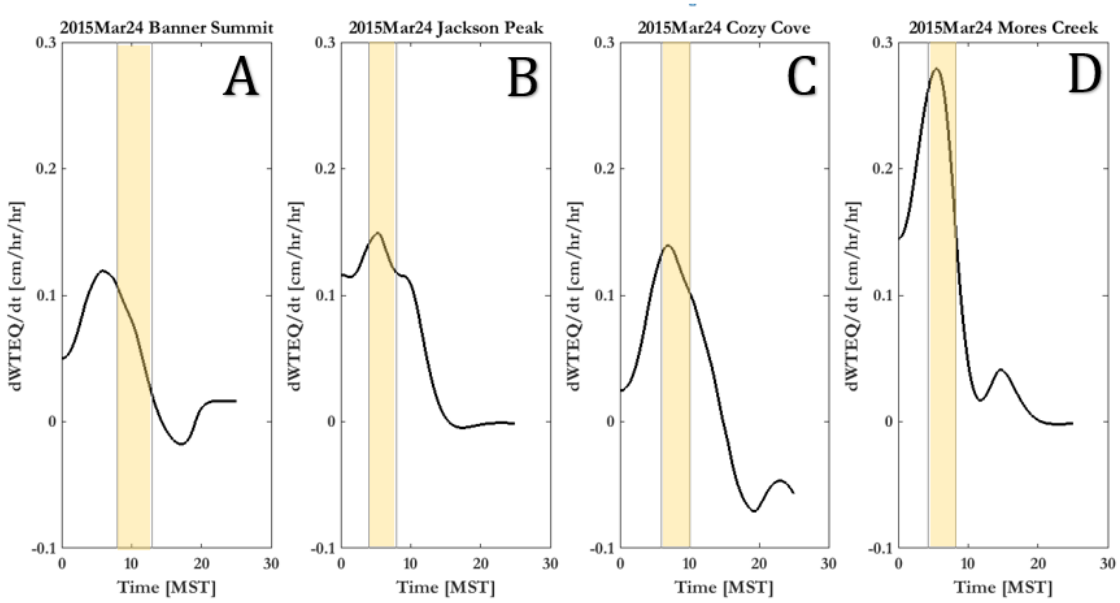

Figure D.5. Yellow highlighted regions delineate times when a seeding signal during the March 24 event. Black lines are a smoothed spline of SNOTEL cumulative precipitation *(Figure B.26)*. The spline better represented what a continuous time series of precipitation intensity looks like (raw SNOTEL data of 1hr at 0.1 inch resolution were too course for precise precipitation intensity estimates).

December 21, 2015 storm

The methods from the March 24 storm are replicated for the December 21, 2015 storm. I chose to analyze this storm because every site in the December 21 storm (with the exception of the contaminated 'control' site) contained three distinct silver 'pulses'. This was the only storm with more than one replicated Ag peak in a given seeded snow storm layer, so it seemed likely to find a correlation to a meteorologic variable.

All four sites sampled for silver for the Dec 21, 2015 storm.

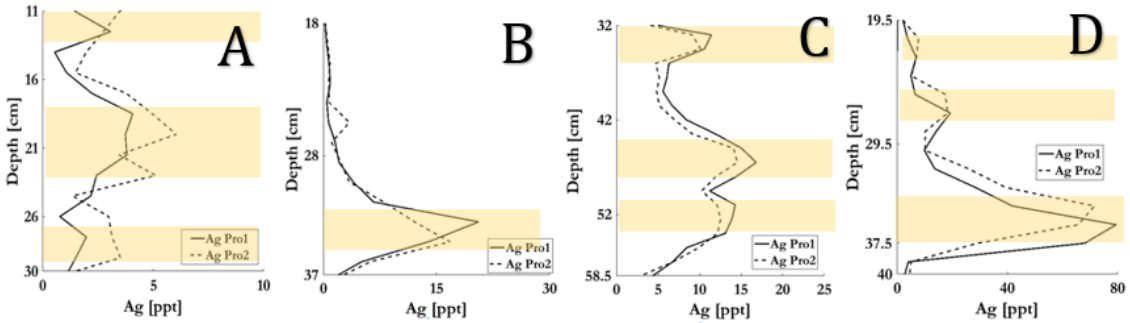

Precipitation intensity of each storm corresponding to the silver profiles above.

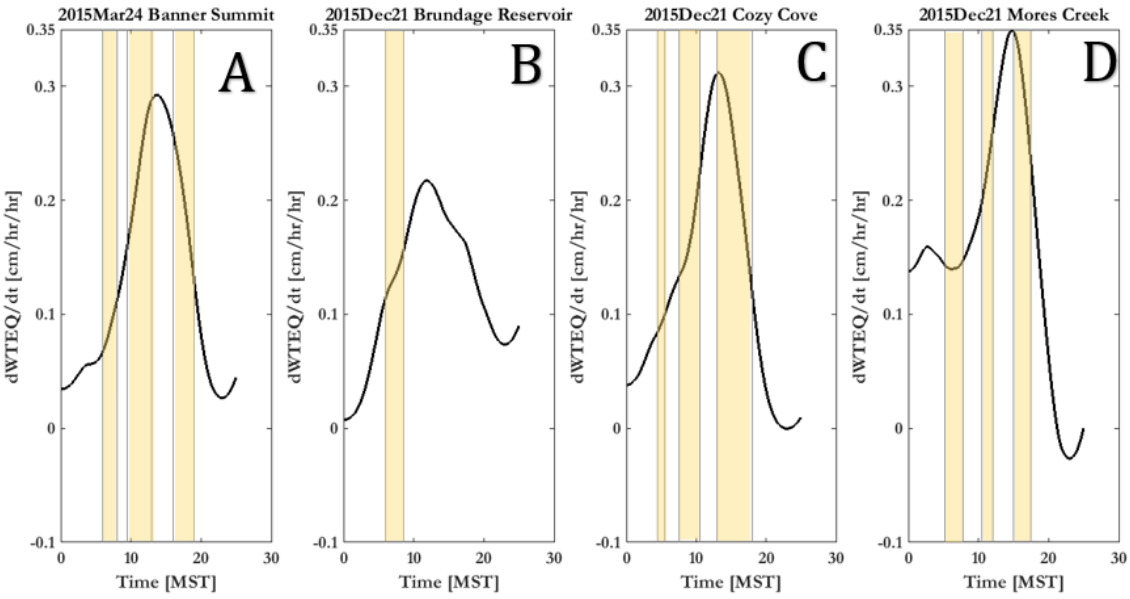

Figure D.6. Black line is the precipitation intensity for December 21, 2015 seeded storm. Seeding signatures are highlighted in yellow on both the snow profile plots (upper A-D subplots) and lower precipitation intensity plots (lower A-D subplots).

Results show that AgI signatures tend to correlate with the highest precipitation intensities, much like the findings on the March 24, 2015 storm. One notable exception is the top and bottom plot D's in *Figure B.28*. This site had the highest silver concentration and enrichment ever measured in both winter seasons (80 ppt!) but corresponded to a 'local min' in precipitation intensity.

D.4.3. Discussion

On a related note, Warburton found that areas with more snowfall should have higher peak concentrations of Ag in snow. This indirectly relates to efficacy of cloud seeding and thus, the finding that precipitation is positively correlated with silver is not surprising.

Temperature was also positively correlated with silver signatures. However, it is unclear how this relates to the silver concentrations in snow. For instance, it is likely that since AgI signatures happen to occur during periods of highest precipitation intensity, it is expected that temperature too will rise with precipitation intensity. Latent heat releases from ice nucleation should warm the air a few degrees above background temperatures.

Using surface wind speed measurements from a NOAA station in Stanley, ID (15 km east of the target zone), we found no correlation between wind speed and seeding signals. It is possible that there is a correlation between other wind speeds (at the 700 mb level, for example), but we do not have the supplementary data to address such a question.

D.4.4. Conclusions

Like literature would suggest, Ag concentrations appear to be positively correlated with precipitation intensity and temperature. Wind speed is not correlated with Ag concentrations. Wind speeds at the time of highest silver concentrations tended to be one-third that of the daily high (excluding gusts).